

X-602-74-272

PREPRINT

NASA TM X- 70759

# GAMMA RAY ASTROPHYSICS

(NASA-TM-X-70759) GAMMA RAY ASTROPHYSICS  
(NASA) 126 p HC \$9.50 CSCL 03B

N74-35217

Unclas  
G3/29 52012

F. W. STECKER



SEPTEMBER 1974



**GODDARD SPACE FLIGHT CENTER**  
**GREENBELT, MARYLAND**

**"This paper presents the views of the author(s), and does not necessarily reflect the views of the Goddard Space Flight Center, or NASA."**

**For information concerning availability  
of this document contact:**

**Technical Information Division, Code 250  
Goddard Space Flight Center  
Greenbelt, Maryland 20771**

**(Telephone 301-982-4488)**

**GAMMA RAY ASTROPHYSICS**

**F. W. Stecker**

**September 1974**

**Goddard Space Flight Center  
Greenbelt, Maryland**

CONTENTS

	<u>Page</u>
1. INTRODUCTION . . . . .	1
2. GAMMA RAY PRODUCTION PROCESSES . . . . .	3
A. Compton Scattering Between Cosmic-Ray Electrons and Starlight and Microwave Background Photons. . . . .	3
B. Synchrotron Radiation . . . . .	7
C. Bremsstrahlung Interactions. . . . .	10
D. Cosmic-Ray Produced $\pi^0$ Meson Decay . . . . .	13
E. Nucleon-Antinucleon Annihilations . . . . .	24
F. Form of the Spectrum from Pion Production at High Energies . . . .	24
3. $\gamma$ -RAY ABSORPTION MECHANISMS . . . . .	28
A. Absorption through Interactions with Radiation . . . . .	28
B. Absorption by Interactions with Matter . . . . .	31
4. $\gamma$ -RAYS OBSERVED FROM THE GALAXY . . . . .	35
5. EXTRAGALACTIC $\gamma$ -RAYS . . . . .	68
A. Redshifts and Cosmology . . . . .	68
B. Gamma-Ray Fluxes . . . . .	71
6. GAMMA RAY ABSORPTION PROCESSES AT HIGH REDSHIFTS . . . .	82
REFERENCES. . . . .	110

TABLE

<u>Table</u>	<u>Page</u>
1 Lifetime of Cosmic-Rays in the 4 to 5 kpc Region Calculated from the Acceleration-Compression Model . . . . .	62

## LIST OF ILLUSTRATIONS

<u>Figure</u>		<u>Page</u>
1	Cross section times multiplicity for neutral pion production in p-p interactions as a function of incident kinetic energy (Stecker 1973a) . . . . .	15
2	Differential neutral pion production function from p-p interactions (Stecker (1973a). . . . .	16
3	The calculated differential production spectrum of $\gamma$ -rays produced in cosmic-ray interactions in the galaxy based on the "isobar (i) -plus-fireball (f)" model of Stecker (1970) . . .	21
4	A comparison of the shapes of the integral galactic pion-decay energy spectra calculated by Stecker (1970) and Cavallo and Gould (1971). The total production rate is normalized to unity . . . . .	22
5	Total calculated galactic $\gamma$ -ray production spectrum from cosmic-ray interactions (Stecker 1971a) . . . . .	23
6	Normalized local differential $\gamma$ -ray spectrum from p- $\bar{p}$ annihilation at rest (Stecker 1971a) . . . . .	25
7	Absorption probability per unit distance by $\gamma + \gamma \rightarrow e^+ + e^-$ as a function of photon energy for $\gamma$ -rays passing through various universal radiation fields. The contributions from the optical ( $0_1$ and $0_2$ ) infrared (IR) 2.7 k blackbody microwave (M) and radio (R) fields are shown. Absorption at lower energies from X-rays is negligible. $0_1$ represents the contribution from the light of population II stars; $0_2$ that from population I stars (from Gould and Schröder 1967a, b); M is corrected to 2.7 K (Stecker 1971a) . . . . .	32
8	Compton scattering ( $\sigma_s$ ), Compton absorption ( $\sigma_a$ ), pair-production ( $\sigma_p$ ) and total ( $\sigma_a + \sigma_p$ ) cross sections as a function of $\gamma$ -ray energy for absorption of $\gamma$ -rays in hydrogen gas (based in part on work of Nelmes, 1953) from Stecker (1971a) . .	36
9	Contour map of $N_H$ , the number of atomic hydrogen atoms per $\text{cm}^2$ along the line of sight in galactocentric coordinates (from Garmire and Kraushaar (1964)) . . . . .	41
10	A smoothed spatial diagram of the locations of the maxima of the matter density deduced from the 21-cm neutral H line measurements and the density-wave theory by Simonson (preprint) . . . . .	42
11	The neutral hydrogen density $n_{H1}(\tilde{\omega})$ based on the discussion of Kerr (1969), Shane (1972), and Sanders and Wrixon (1973) . . .	43

Page intentionally left blank

Page intentionally left blank

<u>Figure</u>		<u>Page</u>
12	Distribution in galactic longitude of the galactic $\gamma$ -ray line flux as observed by OSO-3 (Kraushaar, et al. 1972) and SAS-2 (Kniffen, et al. 1973) normalized arbitrarily for purposes of comparison. Statistical uncertainties quoted for these results (not plotted) are significantly greater for the OSO-3 results as compared with the SAS-2 results. The interpolation of the SAS-2 data was obtained on the assumption of a smooth average variation in the $\gamma$ -ray production rate (Puget and Stecker 1974) . . . . .	45
13	Distribution of high-energy (>100 MeV) gamma-rays along the galactic plane. The diffuse background level is shown by a dashed line. The SAS-2 data are summed over $ b^{II}  < 10^\circ$ . The ordinate scale is approximately in units of $10^{-4}$ photons $\text{cm}^{-2}$ $\text{rad}^{-1}$ $\text{sec}^{-1}$ (Thompson, et al. 1974) . . .	46
14	(a) Distribution of high-energy ( $E_\gamma > 100$ MeV) gamma-rays summed over $335^\circ < \ell_{II} < 25^\circ$ as a function of $b^{II}$ . The solid line represents the sum of the two distributions with equal areas, one representing only the detector resolution, the other a gaussian with a width $\sigma = 6^\circ$ (Thompson, et al. 1974). (b) Distribution of $> 100$ MeV gamma-rays summed from $90^\circ < \ell_{II} < 170^\circ$ and $200^\circ < \ell_{II} < 270^\circ$ where data exists, (Thompson, et al. 1974) . . . . .	47
15	Schematic diagram of relative intensity of the gamma radiation above 100 MeV as deduced from preliminary data from SAS-2. Increasing shading indicates higher intensity, but no single ( $4^\circ \times 4^\circ$ ) box has sufficient numbers of gamma rays to justify statistically conclusions to be deduced for it alone. It is clear, however, that the galactic plane stands out sharply (Fichtel, Hartman, Kniffen, and Thompson, 1973) . . . . .	48
16	The value for $hQ(\tilde{\omega})$ ( $\gamma$ -ray emissivity times disk width) given by Puget and Stecker (1974). A constant value for $hQ$ is assumed for $R_\odot \tilde{\omega} > 8$ kpc. Uncertainties in the determination of the value of $hQ(\tilde{\omega})$ as evaluated from an integral equation of Puget and Stecker grow quite large in the central region $R_\odot \tilde{\omega} < 4$ kpc . . . . .	49
17	Comparison of SAS-2 (Kniffen, et al. 1973) spectral data on $\gamma$ -radiation from the inner galaxy with a two-component model based on 70 percent pion decay (Stecker 1970) and an $E^{-1}$ integral Compton spectrum (Stecker, et al. 1974) . . . . .	51

<u>Figure</u>		<u>Page</u>
18	Summary of the integral flux measurements for the galactic center region given by various experimental groups . . . . .	53
19	The differential photon spectrum of $\gamma$ -rays as determined from the emulsion measurements of Samimi, et al. (1974) with the detector response unfolded. (a) only $\gamma$ -rays coming from the enhanced $3^\circ$ band $-3^\circ \leq b^{II} \leq 0^\circ$ , (b) atmospheric $\gamma$ -rays . . . . .	54
20	Longitudinal distributions of galactic gamma-flux integrated over $\pm 10^\circ$ in $b^{II}$ from Bignami and Fichtel (1974). SAS-II points are given together with their error bars (Kniffen, et al. 1973). The thick line represents the model of Bignami and Fichtel smoothed in $10^\circ$ $l^{II}$ intervals. The thin line represents the model in $2^\circ$ intervals. The dashed line (----) gives the contribution of the Sagittarius and Norma-Scutum arms and dash-dot (-.-.-) the contribution of the Sagittarius arm alone. . . . .	57
21	The specific compression rate $\alpha(\tilde{\omega})$ obtained from the radial velocity data $v_r(\tilde{\omega})$ based on the observations of Shane (1972) and Sanders and Wrixon (1972, 1973) . . . . .	61
22	The intensity distribution of 2.6mm line emission in the galactic plane from the $J = 1 \rightarrow 0$ transition of carbon monoxide integrated over velocity as a function of galactic longitude (Scoville and Solomon, to be published; Scoville, Solomon and Jefferts 1974) . . . . .	64
23	Sample CO line emission spectra obtained in the survey of Scoville and Solomon (to be published) . . . . .	65
24	The distribution of CO line emission as a function of galactocentric distance (labeled here $\tilde{\omega}$ ) in kpc . . . . .	66
25	Observational data on the gamma-ray background energy spectrum. The highest energy point of Vette, et al. (1970), shown with a dashed line, and possibly the neighboring point are now thought to be erroneously high due to an inefficiency in the anticoincidence circuit of their detector which should not significantly affect the points at lower energies (Vette, private communication) . . . . .	69

<u>Figure</u>		<u>Page</u>
26	The redshift at which the universe becomes opaque to photons given as a function of observed gamma-ray energy. Gamma-rays originating at all redshifts below the curve can reach us unattenuated with the energy indicated. The two curves on the left side of the figure are for attenuation by Compton scattering with intergalactic electrons having the densities indicated and for pair production and are based on the calculations of Arons and McCray (1969). The right-hand curve results from attenuation of gamma-rays by interactions with the microwave blackbody radiation and is based on the discussion of Fazio and Stecker (1970) . . . . .	86
27	The cosmological $\gamma$ -ray spectrum from matter-antimatter annihilation calculated by solving the CPT equation numerically for $\Omega = 1$ . The solid line represents the complete solution. The other curves represent the effect of neglecting the absorption and scattering (transport) terms in equation (158) . . . . .	94
28	The effect of absorption of $\gamma$ -rays at high redshifts by the protogalactic gas . . . . .	95
29	Comparison of the observed background with a two-component model involving the production and decay of neutral pions produced in intergalactic cosmic-ray interactions at red-shifts up to 100 . . . . .	96
30	A comparison of the data given in Figure 25 with the annihilation model discussed by Stecker, Morgan and Bredekamp (1971) and Stecker and Puget (1972) . . . . .	99
31	Outline of the galaxy formation theory of Stecker and Puget (1972) . . . . .	101
32	Observational implications of baryon symmetric cosmology . . . . .	102
33	Energy flux spectrum of the x-ray and gamma-ray background based on Schwartz and Gursky (1973) and the data given in Figure 25. The straight diagonal line indicates an extrapolation of the 30 keV to 1 MeV spectrum . . . . .	104
34	Predicted energy flux spectra from the annihilation model (A) and cosmic ray (protar) model (CR) as discussed in the text. Also shown is the scatter area covered by the observational data (shaded) and the extrapolated x-ray background spectrum (X). The two curves shown for the CR spectrum above 7 GeV are for closed (Einstein-de Sitter) and open universes as discussed in the text (Stecker 1971a) . . . . .	107

<u>Figure</u>		<u>Page</u>
35	The $\gamma$ -ray background calculated from the Hillas model by Strong, et al. (1973 (SW <sup>2</sup> ). Also shown are the data from Figure 25 for comparison . . . . .	108

## GAMMA RAY ASTROPHYSICS\*

F. W. Stecker  
Theoretical Studies Group  
NASA Goddard Space Flight Center  
Greenbelt, Maryland 20771

### 1. INTRODUCTION

In the context of an advanced study institute on the origin of cosmic rays, one can look at the subject of theoretical gamma-ray astrophysics from two points of view. The first seeks to answer the question, "What is the origin of the observed cosmic gamma radiation?", considering this radiation as a component of cosmic radiation. The second seeks to answer the question, "What does the observed cosmic gamma radiation tell us about the origin of cosmic rays?" with the term "cosmic rays" meant to be the primary nuclear component of cosmic radiation (or perhaps the electronic component) and the gamma radiation considered to be a secondary product of various interactions between primary radiation and fields, photons and nuclei in the cosmos. This latter question, in which most, of you here I'm sure are "primarily" interested, is the historically older question, but it is inherently a much more difficult one to answer and is one which cannot be unambiguously answered at this point in time, given our relatively primitive observations and the context of our present theoretical

---

\* Lectures presented at NATO Advanced Study Institute on "The Origin of Cosmic Rays" Aug. 26-  
Sep. 6, 1974.

understanding. Indeed it may well be that the gamma ray background radiation is not even a product of cosmic ray interactions, at least up the energies thus far observed, and we will discuss this possibility later. Thus, of necessity, we will spend most of our time here discussing the origin of the gamma radiation itself, bearing in mind the relation of this problem with that of the origin of the nuclear component of cosmic radiation.

The possible existence of a secondary component of cosmic gamma radiation first appeared in the literature almost incidental to problems bearing on the question of the origin and propagation of the primary cosmic radiation. After it had been determined that overwhelming component of primary cosmic radiation impinging on the upper atmosphere consists of high-energy protons, Feenberg and Primakoff (1947) addressed themselves to an explanation of the conspicuous absence of electrons in significant quantities in the primary radiation. To do this, they examined the various interactions which cosmic ray electrons and protons could be expected to undergo with low-energy starlight photons in interstellar space and found that electrons could be effectively depleted of their energy by Compton interactions in a fraction of the age of the universe. In this process, the energy of the electrons is transferred to the photons which can be boosted to X-ray or gamma ray energy. Similarly, Hayakawa (1952), in examining the propagation of cosmic radiation through interstellar space, pointed out the effect of meson-producing nuclear interactions between cosmic rays and interstellar gas. Hayakawa noted that the neutral pions produced would decay to

produce cosmic gamma radiation. The production of bremsstrahlung radiation by cosmic rays was discussed by Hutchinson (1952). However, the idea of establishing a science of gamma ray astronomy itself as a tool for answering questions in high-energy astrophysics and cosmology appears to have been stimulated in an important article by Morrison (1958). Morrison (1958) and Felten and Morrison (1963) pointed out that the processes of most significance for producing cosmic gamma rays were (1) electron bremsstrahlung, (2) electron-photon interactions (Compton effect), (3) cosmic-ray produced pion decay, (4) synchrotron radiation, (5) annihilation produced pion decay, and (6) line emission from electron-positron annihilation and nuclear deexcitation.

We will first review here these various processes for producing cosmic gamma radiation, as well as the significant processes for absorption of cosmic gamma radiation, discussing the basic physics of these processes. We will then attempt to place these processes in their astrophysical context in the galaxy and the universe as a whole. We will then turn to the interpretation of the present data on cosmic gamma radiation and its implications for cosmology and cosmic ray origin.

## 2. GAMMA RAY PRODUCTION PROCESSES

### A. Compton Scattering Between Cosmic-Ray Electrons and Starlight and Microwave Background Photons.

Compton scattering is the relativistic limit of the electron-photon scattering process which is referred to as Thomson scattering in the non-relativistic case.

The traditional Compton effect is one in which a  $\gamma$ -ray scatters off an electron at rest in the laboratory. In the case of astrophysical interest, the electron is a cosmic-ray of energy  $E = \gamma mc^2$  and velocity  $v = \beta c$ . A photon of initial energy  $\epsilon$  then scatters off the electron, coming out of the interaction with an energy  $\epsilon'$ . Denoting quantities in the electron rest system by asterisks and denoting the scattering angle of the photon by  $\nu^*$ , the initial and final energy of the photon in the electron rest system are related by

$$\epsilon'^* = \frac{\epsilon^*}{1 + \frac{\epsilon^*}{mc^2} (1 - \cos \nu^*)} \quad (1)$$

Denoting the angle between the electron and the photon by  $\alpha$ , it then follows that

$$\epsilon^* = \gamma \epsilon (1 + \beta \cos \alpha)$$

$$\epsilon' = \gamma \epsilon'^* (1 - \beta \cos \alpha'^*)$$

and (2)

$$\tan \alpha^* = \frac{\sin \alpha}{\gamma(\cos \alpha + \beta)}$$

so that

$$\epsilon' = \frac{\gamma^2 \epsilon (1 + \beta \cos \alpha) (1 - \beta \cos \alpha'^*)}{1 + \frac{\gamma \epsilon}{mc^2} (1 + \beta \cos \alpha) (1 - \cos \nu^*)} \quad (3)$$

and, on the average, the final photon energy in the observers frame is

$$\epsilon' \sim \gamma^2 \epsilon \quad (\gamma \epsilon \ll mc^2) \quad (4)$$

For the astrophysical conditions we will primarily be concerned with here, the condition  $\gamma \epsilon \ll mc^2$  holds and the cross section for the scattering is

$$\sigma_c \rightarrow \sigma_T = \frac{8}{3} \pi \left( \frac{e^2}{mc^2} \right)^2 = 6.65 \times 10^{-25} \text{ cm}^2 \quad (5)$$

(Heitler 1960).

In the other extreme, the Klein-Nishina form of the cross section holds, which has the asymptotic form.

$$\sigma_c \rightarrow \pi \left( \frac{e^2}{mc^2} \right)^2 \left( \frac{mc^2}{\epsilon} \right) \left[ \frac{1}{2} + \ln \left( \frac{2\epsilon}{mc^2} \right) \right] \quad (\gamma \epsilon \gg mc^2) \quad (6)$$

Also in this extreme

$$\epsilon' \sim \gamma mc^2 \sim E \quad (7)$$

However in most cases, i.e. whenever  $\epsilon E_\gamma \ll (mc^2)^2$ , the energy of the  $\gamma$ -ray produced is on the average

$$\langle E_\gamma \rangle = \frac{4}{3} \gamma^2 \langle \epsilon \rangle \quad (8)$$

In the important case of astrophysical interest where the cosmic ray electrons are assumed to have an energy distribution of power-law form

$$I_e(E) = KE^{-\Gamma} \quad (9)$$

if we make the delta-function approximation for the differential production function

$$\sigma(E_\gamma | \epsilon, E) \simeq \sigma_T \delta \left( E_\gamma - \frac{4}{3} \langle \epsilon \rangle \gamma^2 \right) \quad (10)$$

the  $\gamma$ -ray production rate as a function of energy is given by

$$\begin{aligned} q(E_\gamma) &= 4\pi n_{\text{ph}} \sigma_T \int dE K E^{-\Gamma} \delta \left( E_\gamma - \frac{4}{3} \langle \epsilon \rangle \gamma^2 \right) \\ &= 4\pi n_{\text{ph}} K \left[ \left( \frac{3}{4} \right)^{1/2} E_\gamma^{-1/2} \langle \epsilon \rangle^{-1/2} mc^2 \right]^{-\Gamma} \frac{dE}{dE_\gamma} \\ &= 2\pi n_{\text{ph}} \sigma_T K (mc^2)^{1-\Gamma} \left( \frac{4}{3} \langle \epsilon \rangle \right)^{(\Gamma-1)/2} E_\gamma^{-\left(\frac{\Gamma+1}{2}\right)} \\ &= \frac{8\pi}{3} \sigma_T \rho_{\text{ph}} (mc^2)^{1-\Gamma} \left( \frac{4}{3} \langle \epsilon \rangle \right)^{\left(\frac{\Gamma-3}{2}\right)} K E_\gamma^{-\left(\frac{\Gamma-1}{2}\right)} \end{aligned} \quad (11)$$

where  $n_{\text{ph}}$  is the number density of target photons of low energy in the interstellar or intergalactic medium (usually in the form of starlight photons of  $\sim 1$  eV energy or universal microwave blackbody photons of energy  $\sim 0.6 \times 10^{-3}$  eV) and  $\rho_{\text{ph}} = n_{\text{ph}} \langle \epsilon \rangle$  is the energy density of the radiation.

In particular, for blackbody radiation of temperature  $T$

$$\left\langle \frac{4}{3} \epsilon \right\rangle \simeq 3.6 kT \simeq 3.1 \times 10^{-10} T \text{ MeV}$$

and

$$\rho_{\text{ph}} = 4.75 \times 10^{-9} \text{ T}^4 \text{ MeV/cm}^3 \quad (12)$$

### B. Synchrotron Radiation

Synchrotron radiation, or magnetic bremsstrahlung, is the radiation emitted by a relativistic particle spiraling in a magnetic field. Its mathematical description has been given by Schwinger (1949). An electron suffers energy losses by synchrotron radiation at a rate

$$\left(\frac{dE}{dt}\right)_{\text{synch}} = -\frac{4}{3}\sigma_{\text{T}}c\gamma^2\rho_{\text{H}}$$

where the magnetic energy density  $\rho_{\text{H}}$  is equal to  $H^2/8\pi$ . This rate can be compared with the energy loss suffered by an electron through Compton interactions with a photon field of energy density  $\rho_{\text{ph}}$ . That rate is

$$\left(\frac{dE}{dt}\right)_{\text{c}} = -\frac{4}{3}\sigma_{\text{T}}c\rho_{\text{ph}} \quad (14)$$

The equivalence of equations (13) and (14) can be shown to be a direct consequence of electromagnetic theory (Jones 1965). The photons emitted as synchrotron radiation have a characteristic frequency given by

$$\omega_{\text{c}} = \frac{3}{2}\gamma^2\left(\frac{eH}{mc}\right) \quad (15)$$

The synchrotron effect can be thought of as the interactions of an electron with "virtual" photons of the magnetic field. Denoting these photons by the subscript v, it is found that they have an average energy

$$\epsilon_v = \frac{8}{8\pi\sqrt{3}} \left( \frac{\hbar}{mc} \right) eH \quad (16)$$

and a number density

$$n_v = \frac{H^2}{8\pi\epsilon_v} \quad (17)$$

(Jones 1967).

The resultant  $\gamma$ -rays have a characteristic energy found from equation (15) to be

$$E_{\gamma,c} = \frac{3}{2} \gamma^2 \left( \frac{\hbar}{mc} \right) eH \quad (18)$$

Because this is the same type of energy dependence as that for Compton radiation, a power-law cosmic-ray electron spectrum of the form  $KE^{-\Gamma}$  will again generate a synchrotron radiation spectrum of the form

$$q(E_\gamma) \propto E_\gamma^{-\frac{\Gamma+1}{2}} \quad (19)$$

The above equations can be used to find some useful numerical relations involving  $\gamma$ -ray production by synchrotron radiating electrons, with the synchrotron radiation being determined from radio observations (e.g., in the 10-1000 MHz range) and the  $\gamma$ -radiation being produced from Compton interactions of the same electrons responsible for the synchrotron radio emission. Typical galactic magnetic fields are of the order of a few  $\mu$ G. From equation (15) it follows that the frequency of a synchrotron radiating electron  $\nu_s$  as a

function of electron energy is given by

$$\nu_s \simeq 4.2 \gamma^2 H_{\perp} \text{ MHz} \quad (20)$$

with the magnetic field strength given in gauss. It then follows from equations (12) and (20) that the energy of a Compton  $\gamma$ -ray produced by an electron which synchrotron radiates at frequency  $\nu_s$  is given by

$$E_{\gamma} = \frac{4}{3} \langle \epsilon \rangle \gamma^2 = 0.74 \times 10^{-10} \left( \frac{T}{H_{\perp}} \right) \nu_s \text{ MeV} \quad (21)$$

To determine the relative importance of synchrotron radiation and Compton scattering in producing  $\gamma$ -radiation under astrophysical conditions, we note that the energy of a synchrotron photon is

$$E_{\gamma, s} = h\nu_s = 2.8 \times 10^{-15} \gamma^2 H_{\perp} \text{ MeV} \quad (22)$$

We then specify that an electron of energy  $\gamma_c mc^2$  will radiate a Compton photon at the same mean energy as an electron of energy  $\gamma_s mc^2$  will radiate a synchrotron photon. It then follows from equations (8), (12) and (22) that the ratio

$$\frac{\gamma_s}{\gamma_c} \simeq 10^2 \left( \frac{T}{H_{\perp}} \right)^{1/2} \quad (23)$$

The relative production rates from synchrotron and Compton radiation are then related by

$$\frac{Q_s}{Q_c} = \frac{\rho_H}{\rho_{ph}} \frac{I_e(\gamma_s)}{I_e(\gamma_c)} \quad (24)$$

In the galaxy, for example,  $\rho_{\text{ph}} \simeq \rho_{\text{H}}$ , but  $\gamma_s \gg \gamma_c$  so that  $I_e(\gamma_s) \ll I_e(\gamma_c)$  and synchrotron radiation is negligible compared to Compton scattering as a  $\gamma$ -ray production mechanism.

### C. Bremsstrahlung Interactions

Bremsstrahlung, which is a German word meaning "braking radiation" is the radiation emitted by a charged particle accompanying deceleration. The cross sections for  $\gamma$ -ray production from bremsstrahlung are derived in Heitler's book (Heitler 1954). In the case of bremsstrahlung from non-relativistic electrons radiating in the field of a target nucleus, the cross sections for production of a  $\gamma$ -ray of energy  $E_\gamma$  by an electron of energy  $E$  in the field of a nucleus or charge  $Z$  is given by

$$\sigma_b(E_\gamma | E) \equiv \sigma_b(E, E_\gamma) f(E_\gamma | E) \quad (25)$$

where  $f_b(E_\gamma | E)$  is the normalized distribution function for  $\gamma$ -ray production, and where, in terms of the kinetic energy  $T = E - mc^2$

$$\sigma_b(E, E_\gamma) = \frac{aZ^2}{\pi} \sigma_T \left( \frac{mc^2}{T} \right) \ln \left\{ \frac{\sqrt{T} + \sqrt{T - E_\gamma}}{E_\gamma} \right\} \left( \frac{T}{E_\gamma} \right) \quad (26)$$

$$\text{for } 2\pi Z a \ll \beta \ll 1$$

The cross section for bremsstrahlung by relativistic electrons is given by

$$\sigma_b(E, E_\gamma) = \frac{4aZ^2}{\pi} \sigma_T \ln \left\{ \frac{2E}{mc^2} - \frac{1}{3} \right\} \left( \frac{E}{E_\gamma} \right) \text{ for } mc^2 \ll E \ll a^{-1} Z^{-1/3} mc^2 \quad (27)$$

In the ultrarelativistic case, where the cross section is calculated by taking into account the screening of the charge of the atomic nucleus by atomic electrons, the resultant cross section is given by

$$\sigma_b(E, E_\gamma) = \frac{4\alpha Z^2}{\pi} \sigma_T \ln \left( 183 Z^{-1/3} + \frac{1}{18} \right) \left( \frac{E}{E_\gamma} \right) \quad (28)$$

$$\text{for } E \gg \alpha^{-1} Z^{-1/3} mc^2$$

Of course, in the case of an ionized gas, equation (27), which holds for the case when screening effects are unimportant, is applicable at all relativistic energies. The cross sections given in equations (26) and (27) may be corrected for additional contributions from interactions between cosmic ray electrons and atomic electrons by the replacement  $Z^2 \rightarrow Z(Z+1)$ .

Another case which may be of astrophysical interest for gamma-ray production may be that of bremsstrahlung from nonrelativistic protons, as has been pointed out by Boldt and Serlinitos (1969). In this case, it is the electrons which is at rest and the proton which has the kinetic energy in the laboratory system (observers system). The appropriate cross section for this interaction, which corresponds to equation (26) for cosmic ray electrons, is then

$$\sigma_b(E_{ph}, E_\gamma) = \frac{\alpha}{\pi} \sigma_T \left( \frac{M_p c^2}{T_{pr}} \right) \ln \left\{ \frac{\sqrt{(M_e/M_p)} T_{pr} + \sqrt{(M_e/M_p)} T_{pr} - E_\gamma}{E_\gamma} \right\} \left( \frac{(M_e/M_p) T_{pr}}{E_\gamma} \right) \quad (29)$$

It is immediately obvious from equations (27) and (28) that for relativistic particles the bremsstrahlung cross sections have little or no dependence, except

for a linear one, on  $E$ . Indeed, equation (28) may be written in the form

$$\sigma_b(E, E_\gamma) \approx \frac{\langle M \rangle}{\langle X \rangle} \left( \frac{E}{E_\gamma} \right) \quad (30)$$

where  $\langle M \rangle$  is the average mass of the target atoms in grams and  $\langle X \rangle$  is the average radiation length for the gas in grams per  $\text{cm}^2$ . The average radiation length for interstellar matter is

$$X = 65 \text{ g/cm}^2 \quad (31)$$

based on the values given for pure hydrogen and pure helium by Dovshenko and Pomanski (1964) of

$$X_H = 62.8 \text{ g/cm}^2 \quad (32)$$

and

$$X_{He} = 93.1 \text{ g/cm}^2 \quad (33)$$

To a good approximation, especially in the case of relativistic bremsstrahlung (see Heitler 1954) the normalized distribution of gamma-rays produced may be taken to be a square distribution given by

$$f(E_\gamma|E) = \begin{cases} E^{-1} & \text{for } 0 \leq E_\gamma \leq E \\ 0 & \text{otherwise} \end{cases} \quad (34)$$

so that the gamma-ray production spectrum is given by

$$\begin{aligned}
I_b(E_\gamma) &= \frac{\langle M \rangle}{\langle X \rangle} \left[ \int_{E_\gamma}^{\infty} dE I_e(E) \right] E_\gamma^{-1} \\
&= \frac{1}{\langle X \rangle} \int d\vec{r} \rho(\vec{r}) \frac{I_e(>E_\gamma)}{E_\gamma}
\end{aligned}
\tag{35}$$

where  $\rho(\vec{r})$  is the matter density of the gas in grams per  $\text{cm}^3$ . For bremsstrahlung between cosmic-ray electrons and interstellar gas we may use equation (31) to write equation (35) in the form

$$q_b(E_\gamma) = 4.3 \times 10^{-25} n \frac{I_e(>E_\gamma)}{E_\gamma} \text{ cm}^{-3} \text{ s}^{-1} \text{ MeV}^{-1}
\tag{36}$$

where  $n$  is the number density of nuclei in the production region.

#### D. Cosmic-Ray Produced $\pi^0$ Meson Decay

Cosmic-rays of high enough energy can produce various secondary particles of short lifetime upon collision with interstellar or intergalactic gas nuclei. Of these secondaries, the most important for production of  $\gamma$ -radiation is the  $\pi^0$  meson which decays almost 100% of the time into 2 gamma rays. An extensive treatment of these various secondary production processes leading to cosmic  $\gamma$ -ray production has been given elsewhere (Stecker 1970, 1971a, 1973a) and the reader is referred to these references for more detail of the material outlined here.

The collision processes of highest frequency occurring in interstellar and intergalactic space are those between cosmic-ray protons and hydrogen gas

nuclei and are therefore p-p interactions. The threshold kinetic energy which a cosmic-ray proton must have to produce a secondary particle of mass  $m$  in such an interaction is

$$T_{\text{th}} = \left( 2 + \frac{m}{2M_p} \right) m \quad (37)$$

Thus, to produce a single  $\pi^0$  meson of rest mass  $135 \text{ MeV}/c^2$  requires a threshold kinetic energy of  $280 \text{ MeV}/c^2$ . Within the past two decades, many measurements have been made of the cross sections for inclusive production of various secondary particles in high energy interactions using proton accelerators. These data are summarized in Figure 1, taken from Stecker (1973a) wherein the references may be found. Figure 1 shows the product of the production cross section  $\sigma_{\pi^0}$  and multiplicity  $\zeta_{\pi^0}$  given as a function of kinetic energy  $T$ . Utilizing the data shown in Figure 1, and a demodulated cosmic-ray proton spectrum given by Comstock, et al. (1972), Stecker (1973a) calculated a total  $\gamma$ -ray production rate from this process in the solar region of the galaxy to be

$$q_{\gamma} = (1.3 \pm 0.2) \times 10^{-25} n_H \text{ cm}^{-3} \text{ s}^{-1} \quad (38)$$

taking account of the effect of p-He and  $\alpha$ -H interactions as well as that of p-p interactions.

Figure 2, which shows the product of the cosmic-ray energy distribution  $I(T)$  and the function  $\sigma_{\pi^0} \zeta_{\pi^0}$  of Figure 1, is a measure of the kinetic energy of the cosmic-ray protons which are most effective in producing  $\pi^0$  mesons in the

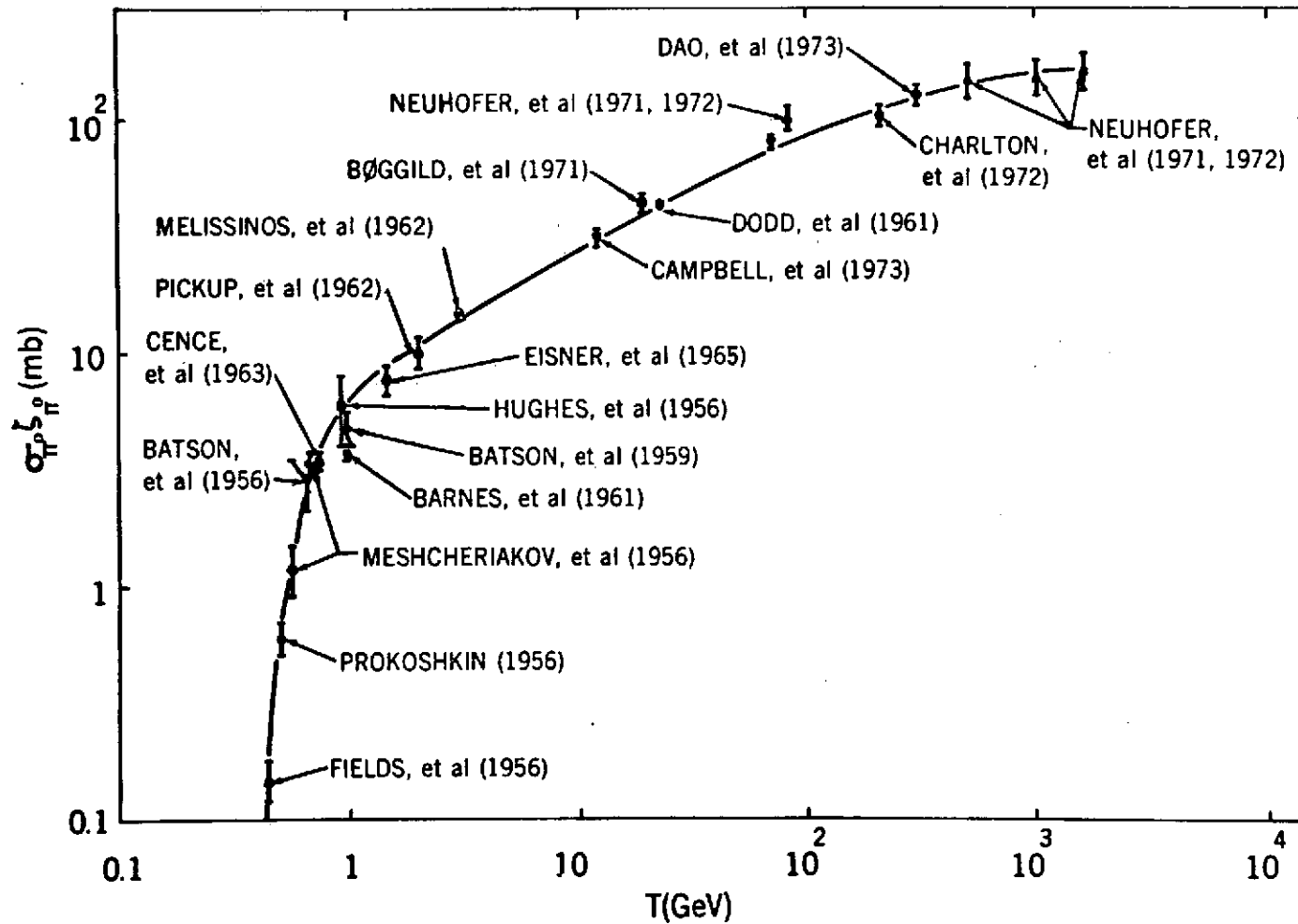


Figure 1. Cross section times multiplicity for neutral pion production in p-p interactions as a function of incident kinetic energy (Stecker 1973a).

$\pi^0$  - PRODUCTION FUNCTION FROM pp INTERACTIONS ONLY

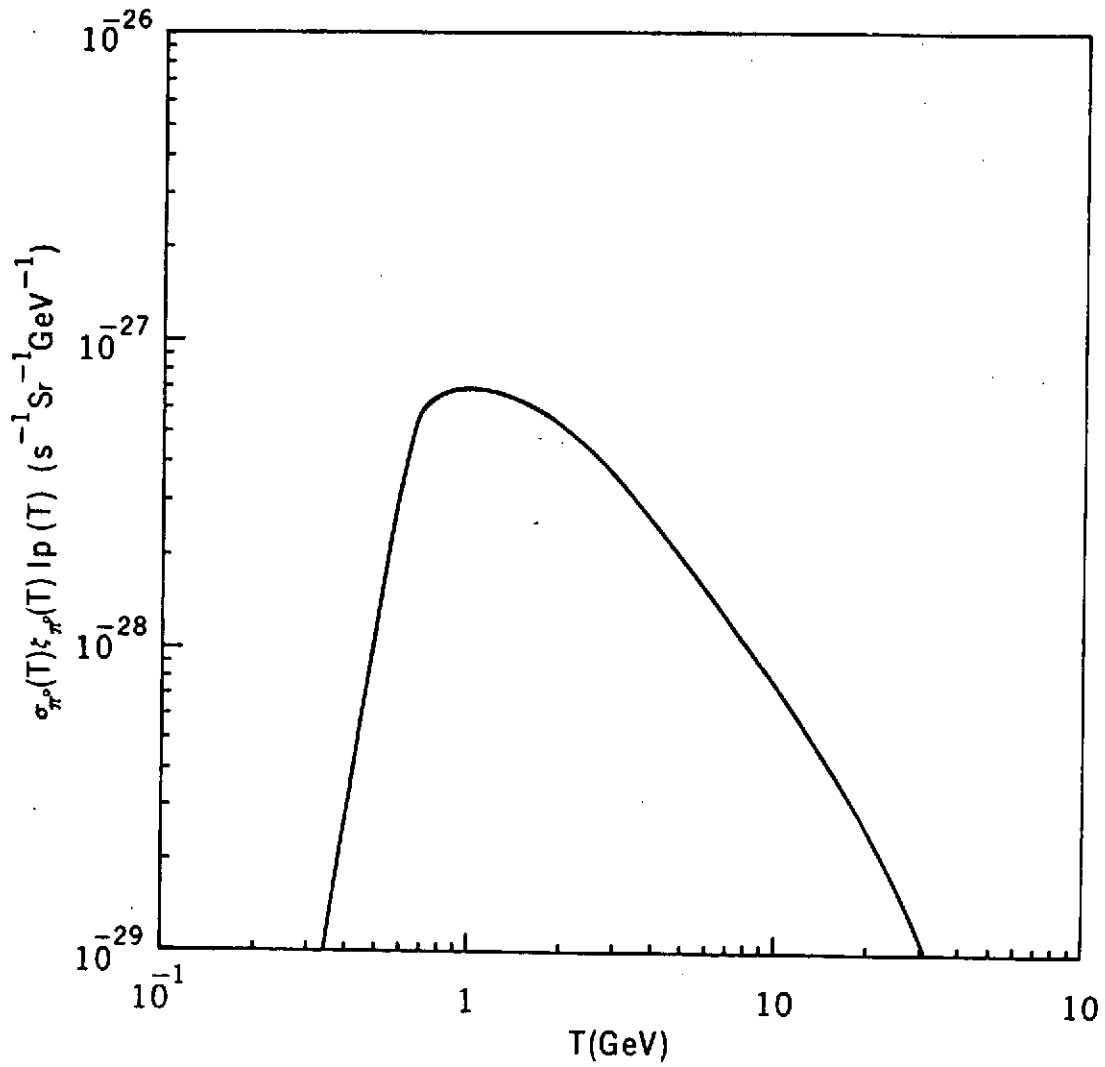


Figure 2. Differential neutral pion production function from p-p interactions (Stecker 1973a).

galaxy. It is found from this figure that the average proton which produces a  $\pi^0$  meson in the galaxy has an energy of about 3.3 GeV and that 85% of the  $\pi^0$  mesons produced in the galaxy are produced by cosmic-ray protons in the energy range between 1 and 10 GeV.

When a  $\pi^0$  meson decays into 2  $\gamma$ -rays, because of conservation of momentum they both are produced with an energy of  $m_\pi c^2/2 = 67.5$  MeV in the rest system of the pion. However, in the system of a terrestrial observer, in general, these  $\gamma$ -rays have unequal energies which are determined by the relativistic Lorentz transformation. To determine the observed  $\gamma$ -ray energy, let  $\gamma_\pi$  and  $\beta_\pi$  refer to the energy and velocity of the parent  $\pi^0$  meson in the observer's system. Let us also define the energy  $\nu = m_\pi c^2/2$ . Then the energies of the  $\gamma$ -rays in the observer's system are given by the Doppler relation

$$E_{\gamma^{1,2}} = \nu \gamma_\pi (1 \pm \beta_\pi \cos \theta) \quad (39)$$

where  $\theta$  is the angle between the  $\gamma$ -ray and the axis of the transformation in the pion rest system. The  $\pm$  sign applies because the  $\gamma$ -rays come off at opposite directions in the pion rest system.

Since there is no preferred direction to the decay in the pion rest system, the distribution in  $\cos \theta$  is isotropic, i.e., the distribution function

$$f(\cos \theta) = \text{const.} \quad (40)$$

and therefore, for a given value of  $\gamma_\pi \beta_\pi$

$$f(E_\gamma | E_\pi) = \text{const.} \quad (41)$$

The extreme upper and lower limits on the  $\gamma$ -ray energy in the observers system,  $E_u$  and  $E_l$  respectively, are defined by letting  $\cos \theta = 1$  in equation (39). We then find

$$E_u = \nu \gamma_\pi (1 + \beta_\pi) \quad (42)$$

and

$$E_l = \nu \gamma_\pi (1 - \beta_\pi)$$

and since  $\gamma_\pi = (1 - \beta_\pi^2)^{-1/2}$ , it follows that  $E_u E_l = \nu^2$  or

$$\ln \nu = \frac{\ln E_u + \ln E_l}{2} \quad (43)$$

From equations (41) and (42), it follows that the normalized  $\gamma$ -ray energy distribution function from the decay of pions of energy  $E_\pi$  is given by

$$f(E_\gamma | E_\pi) = \begin{cases} (E_\pi^2 - M_\pi^2 c^4)^{-1/2} & \text{for } E_l \leq E_\gamma \leq E_u \\ 0 & \text{otherwise} \end{cases} \quad (44)$$

and thus the total production rate from cosmic-ray protons with an energy spectrum  $I(E_p)$  is

$$q(E_\gamma) = 4\pi n \int_{E_{th}}^{\infty} dE_p I(E_p) \cdot 2\zeta(E_p) \quad (45)$$

$$\times \int_{E_{\pi, \min}}^{E_{\pi, \max}} dE_\pi \frac{\sigma(E_\pi | E_p)}{(E_\pi^2 - m_\pi^2 c^4)^{1/2}}$$

To find the limits on the  $E$  integration in equation (45), we note that the relation between the maximum  $\gamma$ -ray energy and  $E_\pi$  can be written as

$$E_\pi = E_u + \frac{\nu^2}{E_u} \quad (46)$$

and we may therefore reverse the criteria to note that  $\gamma$ -rays of energy  $E_\gamma$  may be produced by pions of energy as low as

$$E_{\pi, \min} = E_\gamma + \frac{\nu^2}{E_\gamma} \quad (47)$$

In the upper limit, we note that as  $E_\pi \rightarrow \infty$ ,  $\beta_\pi \rightarrow 1$  and from equation (42),  $E_\ell \rightarrow 0$ . This implies that as we increase the pion energy without limit, the allowed range of  $\gamma$ -rays produced expands in the lower limit to allow for all energies and pions of arbitrarily high energy can produce  $\gamma$ -rays of energy  $E_\gamma$ , i.e.,

$$E_{\pi, \max} \rightarrow \infty \quad (48)$$

and therefore equation (45) becomes

$$q(E_\gamma) = 8\pi n \int_{E_{\text{th}}}^{\infty} dE_p I(E_p) \zeta(E_p) \int_{E_\gamma + \nu^2/E_\gamma}^{\infty} dE_\pi \frac{\sigma(E_\pi | E_p)}{(E_\pi^2 - m_\pi^2 c^4)} \quad (49)$$

It follows from equations (43) and (44) that the  $\gamma$ -ray spectrum from an arbitrary distribution of energies in a decaying pion beam can be looked upon as the superposition of a number of rectangular distributions centered about  $\ln \nu$

on a logarithmic plot. Also, because the energy  $\nu$  is included within the allowed range of  $\gamma$ -ray energies, there is a maximum in the energy spectral distribution at this value. Intuitively, one can also see from equation (43) that the full spectrum from any arbitrary pion energy distribution should be symmetric about the maximum at  $\ln \nu$  on a logarithmic plot. These characteristics can be rigorously proven (Stecker 1971a). The differential  $\gamma$ -ray energy spectrum calculated for galactic cosmic-ray interactions per unit path length and target nucleon density is shown in Figure 3 calculated from a two-component kinematical model for pion production in high-energy cosmic ray interactions (Stecker 1970). The integral  $\gamma$ -ray energy spectrum is shown in Figure 4 along with calculations by Cavallo and Gould (1971) based on a different kinematical model. These spectra have been normalized to compare the shapes obtained. The wiggles in both spectral calculations represent artifacts of the kinematical models assumed and should not be taken too seriously. The shapes of the two spectra are in good agreement and probably represent an accurate approximation to reality within the uncertainty indicated by the wiggles.

Various other secondary products of high-energy cosmic-ray interactions such as other mesons, hyperons and excited nucleon states contribute to the overall cosmic  $\gamma$ -ray spectrum, particularly at high energies. However, their total contribution to the production rate is relatively minor. The kinematics of these reactions is, in general, much more complicated than in the case of pion decay and has been thoroughly discussed elsewhere (Stecker 1971a). Figure 5,

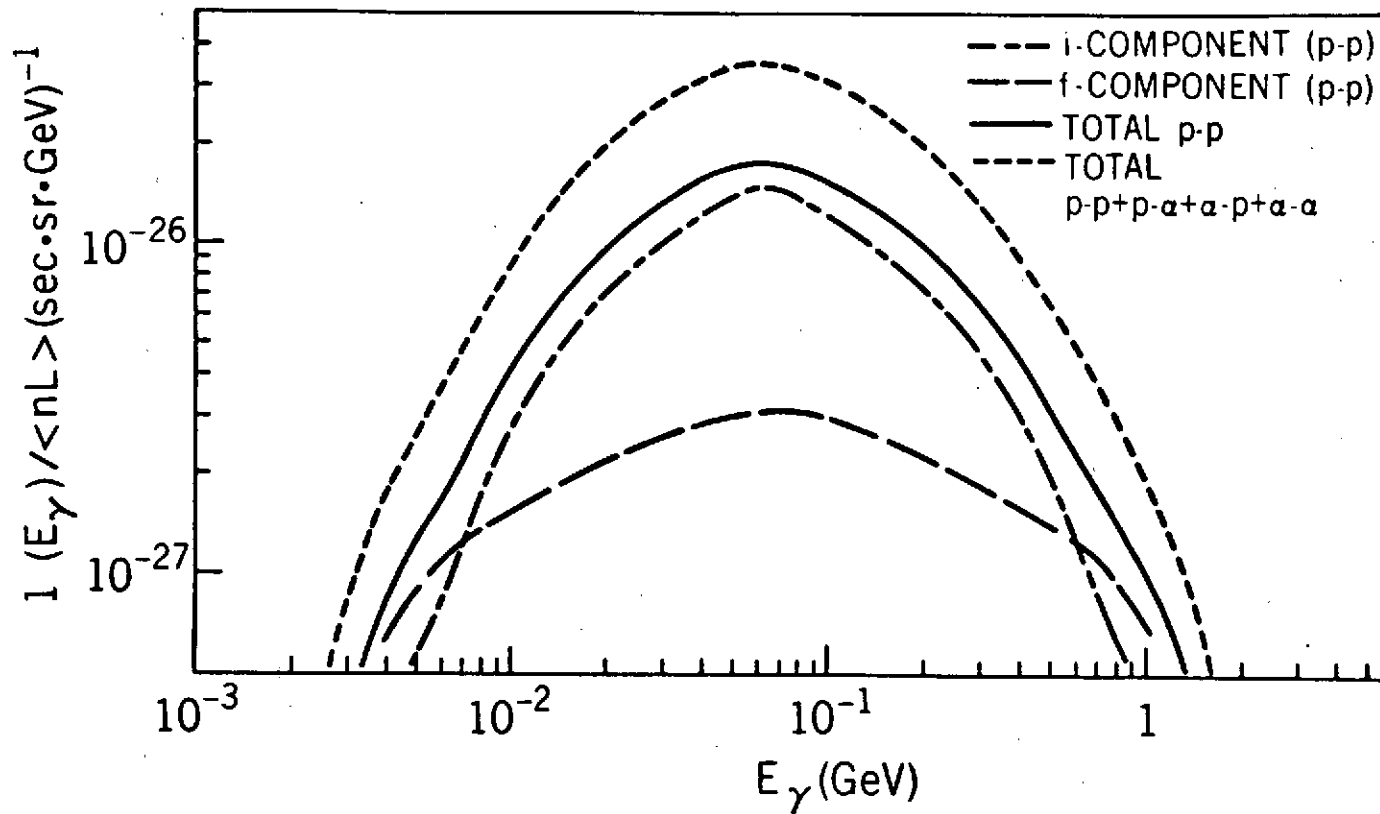


Figure 3. The calculated differential production spectrum of  $\gamma$ -rays produced in cosmic-ray interactions in the galaxy based on the "isobar (i) -plus-fireball (f)" model of Stecker (1970).

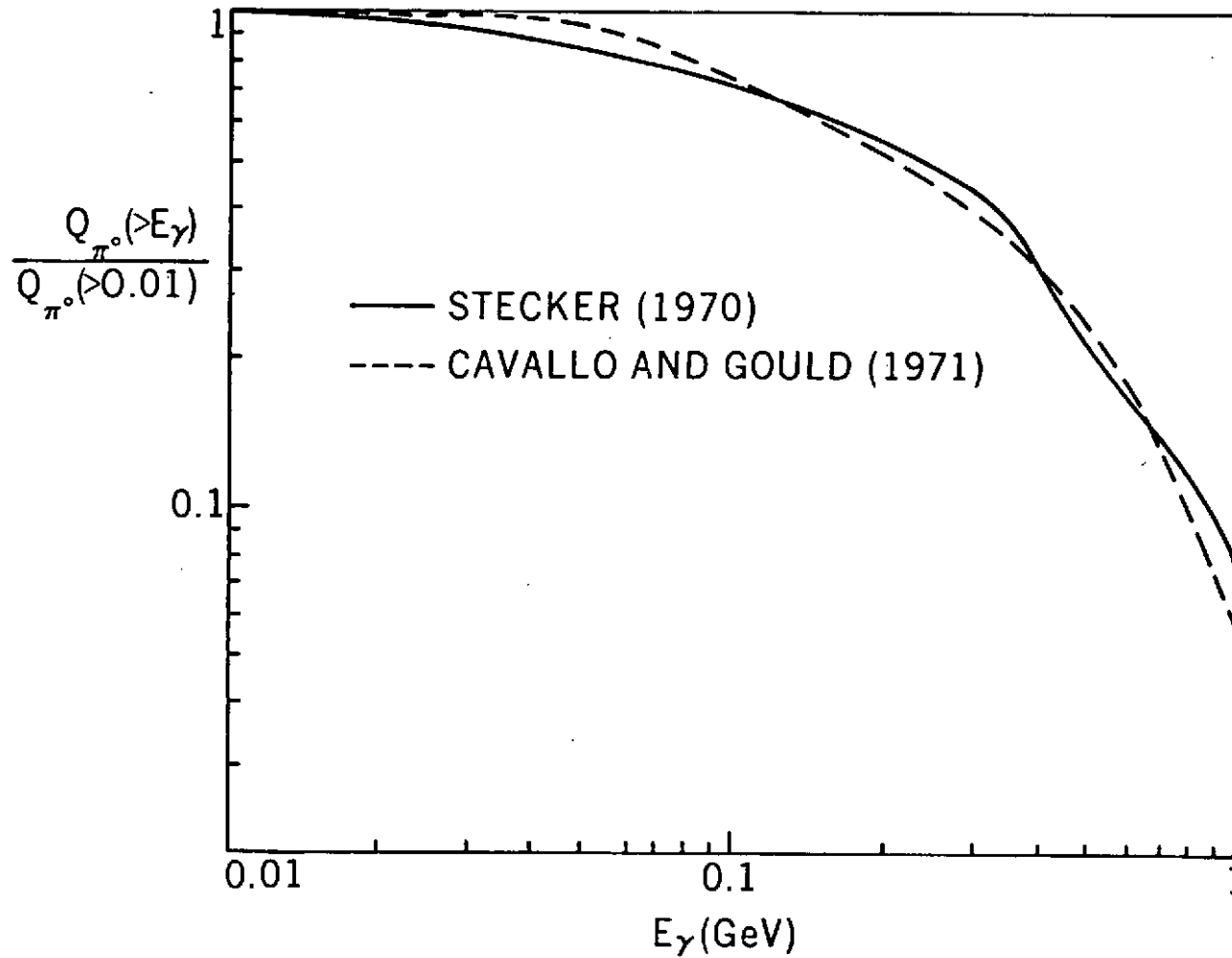


Figure 4. A comparison of the shapes of the integral galactic pion-decay energy spectra calculated by Stecker (1970) and Cavallo and Gould (1971). The total production rate is normalized to unity.

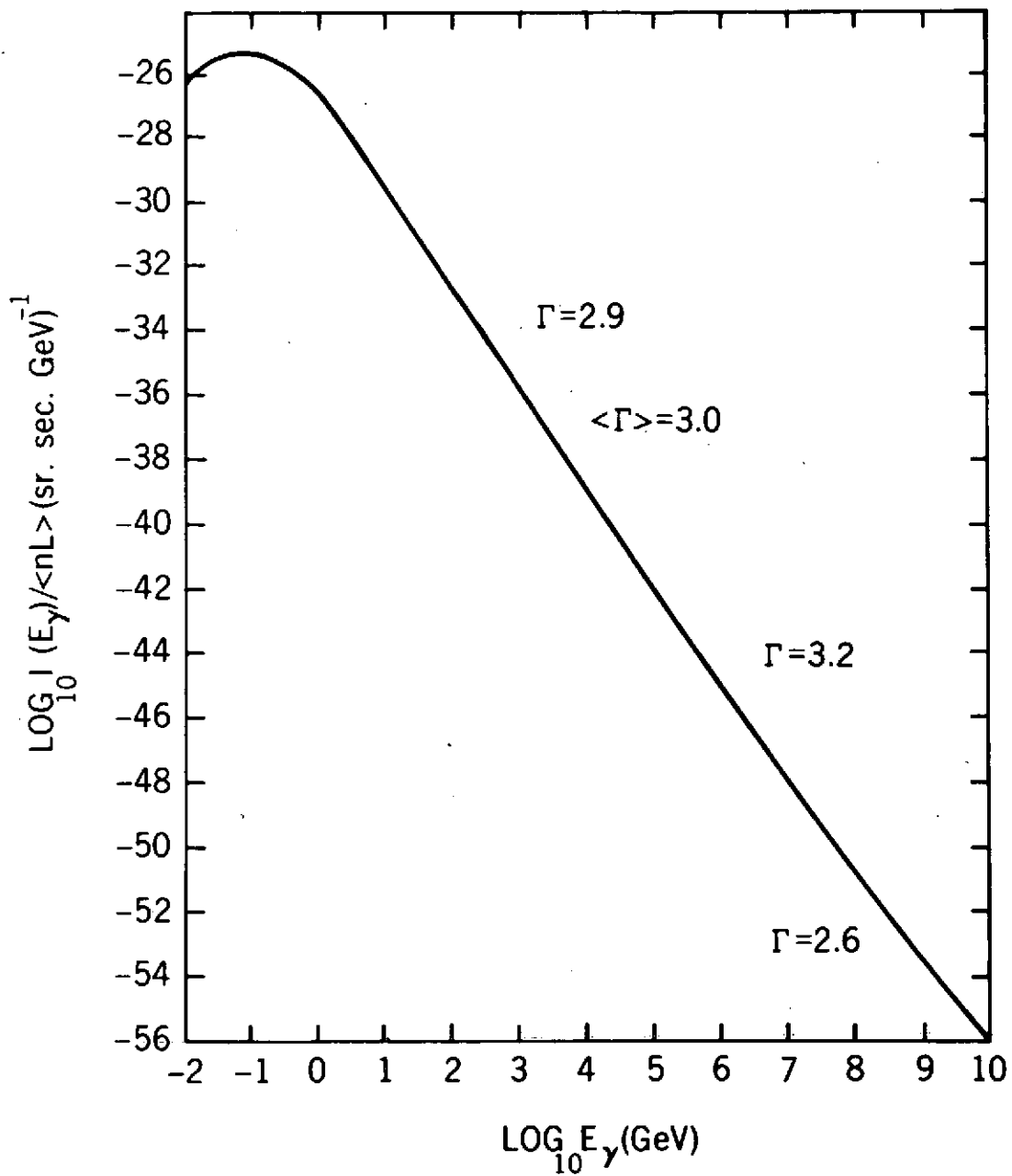


Figure 5. Total calculated galactic  $\gamma$ -ray production spectrum from cosmic-ray interactions (Stecker 1971a).

taken from Stecker (1971a) shows the total  $\gamma$ -ray spectrum calculated for all secondary particles produced by interactions of cosmic rays with interstellar gas in the galaxy.

#### E. Nucleon-Antinucleon Annihilations

If antimatter exists in significant quantities in the universe, secondary particles can result from the annihilation of nucleons and antinucleons. Of these secondaries, the most significant for  $\gamma$ -ray production again are the  $\pi^0$  mesons. Thus, the resultant  $\gamma$ -ray production spectrum is also symmetric about 67.5 MeV on a logarithmic plot, but in this case it is also bounded by the limited rest-mass energy which can be released in the annihilation. Frye and Smith (1966) using accelerator data, and independently Stecker (1967, 1971a) using a theoretical pion production model for nucleon-antinucleon annihilation have calculated the resultant  $\gamma$ -ray spectrum from annihilations at rest. There is excellent agreement between the two calculations and the resultant spectrum is shown in Figure 6.

#### F. Form of the Spectrum from Pion Production at High Energies

It is interesting to examine the asymptotic form of the  $\gamma$ -ray spectrum to be expected from the decay of  $\pi^0$  mesons produced at energies above a few GeV by cosmic rays having a power-law spectrum  $\propto E_p^{-\Gamma}$ . In this case, we assume that the pion production cross section is constant and that the pion multiplicity rises as a power of the primary energy  $\propto E^a$ . We also assume that the average pion energy rises as  $E_p^b$ . We can then write the production function in the form

$$\sigma(E_\pi | E_p) = \sigma_0 E_p^a \delta(E_\pi - \chi_0 E_p^b) \quad (50)$$

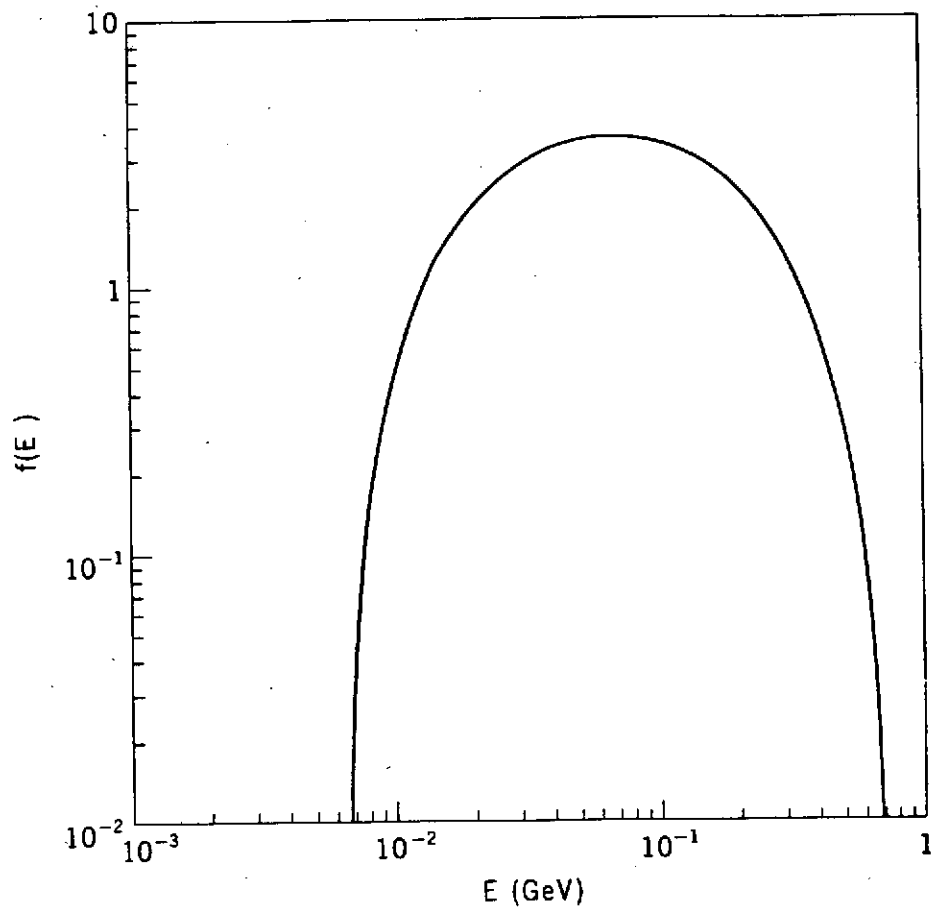


Figure 6. Normalized local differential  $\gamma$ -ray spectrum from  $p$ - $\bar{p}$  annihilation at rest (Stecker 1971a).

where the coefficients  $\sigma_0$  and  $\chi_0$  and the exponents  $a$  and  $b$  are taken to be constants. Equation (49) then reduces to

$$\begin{aligned}
q(E_\gamma) &= 8\pi n K_p \sigma_0 \int_{E_{th}}^{\infty} dE_p E_p^{a-\Gamma} \int_{E_\gamma}^{\infty} dE_\pi \frac{\delta(E_\pi - \chi_0 E_p^b)}{E_\pi} \\
&= 8\pi n K_p \sigma_0 \int_{(E_\gamma/\chi_0)^{1/b}}^{\infty} dE_p \frac{E_p^{-[(\Gamma+b)-a]}}{\chi_0} \\
&= \frac{8\pi n}{g} K_p \sigma_0 \chi_0^{[(g/b)-1]} E_\gamma^{-g/b}
\end{aligned} \tag{51}$$

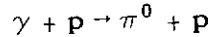
where

$$g \equiv [(\Gamma + b) - (a + 1)]$$

As can be seen from equation (51), the high-energy  $\gamma$ -ray spectrum produced by cosmic rays having an energy spectrum with index  $\Gamma$  is also a power-law, but one which is different and, in general, steeper than the primary spectrum. For example, in the case where  $\Gamma = 2.5$  and  $a = 1/4$ ,  $b = 3/4$  (the Fermi model for meson production), the  $\gamma$ -ray index  $g/b = 2.67$ . The primary and  $\gamma$ -ray spectra have the same index in the important case where a constant and large fraction of the primary energy of the cosmic ray is carried off by a single secondary which decays to produce a  $\pi^0$  meson. This corresponds to the case  $a = 0$ ,  $b = 1$  and therefore  $g/b = \Gamma$ .

### G. $\gamma$ -Rays from Photomeson Production at Ultrahigh Energies

A process which may be important in producing  $\gamma$ -rays of energies in the  $10^{19}$  eV range is that of photomeson production, i.e., reactions of the type



It is now generally believed that the universe is filled with thermal microwave radiation of temperature 2.7 K which is a remnant of the primordial big-bang. This temperature corresponds to an average photon energy of  $2.7kT = 6.4 \times 10^{-4}$  eV and an average photon number density of about 400 photons per  $\text{cm}^3$ . To an ultrahigh energy cosmic ray of energy in the  $10^{20}$  eV range, these microwave photons look like  $\gamma$ -rays of energy equal to hundreds of MeV. These energies are above the threshold for reaction (52) so that various ultrahigh energy mesons can be produced. One very important effect of this is the attenuation of ultrahigh energy cosmic rays in intergalactic space in  $10^8$ - $10^9$  years (Greisen 1966, Zatsepin and Kuz'min 1966, Stecker 1968a). A typical  $\gamma$ -ray produced by reaction (52) carries off about 10% of the primary energy of the cosmic ray (Stecker 1973b). The  $\gamma$ -rays produced may themselves be attenuated by pair production processes of the type



and this process, together with Compton scattering of the electrons and positrons by the 2.7 K radiation may lead to a cascade process which has been treated in detail by Wdowczyk, et al. (1972) and Stecker (1973b).

### 3. $\gamma$ -Ray Absorption Mechanisms

Various processes are of astrophysical importance in depleting  $\gamma$ -rays in the galaxy and the universe. By "absorption" we will mean not only those processes in which the  $\gamma$ -ray completely disappears, such as process (53), but also those processes in which the  $\gamma$ -ray is scattered out of the energy range of interest as can occur in the case of Compton scattering.

We will consider two basic categories of absorption processes: absorption in matter and absorption through interactions with radiation. The later process is of importance because of the existence of the 2.7 K thermal universal radiation field.

#### A. Absorption through Interactions with Radiation

Let us first consider the effects of the universal radiation field on the intensity of cosmic  $\gamma$ -rays. The attenuation process of importance here is the pair-production process (53). This process can only take place if the total energy of the photons in the C.M.S. of the interaction is greater than or equal to  $2mc^2$ . The cross section for reaction (53) can be calculated using quantum electrodynamics and a derivation may be found in Jauch and Rohrlich (1955). The importance of reaction (53) was first pointed out by Nikishov (1961) in considering interactions of  $\gamma$ -rays with ambient starlight photons and with the discovery of the universal radiation Gould and Schröder (1966, 1967a, b) and Jelly (1966) were quick to point out the capacity of the universe to  $\gamma$ -rays of energy above  $10^{14}$  eV.

Stecker (1969b) and Fazio and Stecker (1970) generalized these calculations by including cosmological effects.

In discussing reaction (53), we will generally follow the discussion of Gould and Schröder (1967a, b) with one important difference. At the time Gould and Schröder published their papers, it was generally thought that the universal radiation field had a somewhat higher temperature than the presently accepted 2.7 K. Therefore, the Gould and Schröder results have been corrected here to correspond to a 2.7 K radiation field.

Denoting C.M.S. quantities by primes and noting that for reaction (53)

$$E'_+ = E'_- = E'_e \quad (54)$$

we can determine the threshold energy for the reaction by noting that the relativistic four-momentum invariance condition in this case reduces to the form

$$\begin{aligned} (2E'_e)^2 &= (E_{2.7} + E_\gamma)^2 - |(\vec{p}_{2.7}c + \vec{p}_\gamma c)|^2 \\ &= (E_{2.7}^2 + 2E_{2.7}E_\gamma + E_\gamma^2) - (E_{2.7}^2 + E_\gamma^2 - 2E_{2.7}E_\gamma \cos \theta) \quad (55) \\ &= 2E_{2.7}E_\gamma(1 - \cos \theta) \end{aligned}$$

At threshold, both the electron and positron are produced at rest in the C.M.S. of the interaction. The minimum energy required corresponds to a head-on collision ( $\cos \theta = -1$ ). Equation (55) then reduces to the relation

$$E_{\gamma, \text{th}} = \frac{m_e c^2}{E_{2.7}} \quad (56)$$

If we consider a typical blackbody photon to have an energy of approximately  $10^{-9}$  MeV, then from (56) we find a threshold energy of approximately  $2.5 \times 10^8$  MeV for reaction (53). However, this threshold is somewhat blurred due to the fact that the blackbody photons are not all at the same energy but have a Bose-Einstein distribution given by the well-known relation

$$n(E_{2.7}) = \frac{1}{\pi^2 \hbar^3 c^3} \frac{E_{2.7}^2}{1 - e^{-E_{2.7}/kT}} \quad (57)$$

and also various possible values of  $\cos \theta$  must be allowed for.

The cross section for reaction (53) is given by (Jauch and Rohrlich, 1955)

$$\sigma(E_{2.7}, E_{\gamma}) = \frac{\pi}{2} \left( \frac{e^2}{m_e c^2} \right)^2 (1 - \beta_e'^2) \left[ (3 - \beta_e'^4) \ln \frac{1 + \beta_e'}{1 - \beta_e'} - 2\beta_e'(2 - \beta_e'^2) \right] \quad (58)$$

where the C.M.S. velocity of the electron (positron) is given by

$$\beta_e' = \left( 1 - \frac{m_e^2 c^4}{E_{2.7} E_{\gamma}} \right)^{1/2} \quad (59)$$

The absorption coefficient is then

$$\kappa_{\gamma\gamma}(E_{\gamma}) = \iint dE_{2.7} d\theta \frac{\sin \theta}{2} n(E_{2.7}) \sigma(E_{2.7}, E_{\gamma}) (1 - \cos \theta) \quad (60)$$

Gould and Schröder (1967a, b) have reduced equation (60) to the form

$$\kappa_{\gamma\gamma}(E_{\gamma}) = \frac{\alpha^3}{\pi} \left( \frac{m_e c^2}{e^2} \right) \left( \frac{kT}{m_e c^2} \right)^3 f(\nu) \quad (61)$$

where

$$\nu \equiv \frac{(m_e c^2)}{E_\gamma kT} \quad (62)$$

They find that the function  $f(\nu)$  has a maximum value  $\simeq 1$  at  $\nu \simeq 1$  and that  $f(\nu)$  has the asymptotic forms given by

$$f(\nu) \rightarrow \frac{\pi^3}{3} \nu \ln \left( \frac{0.117}{\nu} \right) \text{ for } \nu \ll 1$$

(63)

and

$$f(\nu) \rightarrow \left( \frac{\pi\nu}{4} \right)^{1/2} e^{-\nu} \left( 1 + \frac{75}{8\nu} + \dots \right) \text{ for } \nu \gg 1.$$

They have also calculated  $\kappa_{\gamma\gamma}$  for  $\gamma$ -ray interactions with various photon fields in interstellar space. The results of their numerical calculation are shown in Figure 7.

#### B. Absorption by Interactions with Matter

There are two types of interactions of importance to consider here. The first is the Compton scattering interaction



which we have discussed in connection with  $\gamma$ -ray production.

Electrons play the dominant role in the Compton scattering of  $\gamma$ -rays. For  $\gamma$ -rays of energy  $E_\gamma \gg mc^2$ , almost all of the energy of the  $\gamma$ -ray is absorbed and then we can consider that the  $\gamma$ -ray has disappeared.

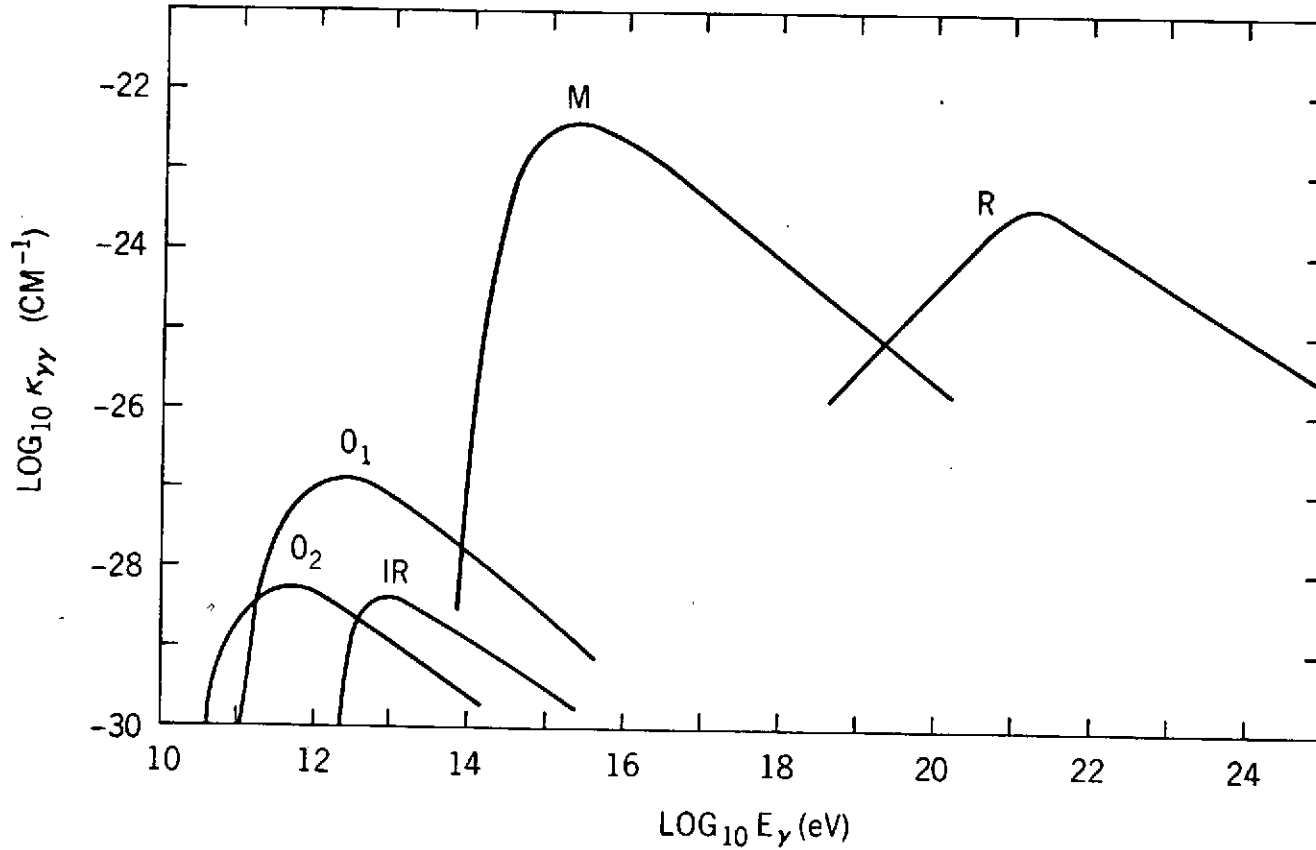


Figure 7. Absorption probability per unit distance by  $\gamma + \gamma \rightarrow e^+ + e^-$  as a function of photon energy for  $\gamma$ -rays passing through various universal radiation fields. The contributions from the optical ( $O_1$  and  $O_2$ ) infrared (IR) 2.7 k blackbody microwave (M) and radio (R) fields are shown. Absorption at lower energies from X-rays is negligible.  $O_1$  represents the contribution from the light of population II stars;  $O_2$  that from population I stars (from Gould and Schröder 1967a, b); M is corrected to 2.7 K (Stecker 1971a).

In some cases it is useful to define an "absorption cross section",  $\sigma_a$ , such that

$$\sigma_a = \left( \frac{\Delta E_\gamma}{E_\gamma} \right) \sigma_c \quad (65)$$

where  $\Delta E_\gamma$  is the average amount of energy transferred from the gamma-ray to the electron. It is then found that (Heitler, 1954) with  $\epsilon \equiv \epsilon_\gamma/m_e c^2$

$$\sigma_a = \epsilon \sigma_c \quad \text{for } \epsilon \ll 1 \quad (66)$$

and

$$\sigma_a = \sigma_c \left[ \frac{\ln 2\epsilon - \frac{5}{6}}{\ln 2\epsilon + \frac{1}{2}} \right] \quad \text{for } \epsilon \gg 1 \quad (67)$$

The second type of gamma-ray absorption process in matter that we must consider involves the conversion of a gamma-ray into an electron-positron pair in the electrostatic field of a charged particle or nucleus. If we designate such a charge field by the symbol CF, such an interaction may be symbolically written as



The conversion interaction, or pair-production as it is usually called, has a cross section that involves an extra factor of the fine structure constant,  $\alpha = e^2/\hbar c$ , since it involves an intermediate interaction with an electrostatic field. At nonrelativistic energies, this cross section is a complicated function of energy which must be determined numerically (see Heitler (1954) for further

details) however a closed analytic approximation for this cross section may be given for energies greater than 1 MeV, which happily corresponds to the energy region where the pair-production cross section becomes more important than the Compton scattering cross section in determining the gamma-ray mass absorption coefficient for hydrogen gas.

For pair-production in the field of a nucleus of atomic number  $Z$ , the cross section for reaction (68) is given by

$$\sigma_p = \alpha \left( \frac{e^2}{m_e c^2} \right)^2 \left( \frac{28}{9} \ln 2\epsilon - \frac{218}{27} \right) Z^2 \quad (69)$$

$$\text{for } 1 \ll \epsilon \ll \alpha^{-1} Z^{-1/3},$$

which is the energy region where electron screening of the nuclear charge field may be neglected. The no-screening case, of course, also holds for an ionized gas (plasma).

In the energy region where the complete-screening approximation is valid,

$$\sigma_p = \alpha \left( \frac{e^2}{m_e c^2} \right)^2 \left[ \frac{28}{9} \ln(183 Z^{-1/3}) - \frac{2}{27} \right] Z^2 \quad (70)$$

$$\text{for } \epsilon \gg \alpha^{-1} Z^{-1/3}.$$

The threshold energy for pair production in the field of an atomic nucleus is, of course  $2m_e c^2$ . In the case of pair production in the field of atomic electrons, the threshold energy for is  $4m_e c^2$ . Above this energy, the pair production cross

section must be modified to include the additional contribution of the electrons and this may be done approximately by making the replacement

$$Z^2 \rightarrow Z^2(1 + \xi^{-1}Z^{-1}) \quad (71)$$

in equations (69) and (70), where the quantity  $\xi$  varies from  $\simeq 2.6$  at  $E_\gamma \simeq 6.5$  MeV to  $\simeq 1.2$  at  $E_\gamma \simeq 100$  MeV. For gamma-ray energies above 200 MeV,  $\xi \simeq 1$  and the pair production cross section has the approximately constant value of  $1.8 \times 10^{-26}$  cm<sup>2</sup>, according to the results of Trower (1966). The values of the various cross sections for  $\gamma$ -ray absorption in matter, as discussed in this section, are shown in Figure 8.

#### 4. $\gamma$ -Rays Observed from the Galaxy

In this section, we will now turn our attention to the interpretation of presently existing observations of cosmic  $\gamma$ -radiation. Because of lack of time, we will restrict ourselves to two important topics, galactic diffuse  $\gamma$ -radiation and the diffuse  $\gamma$ -ray background. This means we are omitting a discussion of such important topics as 1. the crab nebula and other possible point sources of  $\gamma$ -rays, 2. positron annihilation in the galaxy and nuclear de-excitation  $\gamma$ -ray lines, 3. cosmic soft  $\gamma$ -ray bursts, 4.  $\gamma$ -rays from supernovae, and 5. solar  $\gamma$ -rays.

Some of these important topics will be touched upon here by Professor Pinkau, Professor Colgate and Professor Reeves. I would also like to recommend the discussion of some of these topics in the reviews published in the Proceedings of the International Symposium and Workshop on Gamma Ray Astrophysics held at NASA Goddard Space Flight Center last May (Stecker and Trombka 1973).

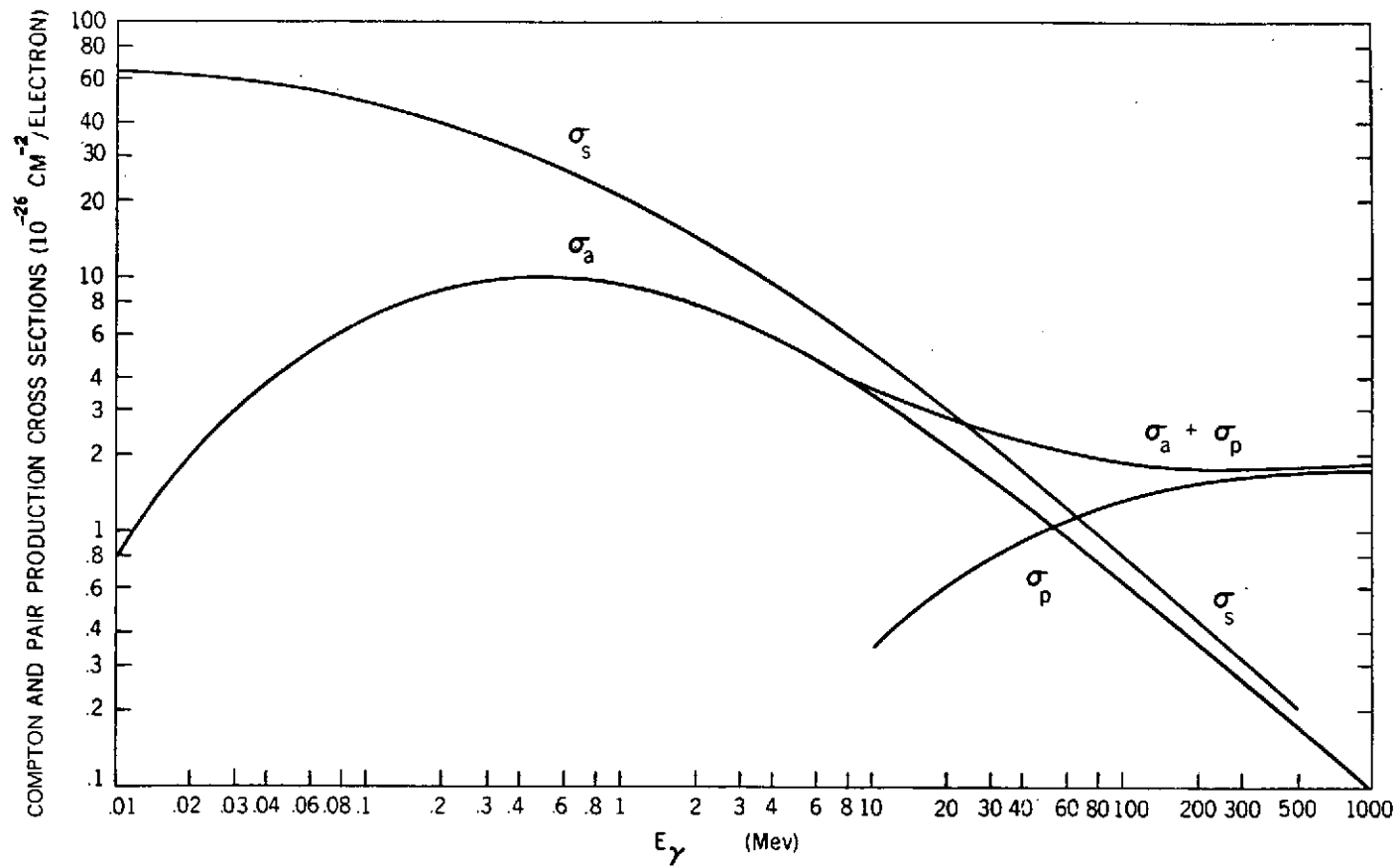


Figure 8. Compton scattering ( $\sigma_s$ ), Compton absorption ( $\sigma_a$ ), pair-production ( $\sigma_p$ ) and total ( $\sigma_a + \sigma_p$ ) cross sections as a function of  $\gamma$ -ray energy for absorption of  $\gamma$ -rays in hydrogen gas (based in part on work of Nelmes, 1953) from Stecker (1971a).

The galaxy is a roughly disk-shaped collection of about  $10^{11}$  stars and a lesser mass of gas and dust having a radial dimension of about 15 kpc. The half-width of the gas disk, according to 21cm radio measurements of atomic hydrogen, is about 100 pc with a general tendency for a somewhat larger thickness in the outer regions. The sun is located approximately 2/3 of the way out from the center at a radial distance of about 10 kpc.

Apart from these general considerations, it should be kept in mind at all times that the galaxy is a very complex object whose detailed general features such as spiral arms have not been charted to undisputed accuracy. Indeed, the required accurate observations to accomplish this are in some situations exceedingly difficult if not outright impossible.

Radio astronomers have for years been mapping accumulations and features involving relatively high densities of atomic hydrogen in the galaxy. They do this by studying the 21cm emission line of atomic hydrogen caused by the hyperfine splitting of the  $1^2S$  ground state of the hydrogen atom as a result of the interaction between the magnetic moments of the proton and the electron in the atom. The separation between these levels is very small because the magnetic moment of the proton is almost 2000 times smaller than that of the electron owing to its proportionally larger mass. The frequency of the emission corresponding to this energy-level separation is in the radio range at 1420 MHz.

Radio source intensities are usually given in terms of brightness temperature  $T_b$  (Kelvin) corresponding to the emission temperature of a blackbody on the

Rayleigh-Jeans (low frequency) side of the Planck distribution. Thus

$$T_b(\nu) = \frac{I(\nu) c^2}{2\nu^2 k} \quad (72)$$

Sometimes these intensities are given in terms of antenna temperature which is equal to the brightness temperature multiplied by antenna efficiency. For a gas radiating at constant temperature  $T$  but with opacity  $\kappa$ , the brightness temperature measured along the line-of-sight in a given direction is

$$T_b = \int ds T e^{-\int_0^s \kappa ds'} = \int ds T e^{-\tau(s)} = T(1 - e^{-\tau}) \quad (73)$$

Thus, at small optical depths  $\tau \ll 1$ ,

$$T_b \simeq T\tau \quad (74)$$

and at large optical depths  $\tau \gg 1$ ,

$$T_b \simeq T \quad (75)$$

The opacity  $\kappa$  can be expressed as the atomic opacity  $\alpha$  times the atomic density  $n$  of absorbing atoms.

Consider an atom with two state levels, the upper level  $u$  and a lower level  $\ell$ . Then according to Boltzmann's law the proportion in each level as a function of  $T$  is

$$\frac{n_u}{n_\ell} = \frac{g_u}{g_\ell} e^{-h\nu_0/kT} \quad (76)$$

where  $\nu_0$  is the transition frequency and  $g_u$  and  $g_l$  are the statistical weights of the two levels. Thus, for the 21 cm transition where  $g_u = 3g_l$  (triplet to singlet)

$$\frac{n_u}{n_l} = 3e^{-h\nu_0/kT} \quad (77)$$

The total absorption coefficient

$$\kappa = an_l \left( 1 - \frac{n_u}{n_l} \frac{g_l}{g_u} \right) \quad (78)$$

where the second term takes account of a stimulated emission. From equation (76) this reduces to

$$\kappa = an_l (1 - e^{-h\nu_0/kT}) \simeq an_l \frac{h\nu_0}{kT} \text{ for } \frac{h\nu_0}{kT} \ll 1 \quad (79)$$

Thus, in the optically thin case, from equation (74).

$$T_b = T\tau = a \frac{h\nu_0}{k} \int n_l ds$$

which is proportional to the total number of atoms along the line-of-sight. In the case of 21 cm emission

$$T_b (21 \text{ cm}) = 5.49 \times 10^{-19} \int n_l ds \quad (80)$$

In general, however, it should be kept in mind that equation (80), which is valid for an optically thin gas, in general only provides a lower limit to the amount of gas along the line-of-sight.

A 21 cm map of the atomic hydrogen density as constructed by Garmire and Kraushaar (1964) and is shown in Figure 9.

In general, line emission is broadened in frequency by the Doppler shift effect of gas moving with various radial velocities  $v_\gamma = \beta_\gamma c$  along the line of sight. Then

$$\nu = \nu_0(1 + \beta_\gamma) \quad (82)$$

What is usually measured is a velocity profile determined by the frequency distribution of the line emission  $f(\nu')$  so that a distribution in brightness temperature versus velocity or frequency is constructed. Then from equation (81)

$$N_H = \int n_\ell ds = 1.82 \times 10^{18} \int T_b(\nu) d\nu \quad (83)$$

From the two dimensional distribution  $n(\ell, \nu)$  where  $\ell$  is galactic longitude, one can use a rotation model of the galaxy to construct a positional map of dense regions of atomic hydrogen. Such a map is shown in Figure 10 with some of the 21 cm atomic hydrogen "arms" of the galaxy named.

One can also plot a graph of the average hydrogen density seen in 21 cm emission as a function of galacto-centric distance in kpc. Such a plot is shown in Figure 11.

The galactic distribution of  $\gamma$ -ray emission was first mapped by Kraushaar, et al. (1972) on OSO-3 with rather limited resolution. More recently, the galactic distribution was remeasured with better angular resolution by Kniffen, et al.

# GALACTIC ATOMIC HYDROGEN

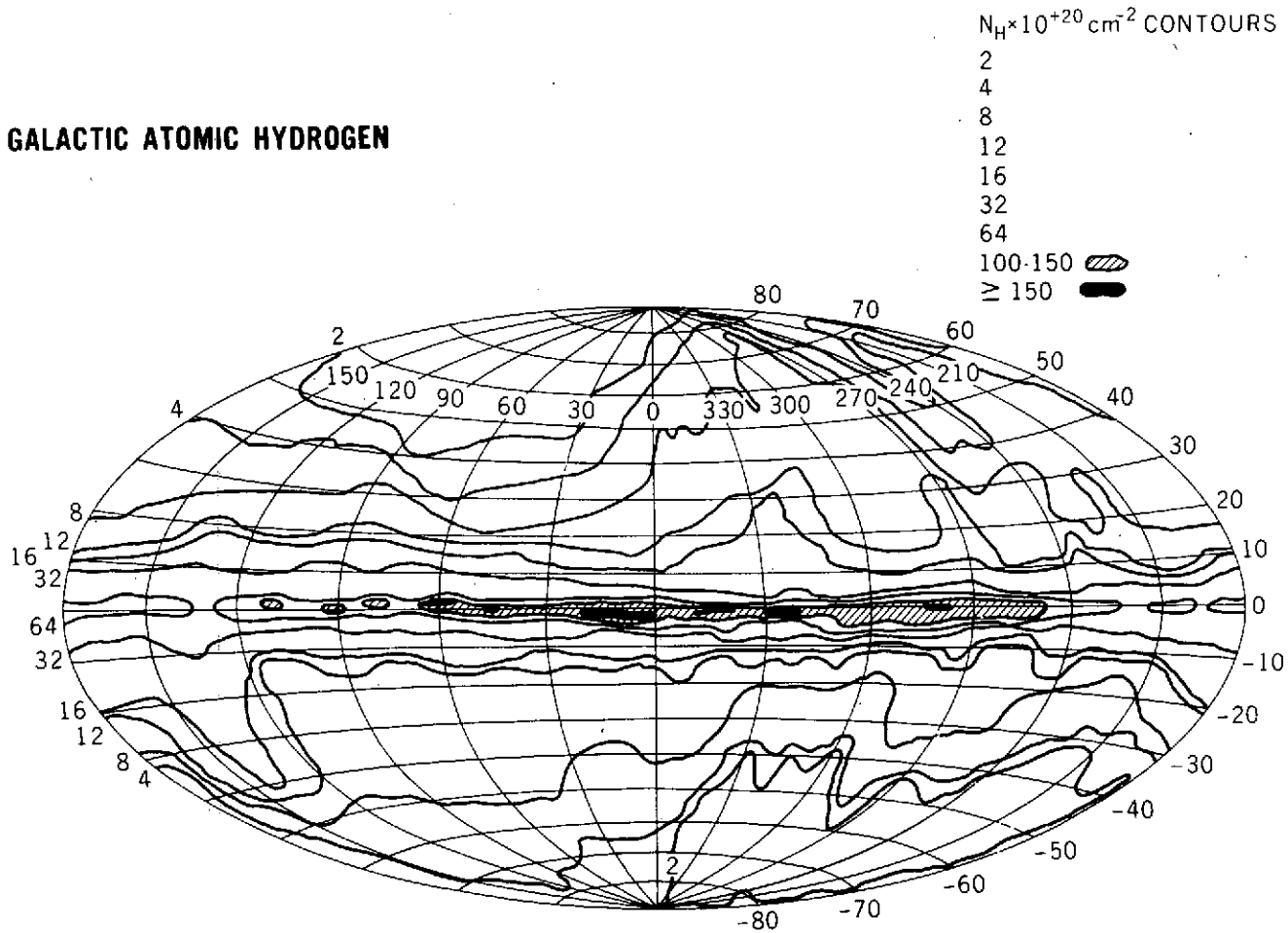


Figure 9. Contour map of  $N_H$ , the number of atomic hydrogen atoms per  $\text{cm}^2$  along the line of sight in galactocentric coordinates (from Garmire and Kraushaar (1964)).

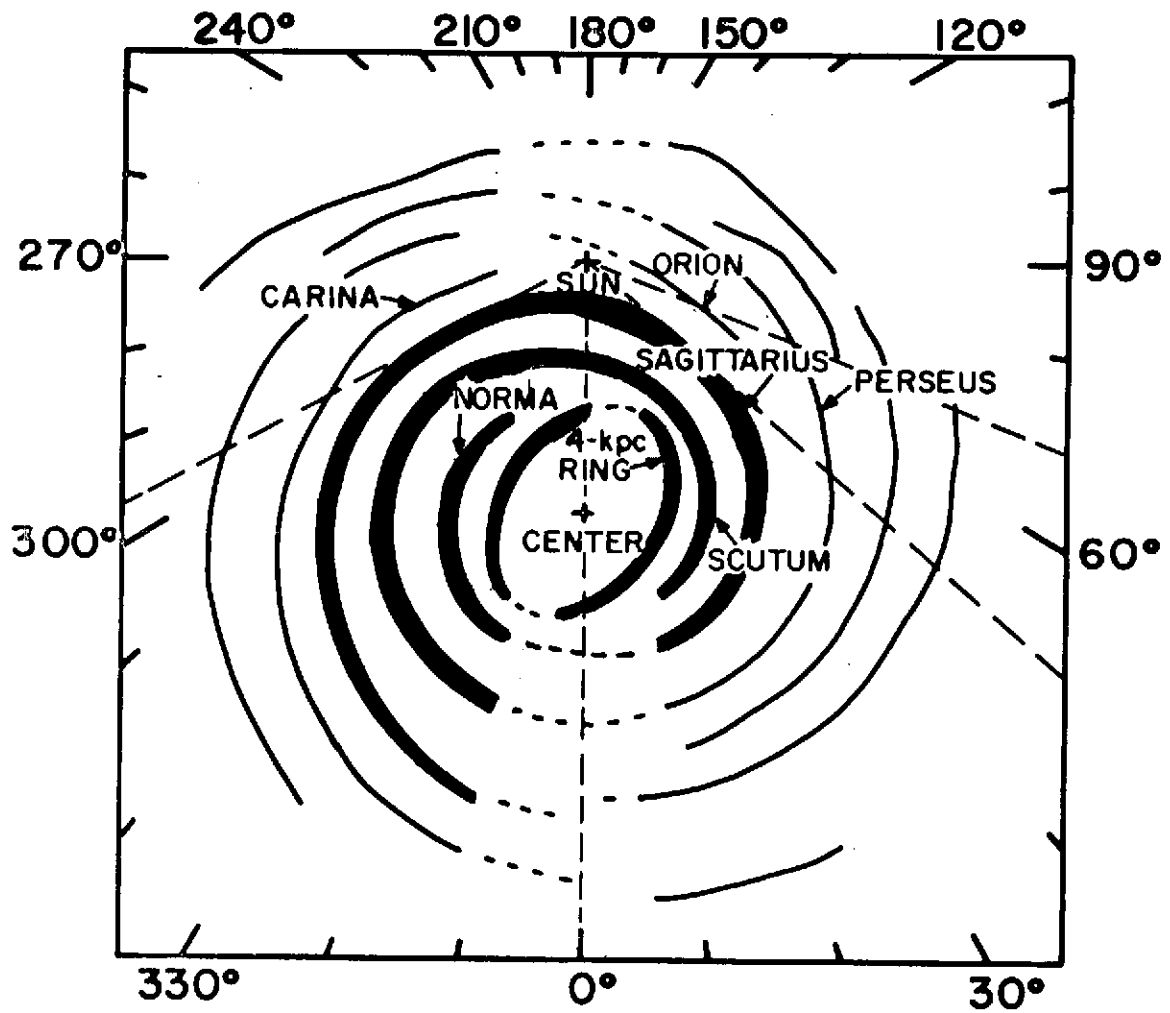


Figure 10. A smoothed spatial diagram of the locations of the maxima of the matter density deduced from the 21-cm neutral H line measurements and the density-wave theory by Simonson (preprint).

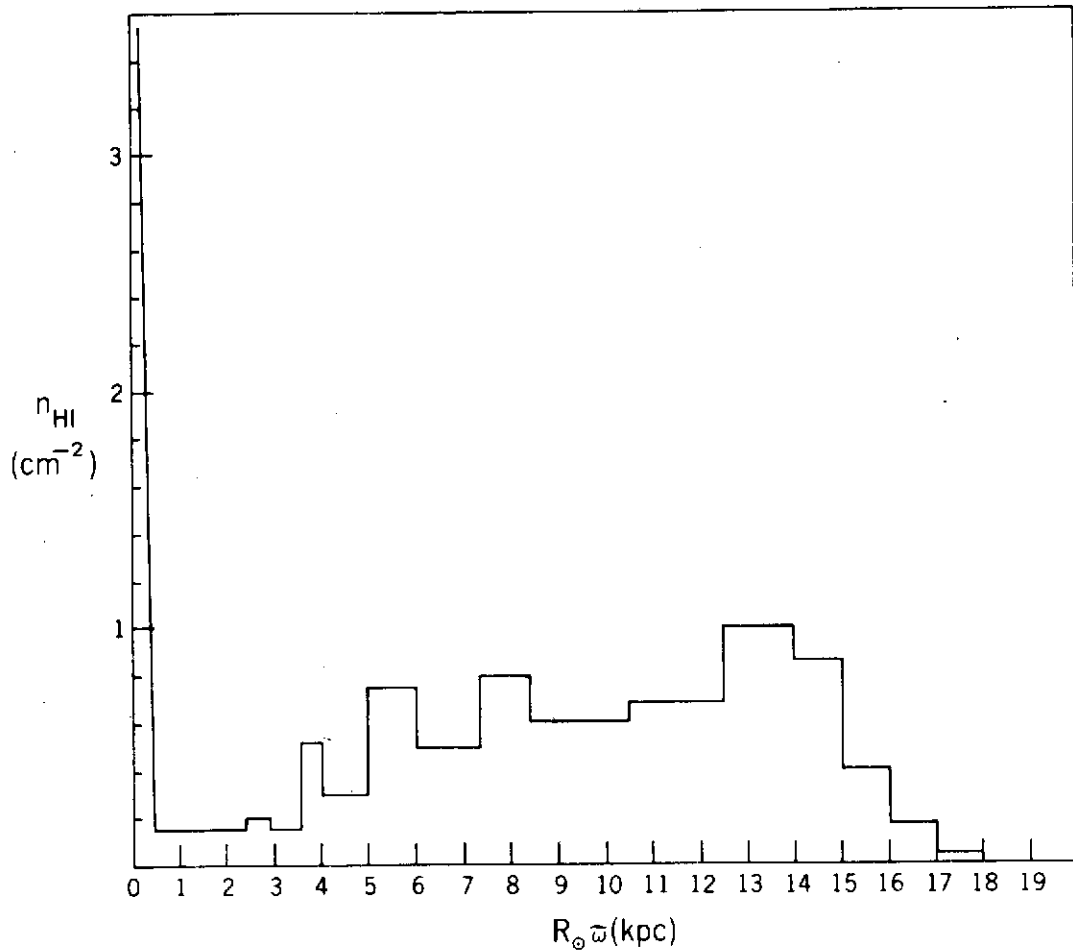


Figure 11. The neutral hydrogen density  $n_{\text{HI}}(\tilde{\omega})$  based on the discussion of Kerr (1969), Shane (1972), and Sanders and Wrixon (1973).

(1973) on SAS-2. The results of both measurements are shown in Figure 12. The map of Kniffen, et al. has recently been updated by the addition of new data having been analyzed and the updated distribution is shown in Figure 13 (Fichtel 1974).

The data from SAS-2 of  $\gamma$ -rays above 100 MeV shows radiation coming from the galactic disk. The galactic latitude distribution of the emission is shown in Figure 14. Figure 14 indicates that the radiation in the anticenter direction comes from within  $6^\circ$  of the galactic plane whereas that in the direction of the galactic center also is limited to within  $6^\circ$  with perhaps a particularly intense component restricted to within  $3^\circ$  of the plane. Since  $3^\circ$  was the angular resolution of the instrument, this narrow source could have a true width of less than  $3^\circ$  corresponding to a source distance of at least 2 to 4 kpc from the sun toward the inner galaxy. A two dimensional SAS-2 map of the galactic disk is shown in Figure 15.

Data obtained by Samimi, et al. (1974) on the latitude distribution of the galactic  $\gamma$ -radiation also indicate a width of  $3^\circ$  for most of the radiation.

The longitude data in Figure 13 show a broad flat region of intense emission within  $30^\circ$  to  $40^\circ$  of the galactic center on either side. This indicates that there is a large emission rate within 5 to 6 kpc of the galactic center.

Puget and Stecker (1974) have geometrically unfolded the SAS-2 distribution shown in Figure 12 and the resultant emissivity as a function of galactocentric distance is shown in Figure 16. Strong (1974) has performed a corresponding

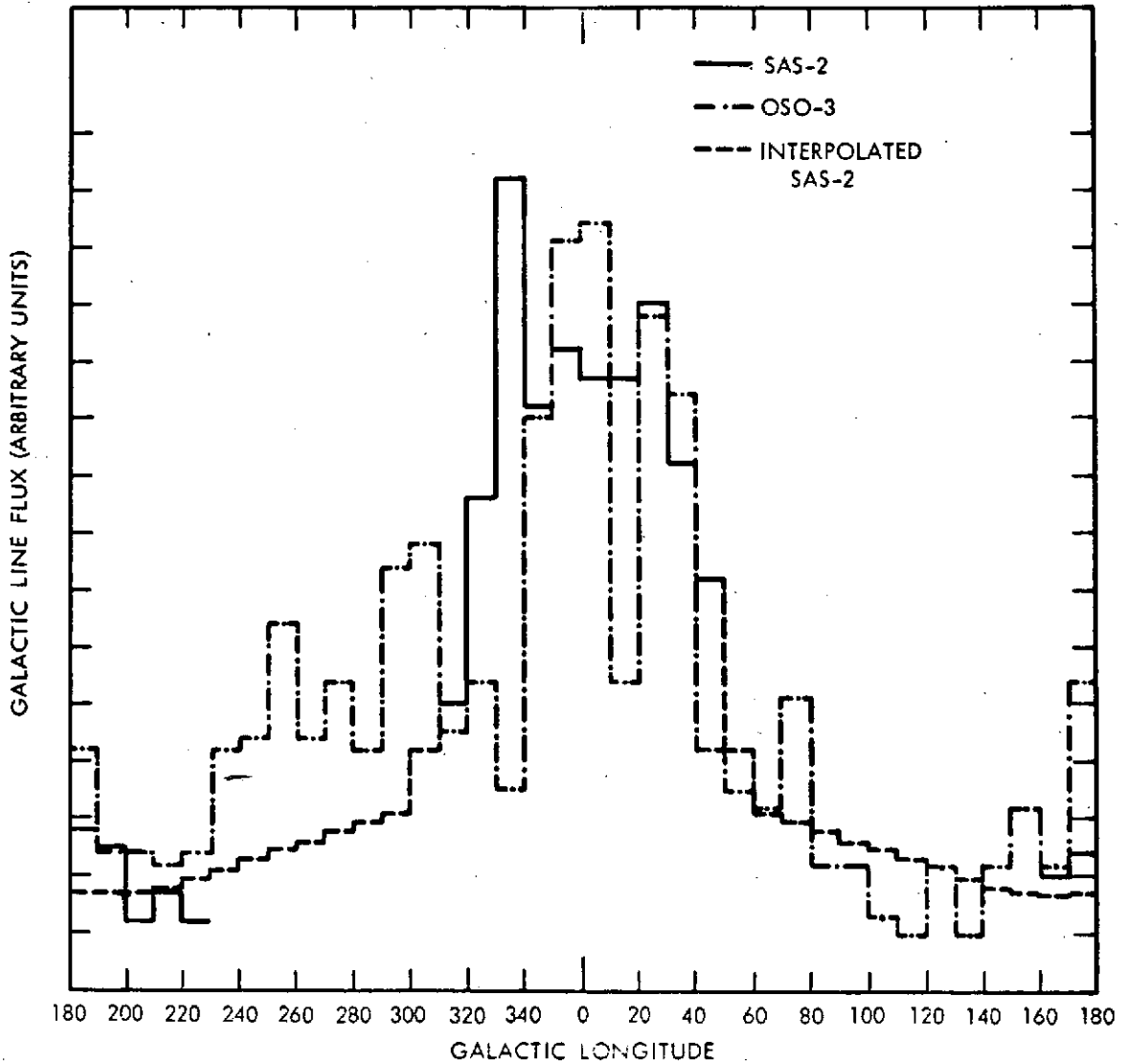


Figure 12. Distribution in galactic longitude of the galactic  $\gamma$ -ray line flux as observed by OSO-3 (Kraushaar, et al. 1972) and SAS-2 (Kniffen, et al. 1973) normalized arbitrarily for purposes of comparison. Statistical uncertainties quoted for these results (not plotted) are significantly greater for the OSO-3 results as compared with the SAS-2 results. The interpolation of the SAS-2 data was obtained on the assumption of a smooth average variation in the  $\gamma$ -ray production rate (Puget and Stecker 1974).

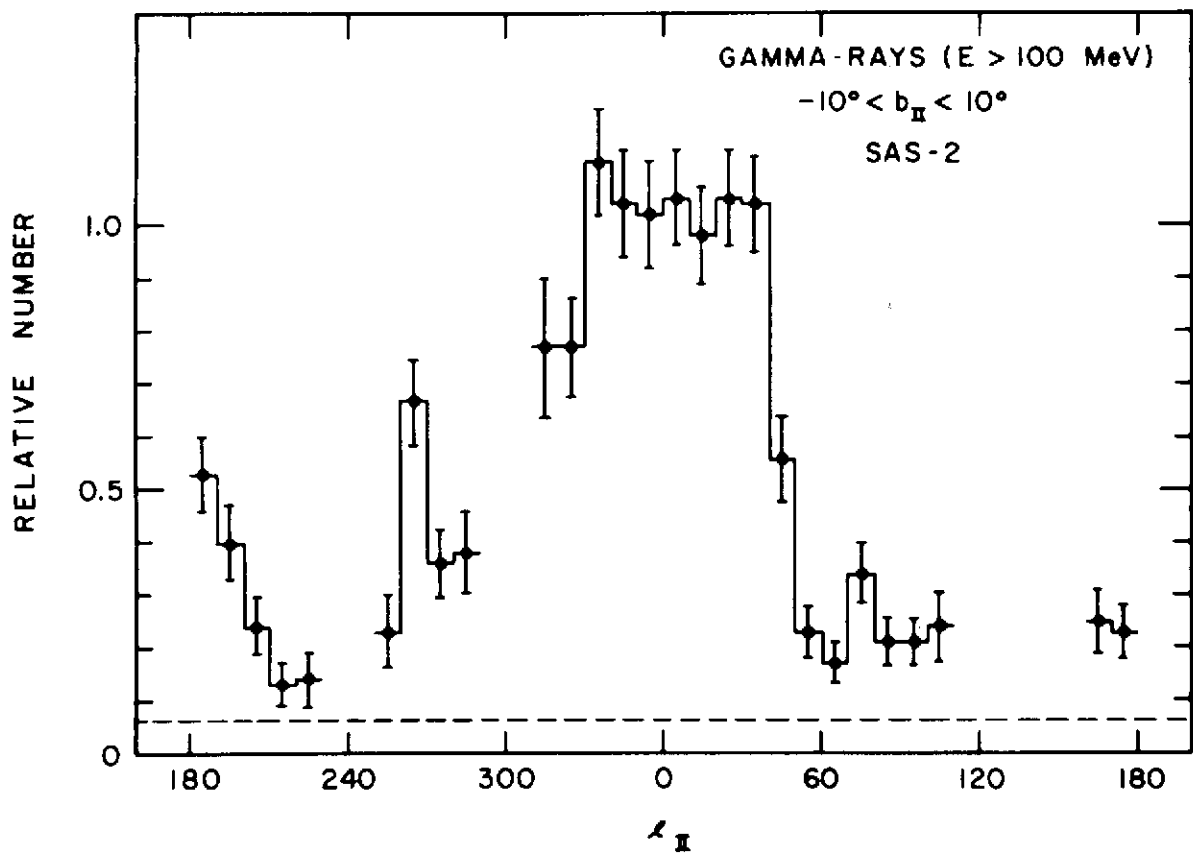


Figure 13. Distribution of high-energy ( $>100$  MeV) gamma-rays along the galactic plane. The diffuse background level is shown by a dashed line. The SAS-2 data are summed over  $|b^{II}| < 10^\circ$ . The ordinate scale is approximately in units of  $10^{-4}$  photons  $\text{cm}^{-2}$   $\text{rad}^{-1}$   $\text{sec}^{-1}$  (Thompson, et al. 1974).

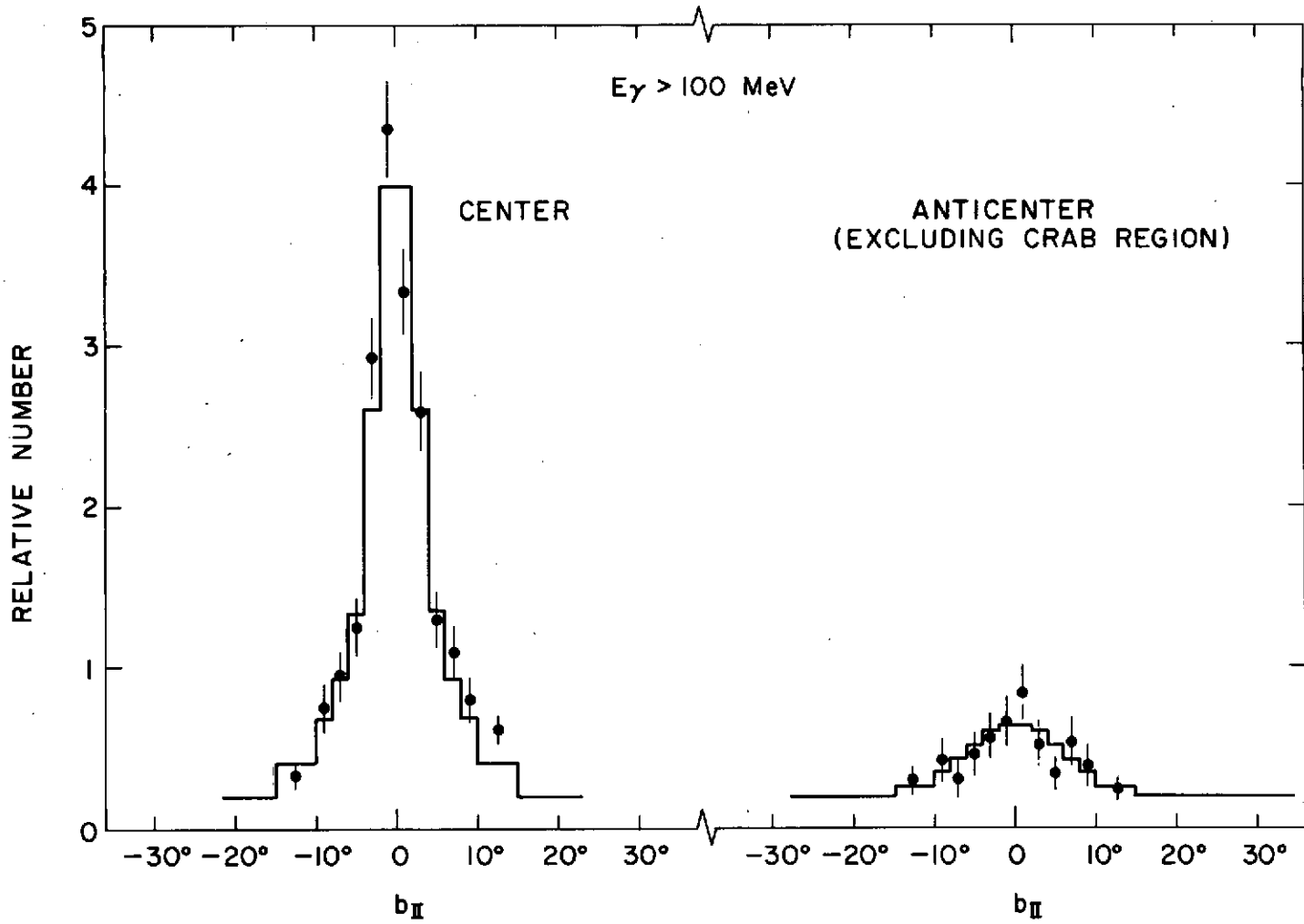


Figure 14a. Distribution of high-energy ( $> 100 \text{ MeV}$ ) gamma-rays summed over  $335^\circ < \ell_{II} < 25^\circ$  as a function of  $b_{II}$ . The solid line represents the sum of the two distributions with equal areas, one representing only the detector resolution, the other a gaussian with a width  $\sigma = 6^\circ$  (Thompson, et al. 1974). (b) Distribution of  $> 100 \text{ MeV}$  gamma-rays summed from  $90^\circ < \ell_{II} < 170^\circ$  and  $200^\circ < \ell_{II} < 270^\circ$  where data exists, (Thompson, et al. 1974).

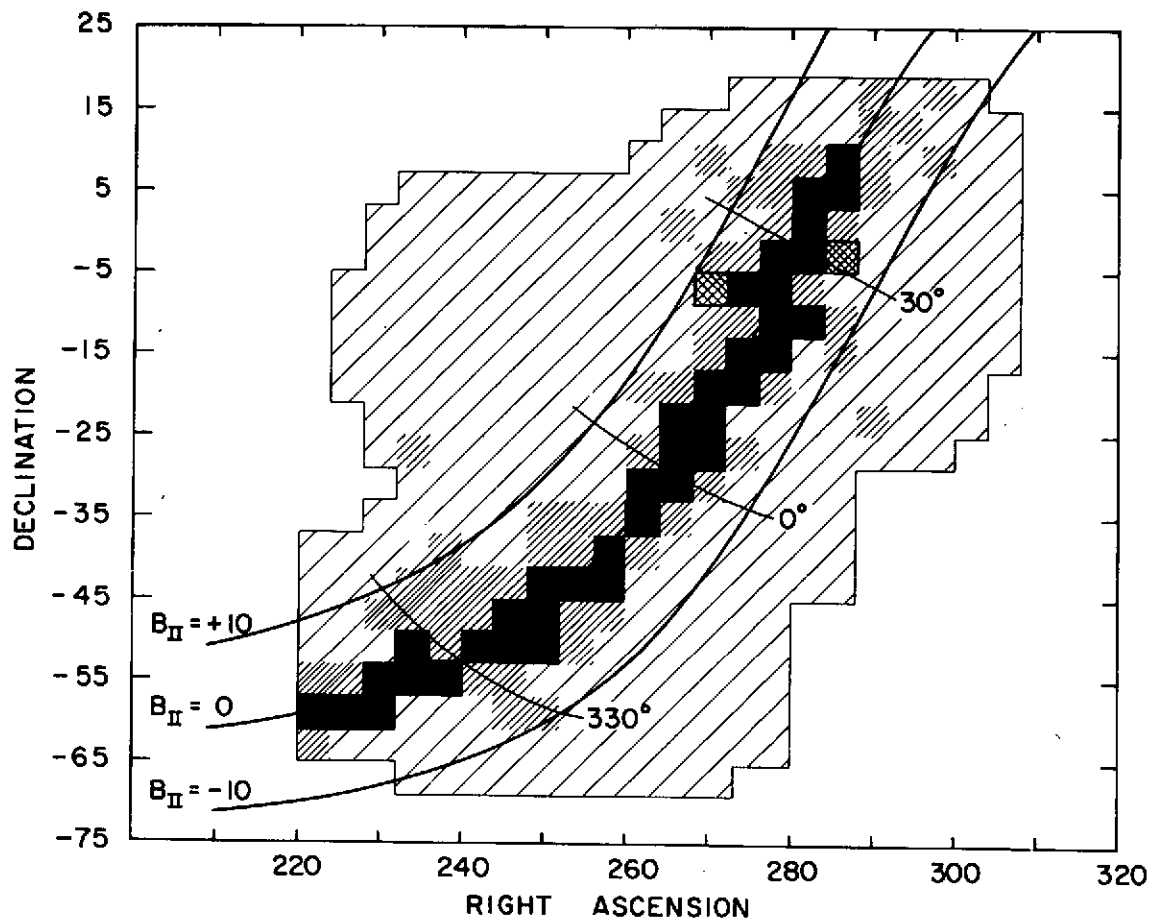


Figure 15. Schematic diagram of relative intensity of the gamma radiation above 100 MeV as deduced from preliminary data from SAS-2. Increasing shading indicates higher intensity, but no single ( $4^\circ \times 4^\circ$ ) box has sufficient numbers of gamma rays to justify statistically conclusions to be deduced for it alone. It is clear, however, that the galactic plane stands out sharply (Fichtel, Hartman, Kniffen, and Thompson, 1973\*).

\*"Gamma Ray Astronomy in the Time of SAS-2", invited talk 140 AAS Meeting Columbus, Ohio, June 1973.

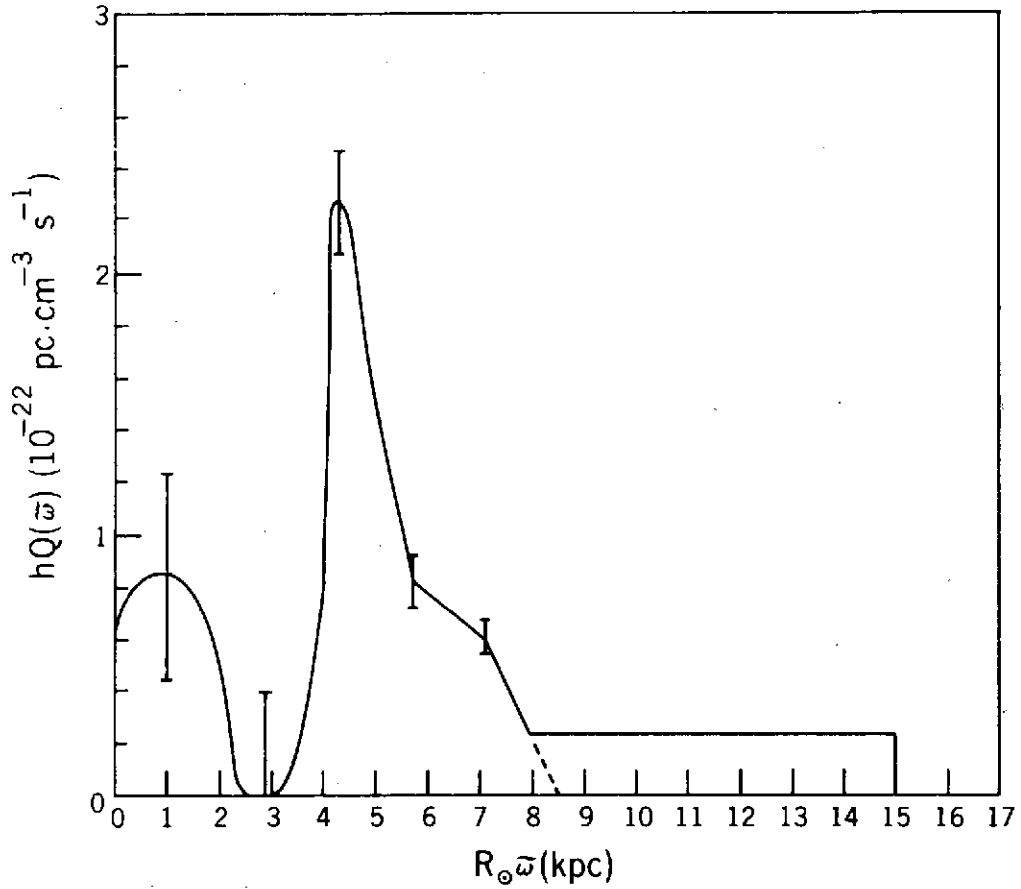


Figure 16. The value for  $hQ(\tilde{\omega})$  ( $\gamma$ -ray emissivity times disk width) given by Puget and Stecker (1974). A constant value for  $hQ$  is assumed for  $R_{\odot} \tilde{\omega} > 8$  kpc. Uncertainties in the determination of the value of  $hQ(\tilde{\omega})$  as evaluated from an integral equation of Puget and Stecker grow quite large in the central region  $R_{\odot} \tilde{\omega} < 4$  kpc.

unfolding of combined data from SAS-2 and OSO-3. He obtained a similar distribution to that shown in Figure 16. The results show a maximum in the  $\gamma$ -ray emissivity at  $\sim 5$  kpc and a reduced emissivity within 3 kpc of the galactic center. An unfolding of Figure 13 would probably show a less pronounced maximum at 5 kpc, but this unfolding has not been attempted here because the SAS-2 group will be publishing their final and complete longitude data in the near future.

Data have also been obtained on the energy spectrum of the galactic  $\gamma$ -radiation in the direction of maximum intensity by Kniffen, et al. (1973). These spectral measurements on the integral  $\gamma$ -ray spectrum are shown in Figure 17 to be consistent with a two-component origin with  $\sim 70$  percent of the radiation above 100 MeV due to  $\pi^0$ -decay as shown in figure 4 and  $\sim 30$  percent due to Compton radiation from cosmic ray electrons interacting with the higher radiation field in the inner galaxy (Stecker, et al. 1974). Under this interpretation, one would expect that almost all of the  $\gamma$ -radiation above 100 MeV in the outer regions of the galaxy would be due to  $\pi^0$ -decay. This interpretation would also be consistent with the  $\gamma$ -ray production rate deduced by Kraushaar, et al. of  $(1.6 \pm 0.5) \times 10^{-25} \text{ cm}^{-3} \text{ s}^{-1}$  above 100 MeV which is only slightly larger than the theoretical calculated value of  $(1.3 \pm 0.2) \times 10^{-25} n_{\text{H}} \text{ cm}^{-3} \text{ s}^{-1}$  for the solar vicinity (Stecker 1973) with  $n_{\text{H}} \sim 0.7 \text{ cm}^{-3}$  for atomic hydrogen alone.

While this interpretation presents a coherent and plausible model for discussion, one should bear in mind that the empirical situation is still in a state of flux and one measure of uncertainty is indicated by the various different

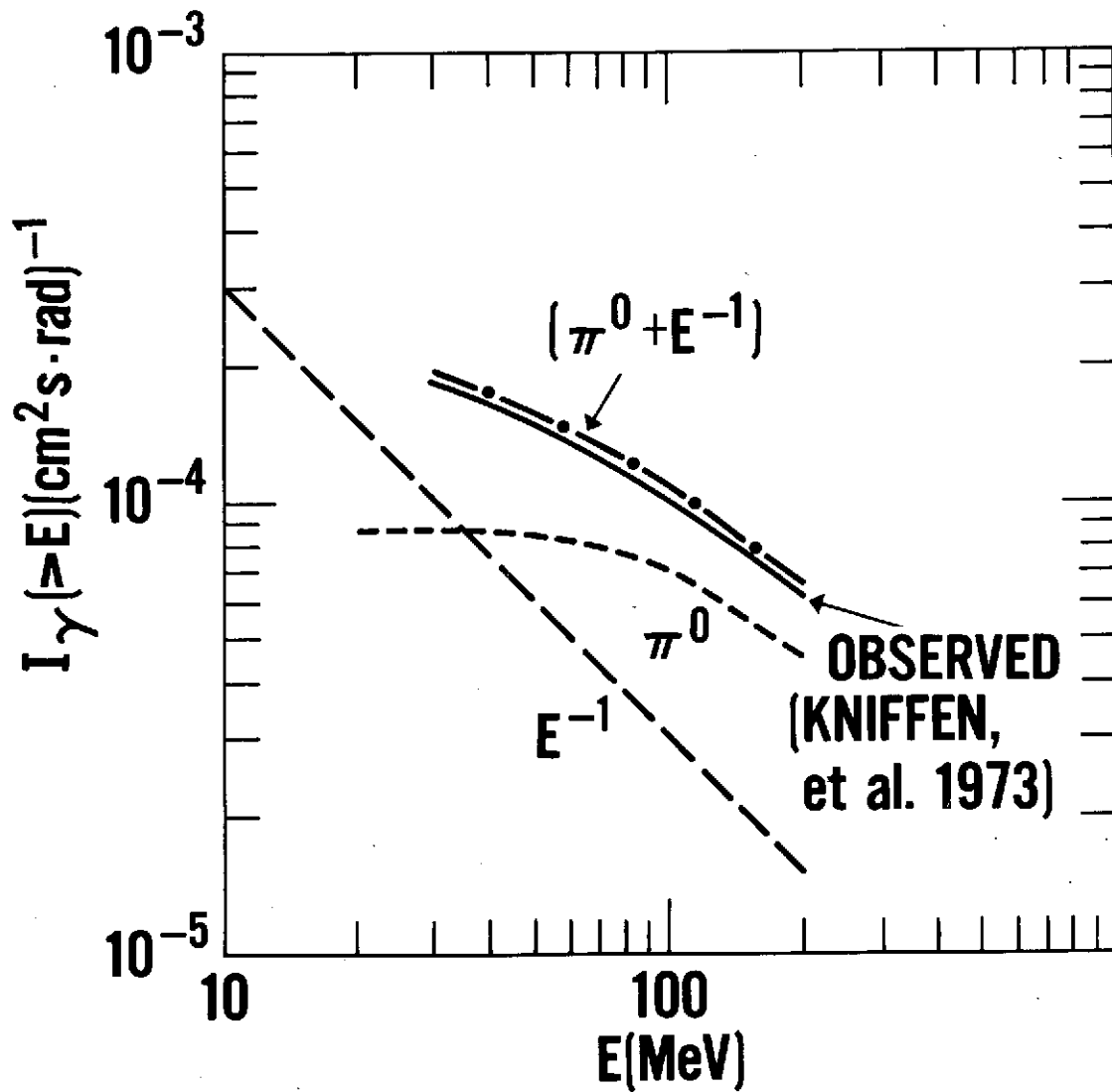


Figure 17. Comparison of SAS-2 (Kniffen, et al. 1973) spectral data on  $\gamma$ -radiation from the inner galaxy with a two-component model based on 70 percent pion decay (Stecker 1970) and  $E^{-1}$  integral Compton spectrum (Stecker, et al. 1974).

measurements of the inner-galactic flux as shown in Figure 18 and the differential data of Samimi, et al. (1974) as shown in Figure 19. In particular, the data summarized in Figures 18 and 19 appear to support the presence of a soft component of radiation at low energies possibly due to Compton interactions or bremsstrahlung.

It is instructive to estimate Compton and bremsstrahlung intensities in the galaxy relative to  $\pi^0$ -decay  $\gamma$ -radiation. First a crude estimate of the Compton radiation in the galactic disk. Starlight photons in the galaxy have an average energy of  $\sim 1\text{eV}$  and a number density of  $\sim 0.4\text{cm}^{-3}$  (Allen 1973). Let us consider the total gas density of atomic and molecular hydrogen to be  $\sim 1\text{cm}^{-3}$ . As pointed out previously, the mean energy of cosmic ray protons which produce  $\pi^0$ -mesons leading to  $\gamma$ -rays in the observed energy range  $\gtrsim 100\text{MeV}$  is  $\sim 3\text{GeV}$ . By a curious coincidence, a 3 GeV electron with  $\gamma \simeq 6 \times 10^3$  interacting with a 1eV photon will produce a  $\gamma$ -ray of energy

$$E_\gamma = \frac{4}{3} \gamma^2 \text{ eV} \simeq 50 \text{ MeV} \quad (84)$$

so that electrons of comparable (or slightly higher) energies will produce  $\gamma$ -rays in the same energy range as protons which produce  $\pi^0$  decay  $\gamma$ -rays. The ratio of electrons to protons at these energies is  $\sim 10^{-2}$ . The ratio of total  $\gamma$ -ray intensities is then

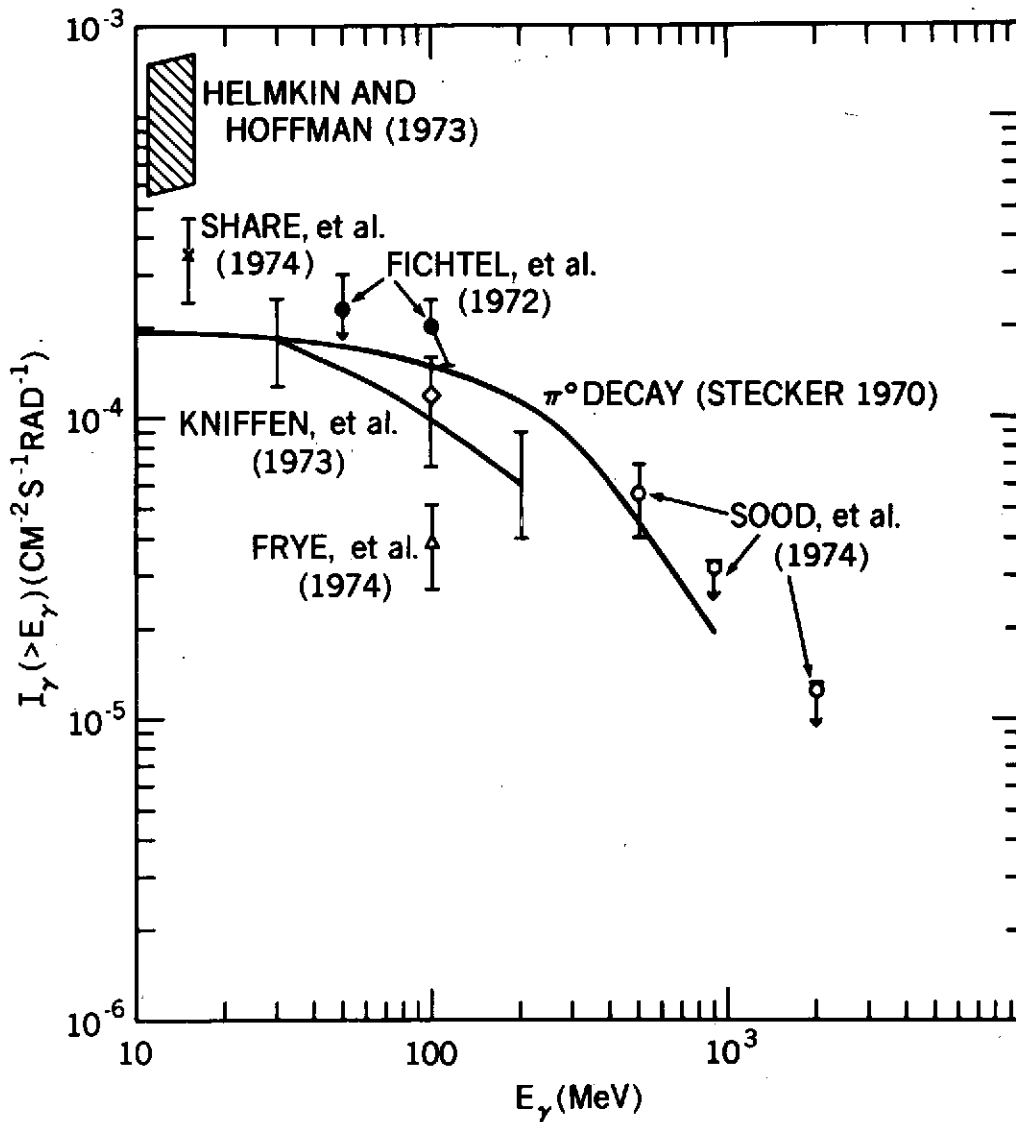


Figure 18. Summary of the integral flux measurements for the galactic center region given by various experimental groups.

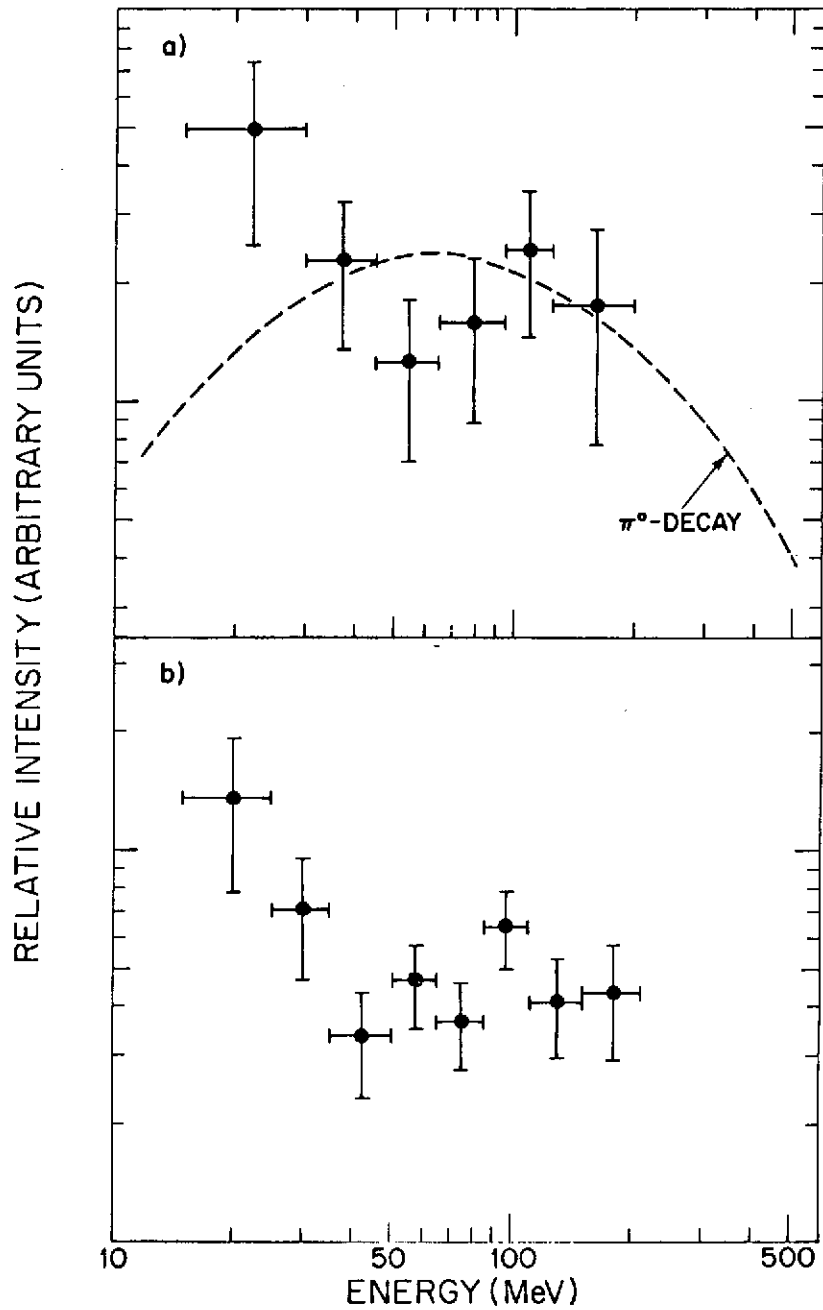


Figure 19. The differential photon spectrum of  $\gamma$ -rays as determined from the emulsion measurements of Samimi, et al. (1974) with the detector response unfolded. a) only  $\gamma$  rays coming from the enhanced  $3^\circ$  band  $-3^\circ \leq b^{\text{II}} \leq 0^\circ$ , b) atmospheric  $\gamma$ -rays.

$$\frac{I_c}{I_\pi} \approx \left( \frac{I_e}{I_p} \right) \left( \frac{\sigma_c}{2\sigma_{\pi^0} \zeta_{\pi^0}} \right) \left( \frac{n_{ph}}{n_H + 2n_{H_2}} \right) \quad (85)$$

$$\approx (10^{-2}) \left( \frac{4.4 \times 10^{-25}}{3 \times 10^{-26}} \right) \left( \frac{0.4}{1} \right) \approx 0.06.$$

More involved calculations using equations (11) and (12) give similar results. Equation (11) and (12) can also be used to calculate the  $\gamma$ -ray spectrum produced by interactions of electrons with the 2.7K universal background radiation. The ratio of 2.7K blackbody Compton  $\gamma$ -rays to starlight Compton  $\gamma$ -rays is

$$\frac{I_{2.7, c}}{I_{*, c}} = \frac{\rho_{2.7}}{\rho_*} \left( \frac{E_{2.7}}{E_*} \right)^{\Gamma-3/2} \approx \left( \frac{0.25}{0.4} \right) (6.4 \times 10^{-4})^{-0.2} \approx 2.7 \quad (86)$$

As can be seen from Figure 13, the  $\gamma$ -ray intensity in the inner galaxy is about 5 times that in the anticenter direction when one subtracts out the peaks due to the crab nebula at  $180^\circ$  and the Vela source (pulsar?) at  $270^\circ$ . A similar large ratio was found by Kraushaar, et al. (1972) on OSO-3. The OSO-3 ratio was speculated by Stecher and Stecker (1970) to be due to two effects: 1)  $\pi^0$  production off  $H_2$  not seen in 21 cm emission and 2) a Compton source from a large infrared radiation field at the galactic center (Hoffman and Frederick 1969). However, the Compton source would produce a clear peak at  $\ell = 0^\circ$  whereas the new SAS-2 data do not indicate such a peak but rather a broad flat region of relatively intense radiation (see Figure 13).

Bignami and Fichtel (1974) have attempted to explain the SAS-2 longitude distribution as due to an  $n^2$  enhancement of the product of gas density  $n$  and cosmic-ray intensity  $I$  with large density contrasts in galactic spiral arms as defined by 21 cm measurements of atomic hydrogen. Their results are shown in Figure 20.

Stecker, et al. (1974) and Puget and Stecker (1974) pointed out that the apparent peak in  $\gamma$ -ray emissivity at  $\sim 5$ kpc implied by the data of Kniffen, et al. corresponded to a maximal dissipation of the kinetic energy of outward gas motion in the galaxy and that possible cosmic-ray compression in that region and first-order Fermi acceleration could enhance the cosmic-ray density in that region to a large enough extent to explain the enhancement in  $\gamma$ -ray emissivity.

An enhancement of cosmic-rays in a localized region of the galaxy can be due to three factors (1) an increase in the density of cosmic-ray sources (or alternatively the production rate) in the region (2) an increase in the trapping time (escape time) of cosmic-rays in the region, and (3) acceleration and compression of cosmic-rays in the region. We may write this as follows:

$$\ln(I_{\text{CR}}/I_{\odot}) = \ln(Q_{\text{CR}}/Q_{\odot}) + \ln(T_{\text{CR}}/T_{\odot}) + \delta \quad (87)$$

where the first term on the right hand side of equation (87) represents the enhancement in the production rate, the second term represents the trapping factor and the third term represents the effect of acceleration and compression. The first term can only be guessed at, given our present lack of knowledge of the

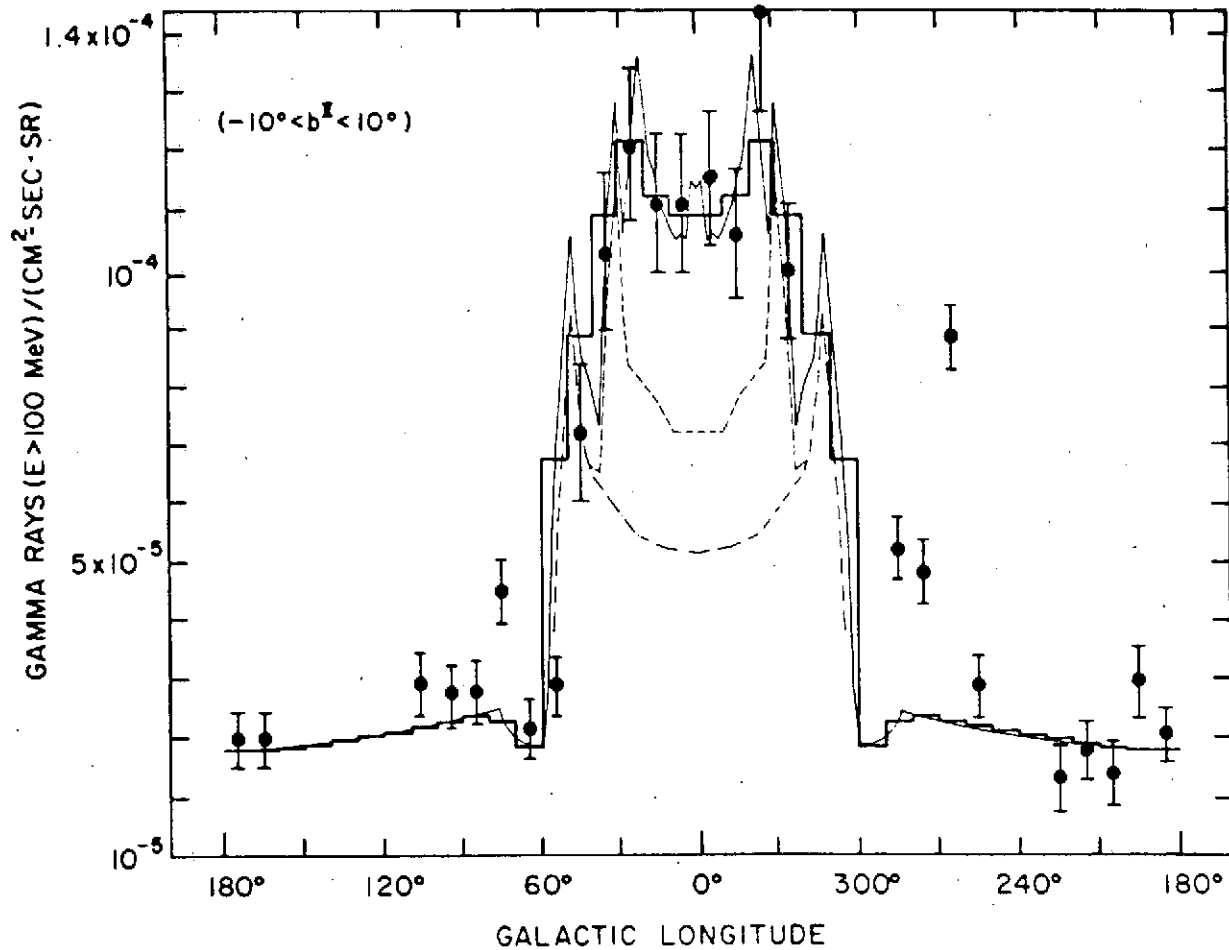


Figure 20. Longitudinal distributions of galactic gamma-flux integrated over  $\pm 10^\circ$  in  $b^{\text{II}}$  from Bignami and Fichtel (1974). SAS-II points are given together with their error bars (Kniffen, et al. 1973). The thick line represents the model of Bignami and Fichtel smoothed in  $10^\circ$   $l^{\text{II}}$  intervals. The thin line represents the model in  $2^\circ$  intervals. The dash line (----) gives the contribution of the Sagittarius and Norma-Scutum arms and dash-dot (-.-.-) the contribution of the Sagittarius arm alone.

ultimate origin of cosmic rays. However, as an indication of the possible effect of source density, one can note the distribution of supernova remnants in the galaxy which may be proportional to the density of cosmic-ray sources if we assume that cosmic-rays are produced by supernova explosions (Ginzburg and Syrovatsky 1964) or in remnant pulsars (Gunn and Ostriker 1969). According to Ilovaisky and Lequeux (1972) the density of supernova remnants increases roughly by a factor of 2 over the local galactic value for  $\tilde{\omega} < 0.8$  and drops sharply for  $\tilde{\omega} > 1.2$ . A more recent study by Clark, et al. (1973) is probably less susceptible to selection effects because their survey included remnants down to lower luminosity levels. The results obtained by Clark, et al. confirm the earlier results of Ilovaisky and Lequeux regarding the general distribution of supernova remnants in the galaxy. We will, therefore, estimate here that  $Q_{cr}/Q_{\odot} \simeq 2$  for the enhanced region  $0.4 < \tilde{\omega} < 0.6$ . This factor, by itself, cannot account for the order-of-magnitude enhancement deduced for  $I_{cr}/I_{\odot}$ .

The second factor,  $T_{cr}/T_{\odot}$  is so difficult to estimate that we will treat it as a free parameter  $> 1$  to be solved for. It is not unreasonable to expect more effective trapping in the inner galaxy (i.e.  $T_{cr}/T_{\odot} > 1$ ) due to compression and a resultant stronger magnetic field strength.

The factor  $\delta$  can be broken up into two parts, acceleration factor  $\delta_{Acc}$  which accounts for acceleration of the more numerous lower energy cosmic-rays (given an assumed power-law differential energy spectrum of the form  $\propto E_{cr}^{-\Gamma}$ ) to an energy above the threshold for  $\pi^0$  production, and a simple density

enhancement  $\delta_D$  due to the lower volume of the compressed region in which the trapped particles find themselves. If we designate the specific volume compression rate by

$$\alpha = - (1/V) (dV/dt) \quad (88)$$

then obviously

$$\delta_D = \alpha T_{cr} \quad (89)$$

The acceleration factor can be estimated thermodynamically. Regardless of the exact details of this process, which may be coherent, first order Fermi acceleration which can transfer the momentum of moving "clouds" with trapped magnetic irregularities to cosmic-rays trapped in the compressed region (Fermi 1954, Stecker et al. 1974). The increase in the energy of the individual cosmic-rays can be treated as an adiabatic compression heating of a "cosmic-ray gas molecule". The energy enhancement factor as

$$\ln(E/E_0) = (\gamma - 1) \alpha T_{cr} \quad (90)$$

where  $\gamma = 4/3$  for relativistic cosmic-rays  $\gamma = 5/3$  for sub-relativistic cosmic-rays. For a cosmic-ray differential energy spectrum of the form  $I_{cr} \propto E^{-\Gamma}$ , we then find

$$\delta_{ACC} = (\Gamma - 1) (\gamma - 1) \alpha T_{cr} \quad (91)$$

and therefore

$$\delta = [(\Gamma - 1) (\gamma - 1) + 1] \alpha T_{cr}$$

(Stecker, et al. 1974). The value of the specific volume compression rate  $\alpha(\tilde{\omega})$  can be given in terms of the radial expansion velocity  $v_r$  of the gas deduced from the 21 cm observations of the "expanding arm" feature. Under this interpretation

$$R_{\odot} \tilde{\omega} = \frac{dv_r}{d\tilde{\omega}} - \frac{v_r}{\tilde{\omega}} \quad (92)$$

where the galactocentric distance  $R = R_{\odot} \tilde{\omega}$

The function  $\alpha(\tilde{\omega})$  deduced from the observations of  $v_r(\tilde{\omega})$  (Shane 1972, Sanders and Wrixon 1972, 1973) is shown in Figure 21. It is positive and maximal in the region of observed maximum  $\gamma$ -ray emission (see Figure 16) and is negative in the inner region  $\tilde{\omega} < 3$  kpc where there may be a significant drop in  $\gamma$ -ray emission, although the uncertainties in that region are very large.

Because of the large uncertainties in  $T_{cr}$  and  $T_{\odot}$  we will consider a range of values for  $T_{cr}$  and  $T_{cr}/T_{\odot}$ . We will consider  $3 \times 10^6 \leq T_{cr} \leq 3 \times 10^7$  yr where the upper limit on  $T_{cr}$  is taken to be the deduced age of the expanding feature (Oort 1970, Van der Kruit 1971). The cosmic-ray lifetime in the local region,  $T_{\odot}$ , is given by O'Dell, et al. (1973) and Brown et al. (1973), to be  $10^6 \text{ yr} \leq T_{cr} \leq 10^7$  yr. Taking  $\alpha = 2 \times 10^{-15} \text{ s}^{-1}$  in the region of maximum compression (see Figure 8) and assuming  $I_{cr}/I_{\odot} \simeq 15$  and  $Q_{cr}/Q_{\odot} \simeq 2$ ,  $\Gamma = 2.5$ ,  $\delta = 1.75$   $\alpha T_{cr} = 1.5 \times 10^{-15} T_{cr}$ , the value given for the parameters  $T_{cr}/T_{\odot}$ ,  $e^{\delta}$  and  $T_{cr}$  and  $T_{\odot}$  consistent with equation (87) are given in Table 1. The factor  $e^{\delta}$  represents the enhancement effect due to acceleration and compression.

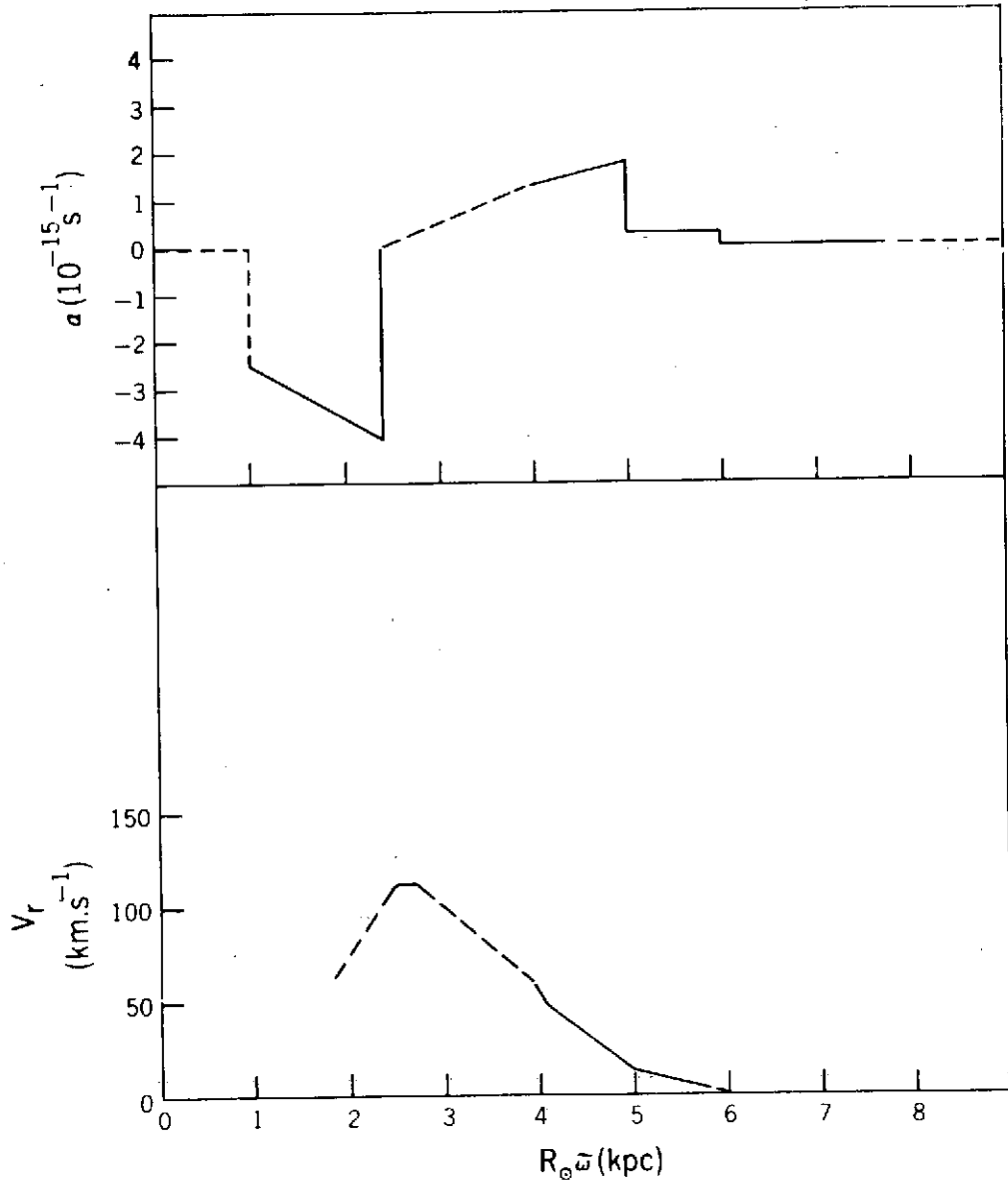


Figure 21. The specific compression rate  $\alpha(\tilde{\omega})$  obtained from the radial velocity data  $v_r(\tilde{\omega})$  based on the observations of Shane (1972) and Sanders and Wrixon (1972, 1973).

Table 1  
Lifetime of Cosmic-Rays in the 4 to 5 kpc Region Calculated  
from the Acceleration-Compression Model

$T_{cr} / T_0$	$e^{\delta}$	$T_{cr} (10^6 \text{ y})$	$T_0 (10^6 \text{ y})$
2	3.7	12.6	6.3
3	2.5	8.7	2.9
4	1.9	6.0	1.5

Aside from the possibility that cosmic-ray enhancement accounts for the large  $\gamma$ -ray emissivity in the 5 kpc region, recent carbon monoxide emission measurements in a 2.6 mm microwave survey of the galaxy by Scoville and Solomon have given new life and strong emphasis to the idea that much if not all of the increase in the  $\gamma$ -ray emissivity could be due to interaction between cosmic rays and large amounts of  $H_2$  not seen in 21 cm emission (Stecker 1969c, 1971; Stecher and Stecker 1970). However, the recent measurements of Scoville and Solomon point up this possibility in a much more specific and meaningful way, since their measurements indicate an increased enhancement in CO and by implication an increased  $H_2$  density in the very region where the  $\gamma$ -ray emissivity appears to be enhanced. This has led Solomon and Stecker (1974) to suggest that both enhancements provide evidence for the existence of a galactic  $H_2$  "ring" or "arm" feature at  $\sim 5$ kpc.

Molecular hydrogen is expected to be the predominant form of hydrogen in cool clouds of sufficient density (Solomon and Wickramasinghe (1969), Hollenbach

and Salpeter (1971), Hollenbach, Werner and Salpeter (1971). However, it is difficult to measure its galactic distribution directly. Strong  $H_2$  absorption lines have been seen in the UV in almost all nearby clouds by the Copernicus satellite (Spitzer, et al 1973) but UV observations of  $H_2$  at distances greater than 1 kpc from us are not feasible because of the large extinction of UV radiation by interstellar dust.

Because  $H_2$  has no permanent dipole moment, it cannot emit electric dipole radiation and, even though quadropole vibration-rotation features can in principle be observed in the infrared, such features are inherently very weak.

CO emission can be used as a tracer of  $H_2$  in molecular clouds because the most important source of CO excitation in these clouds is by collisions with  $H_2$ .

The galactic longitude distribution of CO emission in the galactic plane obtained by Scoville and Solomon (to be published) is shown in Figure 22. The data represent the antenna temperature integrated over the velocity profile of the 2.54mm CO emission line and would therefore be proportional to the number of CO molecules along the line-of-sight in the optically thin case as we discussed previously with the 21 cm line. Measurements were also obtained of the velocity profile function  $T_A(\ell, v)$  for each  $1^\circ$  of longitude from  $0^\circ$  to  $90^\circ$  and sample profiles are shown in Figure 23.

The function  $T_A(\ell, v)$  can be converted into a galactocentric distance distribution by using a model for galactic rotation (Schmidt 1965). Such an unfolding is shown in Figure 24 which can be compared with the  $\gamma$ -ray emissivity function given in Figure 16.

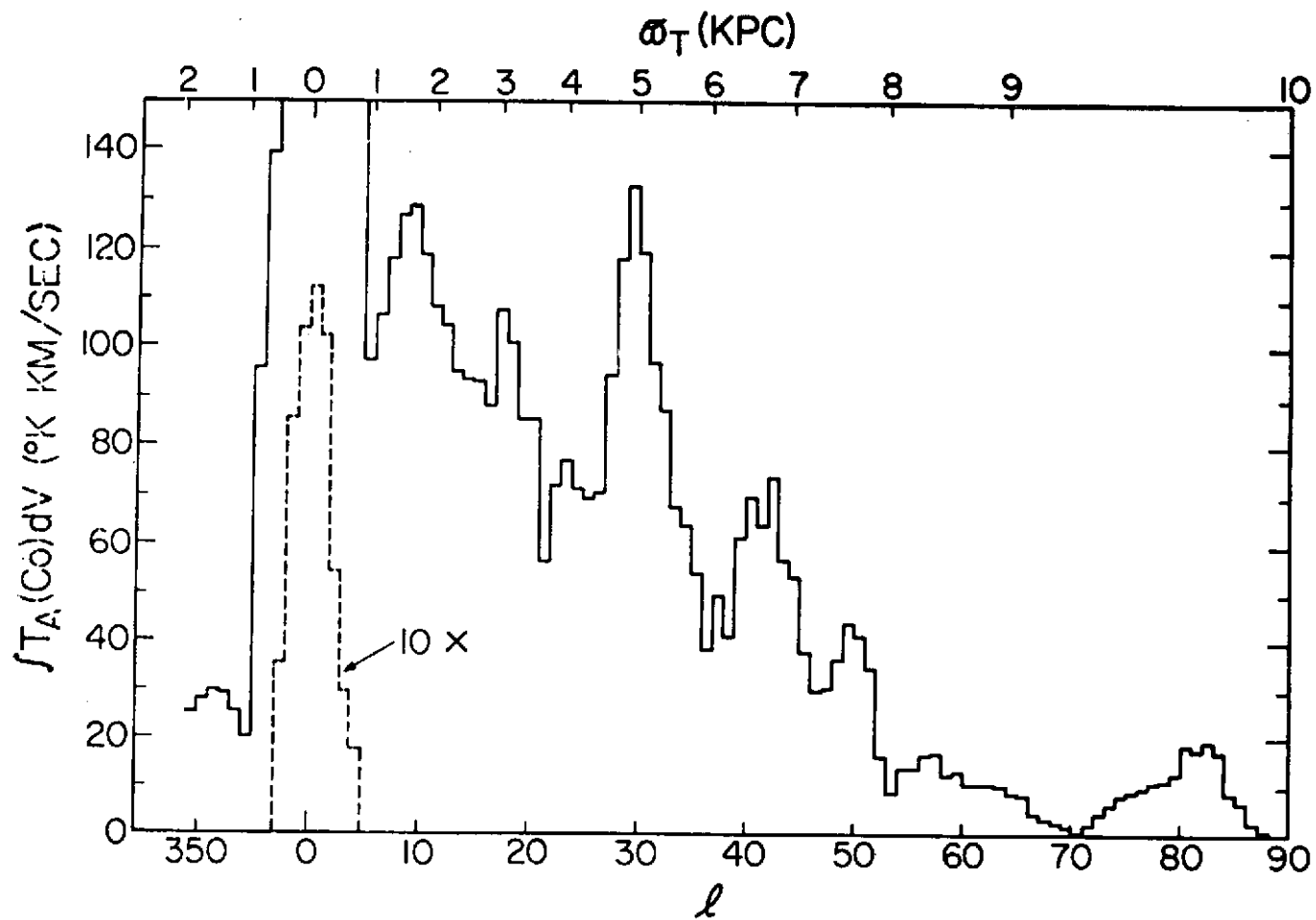


Figure 22. The intensity distribution of 2.6mm line emission in the galactic plane from the  $J = 1 \rightarrow 0$  transition of carbon monoxide integrated over velocity as a function of galactic longitude (Scoville and Solomon, to be published; Scoville, Solomon and Jefferts 1974).

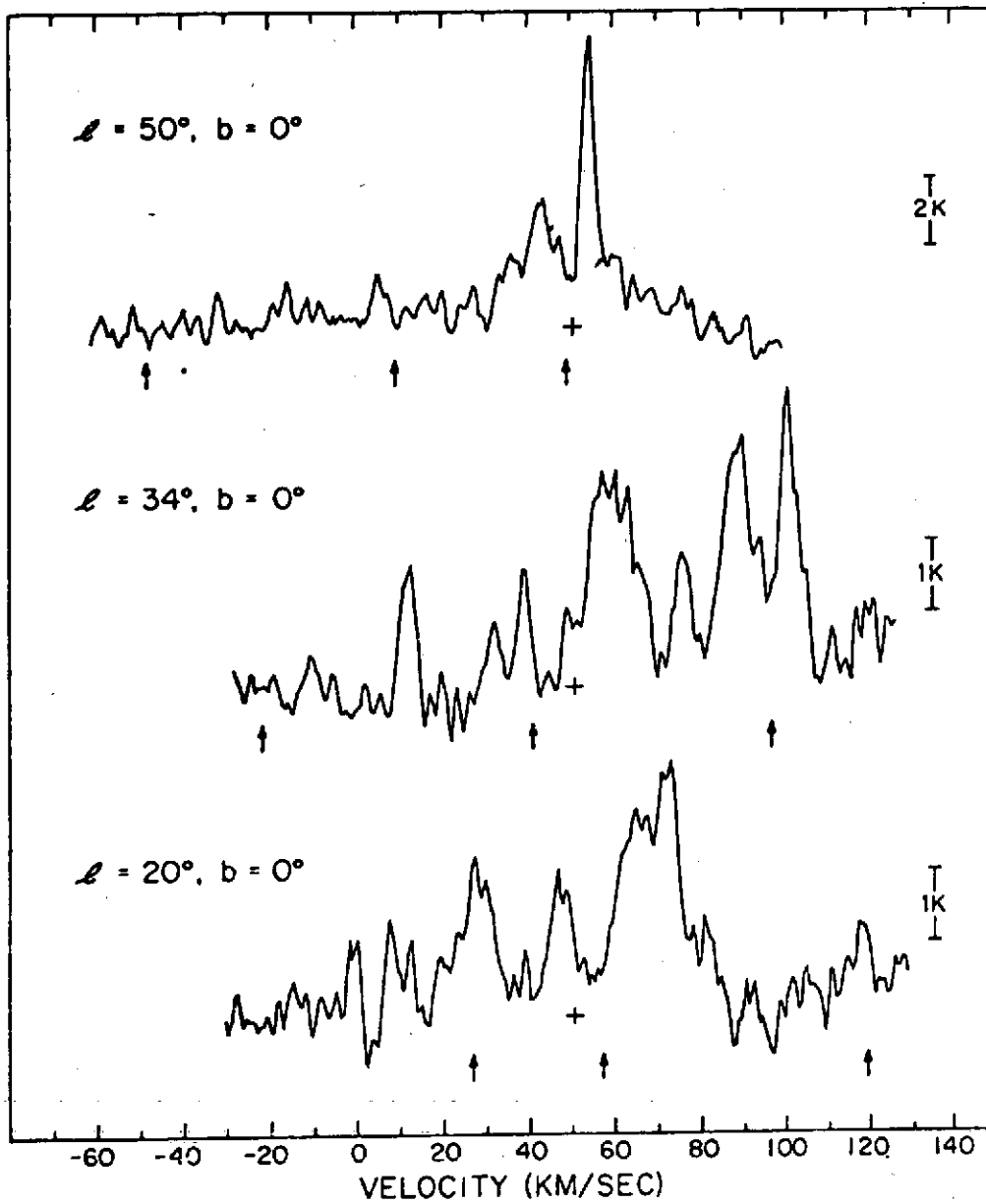


Figure 23. Sample CO line emission spectra obtained in the survey of Scoville and Solomon (to be published).

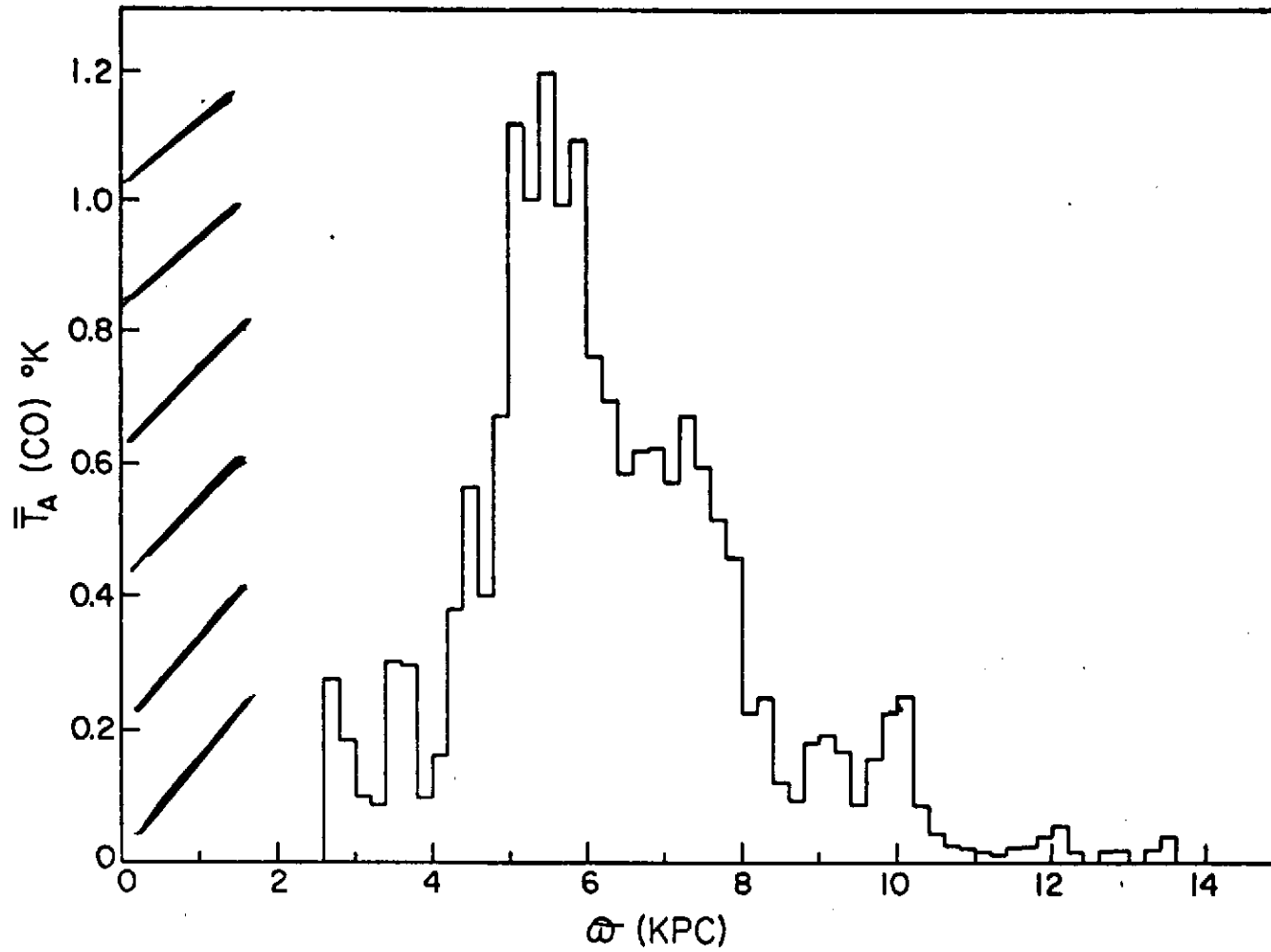


Figure 24. The distribution of CO line emission as a function of galactocentric distance (labeled here  $\bar{r}$ ) in kpc.

Solomon and Stecker (1974) have used the CO emission data and the  $\gamma$ -ray emission data to place limits on the mean density of  $H_2$  in the 5 kpc feature. They have obtained

$$1 \lesssim n_{H_2}(5 \text{ kpc}) \leq 5 \text{ molecules/cm}^3 \quad (93)$$

The lower limit closely corresponds to the optically thin case for CO emission and the upper limit corresponds to optically thick emission of the type observed in nearby dark clouds. In the optically thick case for  $C^{12}O$  in nearby clouds, emission from  $C^{13}O$  is optically thin and one can use the abundance ratio of  $C^{13}/C^{12}$  to deduce that  $C^{12}O$  is in the range 10-20. It should be kept in mind that in order to obtain enough collisional excitation of CO to the  $J = 1$  rotational state to produce a measurable amount of  $J = 1 \rightarrow 0$  2.64 mm emission, the  $H_2$  density in the cloud must be in the range  $10^3 \lesssim n_{H_2} \lesssim 10^4 \text{ cm}^{-3}$ . Therefore, equation (93) represents only a smoothed out mean of a very uneven distribution of  $H_2$ .

It can thus be seen how  $\gamma$ -ray astronomy gives us another window on the study of galactic structure and dynamics. The various implications of the SAS-2 data we have just discussed represent only a first step toward our understanding of  $\gamma$ -ray emission in the galaxy. Improved  $\gamma$ -ray telescopes will someday provide us with a clearer picture of the galaxy.

## 5. Extragalactic $\gamma$ -Rays

### A. Redshifts and Cosmology

Much data have recently been obtained on the diffuse  $\gamma$ -ray background radiation which appears to be isotropic in origin. These data have now defined a continuous background spectrum up to an energy of 200 meV. They are summarized in Figure 25.\*

The cosmological nature of this radiation leads us to examine its origin in the context of the expanding universe model where such radiation is redshifted to lower energies as we see it because of the Doppler effect.

The simplest expanding universe model is one in which the universe is both homogeneous and isotropic. Such a model is quite adequate for our purposes here and support for it comes from the remarkable isotropy of the 2.7K microwave background radiation which is believed to have originated much earlier in the history of the universe than the observed  $\gamma$ -ray background. A homogeneous-isotropic universe can be described by the Robertson-Walker space-time metric of the form

$$ds^2 = -c^2 dt^2 - R^2(t) du^2 \quad (94)$$

where  $R(t)$  is a scale factor which describes the expansion of the universe as a function of time according to the solution of the Einstein equations of general relativity.

---

\*Recent data reported by Tanaka (1974) in the energy range up to 7.5 MeV are not shown in the figure but are consistent with other data in this range.

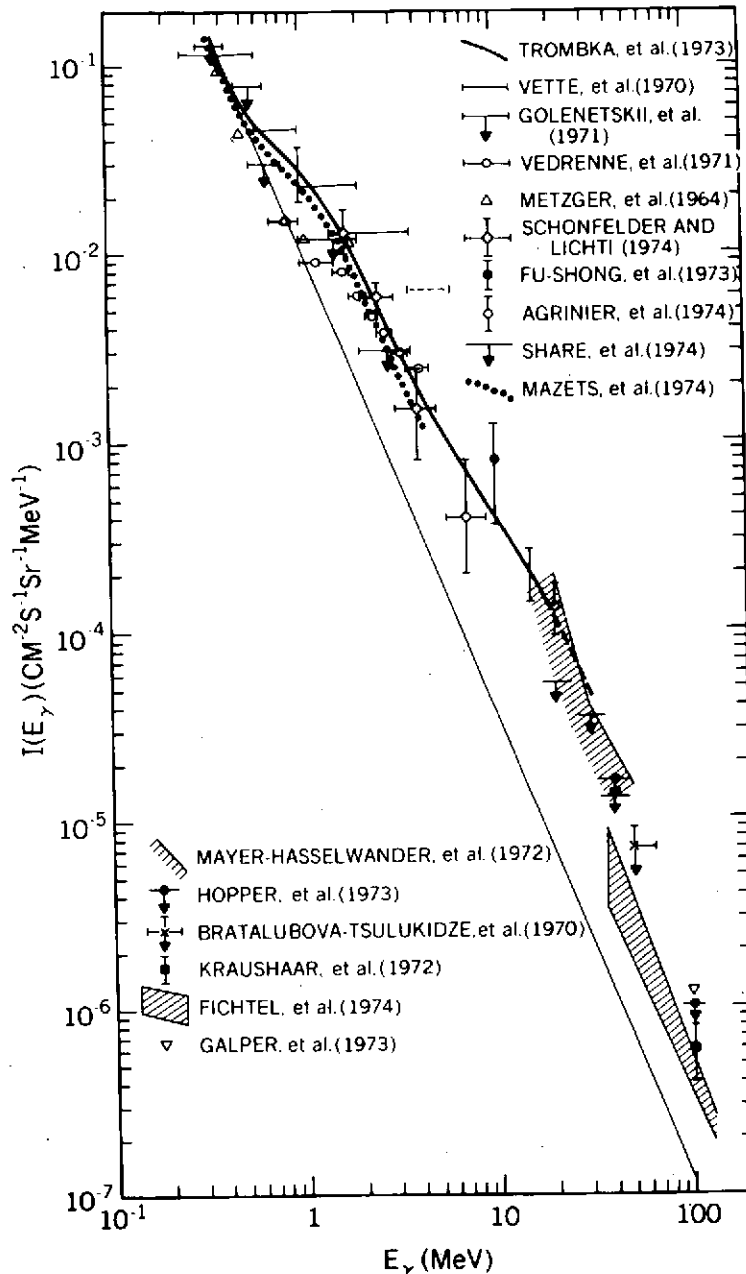


Figure 25. Observational data on the gamma-ray background energy spectrum. The highest energy point of Vette, et al. (1970), shown with a dashed line, and possibly the neighboring point are now thought to be erroneously high due to an inefficiency in the anticoincidence circuit of their detector which should not significantly affect the points at lower energies (Vette, private communication).

Photons travel along the null geodesic which obeys the relation  $ds^2 = 0$ , i.e.,  
from (94)

$$u = c \int_{t_e}^{t_r} \frac{dt}{R(t)} \quad (95)$$

with  $t_e$  being the time the photon was emitted and  $t_r$  being the time the photon is received.

The emitting and receiving points are embedded in the metric so that the distance between them is changing by the scale factor  $R(t)$ ; the dimensionless metric distance,  $u$ , is a constant. If we therefore consider two successive wave crests of a light ray as being emitted at times  $t_e$  and  $t_e + \Delta t_e$  respectively and being received at times  $t_r$  and  $t_r + \Delta t_r$ , then

$$\int_{t_e}^{t_r} \frac{dt}{R(t)} = \int_{t_e + \Delta t_e}^{t_r + \Delta t_r} \frac{dt}{R(t)} = u = \text{const.} \quad (96)$$

Thus

$$\begin{aligned} \int_{t_e + \Delta t_e}^{t_r + \Delta t_r} \frac{dt}{R(t)} - \int_{t_e}^{t_r} \frac{dt}{R(t)} &= \int_{t_r}^{t_r + \Delta t_r} \frac{dt}{R(t)} - \int_{t_e}^{t_e + \Delta t_e} \frac{dt}{R(t)} \\ &= \frac{\Delta t_r}{R(t_r)} - \frac{\Delta t_e}{R(t_e)} = 0 \end{aligned} \quad (97)$$

or

$$\frac{\Delta t_e}{R(t_e)} = \frac{\Delta t_r}{R(t_r)}$$

Since the wavelength of the emitted wave is  $c\Delta t_e$  and that of the wave when received is  $c\Delta t_r$ , the wavelength is shifted by the amount

$$z = \frac{\lambda_r - \lambda_e}{\lambda_e} = \frac{\Delta\lambda}{\lambda} = \frac{R(t_r) - R(t_e)}{R(t_e)}$$

or

(98)

$$\frac{R(t_r)}{R(t_e)} = 1 + z$$

We have observed this shift in the spectral lines of distant galaxies as always being toward longer wavelength so that  $R(t_r) > R(t_e)$ . From this evidence, it has therefore been deduced that our universe is expanding with time.

### B. Gamma-Ray Fluxes

Let us now consider the effect of cosmological factors in calculating gamma-ray fluxes emitted at large redshifts,  $z$ . The number of photons received per second is reduced by a factor  $R(t_e)/R(t_r)$  from the number produced per second at time,  $t_e$ . We consider here gamma rays produced in particle collisions between two components having densities  $n_a(t_e)$  and  $n_b(t_e)$  respectively. We specify the differential photon intensity produced per collision as

$$G(E_\gamma) (\text{cm}^2 \cdot \text{s} \cdot \text{Sr} \cdot \text{MeV} \cdot \text{cm}^{-6})^{-1}$$

Then the differential photon flux received at  $t_r$  is given by

$$dF_r = \frac{4\pi n_a(t_e) n_b(t_e) G(E_{\gamma,e}) dE_{\gamma,e} dV_e dt_e}{4\pi R^2(t_r) u^2} \quad (99)$$

where the numerator represents the photon flux emitted at  $t_e$ , and the denominator indicates the fact that at  $t_r$  this flux is evenly distributed over a spherical wavefront of radius  $R(t_r)$ . We now define the three dimensional length,

$$d\ell = R(t) du \quad (100)$$

so that the volume element

$$dV_e = d\ell [R^2(t_e) u^2 d\Omega] \quad (101)$$

Since

$$dt_e = [R(t_e)/R(t_r)] dt_r \quad (102)$$

and

$$dE_{\gamma,e} = [R(t_r)/R(t_e)] dE_{\gamma,r}$$

because the energy of a gamma-ray is inversely proportional to its wavelength, we may substitute (101) and (102) into (100) and obtain

$$dF_r = n_a(t_e) n_b(t_e) G\{[R(t_r)/R(t_e)] E_{\gamma,r}\} \quad (103)$$

$$\times \frac{4\pi R^2(t_e) u^2 d\Omega d\ell dE_{\gamma,r} dt_r}{4\pi R^2(t_r) u^2}$$

By making use of equation (98) and dropping the subscript, r, since we only measure gamma-rays when they are received, equation (103) reduces to

$$\frac{dF}{d\Omega dt dE_\gamma} = dI = \frac{n_a(z) n_b(z) G[(1+z) E_\gamma] d\ell}{(1+z)^2} \quad (104)$$

$$= \frac{n_a(z) n_b(z) G[(1+z) E_\gamma]}{(1+z)^2} \left( \frac{d\ell}{dz} \right) dz$$

Equation (104) is quite useful in evaluating the metagalactic gamma-ray spectra from various high-energy interactions. The results are obtained from numerical integration of the relation

$$I(E_\gamma) = \int_0^{z_{\max}} dz n_a(z) n_b(z) \frac{G[(1+z) E_\gamma]}{(1+z)^2} \left( \frac{d\ell}{dz} \right) \quad (105)$$

where the factor  $d\ell/dz$  is determined from the Einstein field equations to be

$$\frac{d\ell}{dz} = \frac{c}{H_0} (1+z)^{-2} (1+\Omega z)^{-1/2} \quad (106)$$

where  $H_0$  is the Hubble constant and

$$\Omega = \frac{n_0}{n_c} \quad (107)$$

where  $n_0$  is the present mean density of all the matter in the universe and  $n_c$  is the critical density needed to gravitationally close the universe.

The value for  $cH_0^{-1}$  is in the range

$$10^{28} \lesssim cH_0^{-1} \lesssim 2 \times 10^{28} \text{ cm} \quad (108)$$

and

$$3 \times 10^{-6} \lesssim n_c \lesssim 10^{-5} \text{ cm}^{-3} \quad (109)$$

If absorption effects are included, equation (105) becomes

$$I(E_\gamma) = \frac{c}{H_0} \int_0^{z_{\max}} dz n_a(z) n_b(z) \frac{G[(1+z)E_\gamma]}{(1+z)^4 \sqrt{1+\Omega z}} e^{-\tau(E_\gamma, z)} \quad (110)$$

Since the universal blackbody radiation plays an important role in various high-energy production processes, it is important to determine how this radiation behaves as a function of redshift. At the earliest stages in the evolution of the universe, when the matter in the universe was in thermal equilibrium with the universal blackbody radiation owing to Compton interactions between thermal photons and electrons,  $T_m$  was equal to  $T_r$  (the temperature of the radiation field). Zeldovich, et al. (1969) have shown that even though the intergalactic gas has cooled to the 50% neutral point by the time corresponding to a redshift  $z = 1200-1300$ , the small fraction of ionized material left at lower redshifts is enough to sustain temperature equilibrium between matter and radiation field until a redshift of 150-200.

The photon density of a radiation field at temperature  $T_0$  is given from the Planck formula as

$$n_{r,0}(\epsilon, T_0) d\epsilon = \frac{8\pi}{h^3 c^3} \frac{\epsilon^2 d\epsilon}{e^{\epsilon/kT_{r,0}} - 1} \quad (111)$$

At a redshift  $z \neq 0$ , this distribution is then given by

$$\begin{aligned} n_r(z, \epsilon) d\epsilon &= \frac{8\pi}{h^3 c^3} \frac{(1+z)^3 \epsilon^2 d\epsilon}{e^{(1+z)\epsilon/kT_{r,0}} - 1} \\ &= (1+z)^3 n_{r,0}[\epsilon, T_r(z)] d\epsilon \end{aligned} \quad (112)$$

where

$$T_r(z) = (1 + z) T_{r,0} \quad (113)$$

so we find that the redshifted Planckian maintains its form with the parameter  $T(z)$  in the exponent given by equation (113). The photon number density redshifts in the same manner as the matter density viz.  $n \propto R(t)^{-1} \propto (1 + z)^3$ . The energy density in the radiation field then redshifts as

$$\rho_r = \rho_{r,0} (1 + z)^4 \quad (114)$$

in accord with the definition of  $T_r(z)$  given by equation (11-12) and the relation  $\rho \propto T^4$ .

We therefore find that

$$T_m(z) = T_r(z) = T_{r,p}(1 + z) \quad (115)$$

$$\text{for } z \gtrsim 150 - 200$$

At lower redshifts, when the matter has thermally decoupled from the radiation field, the momentum distribution of the atoms in the intergalactic gas is given by the Maxwellian,

$$n_0(p, T_{m,0}) dp = \text{const.} \times p^2 e^{-p^2/2mkT_{m,0}} dp \quad (116)$$

These atoms lose momentum through collisions due to the effect of the overall adiabatic expansion of the universe; their resultant momentum change is

$$p(z) = p_0 \frac{R_0}{R(z)} = p_0(1 + z) \quad (117)$$

Substituting (117) into (116), we then find

$$n_m(z, p) dp = (1 + z)^3 n_{m,0} [p, T_m(z)] dp \quad (118)$$

with

$$T_m(z) = T_{m,0}(1 + z)^2 \quad (119)$$

From equation (118), it is immediately evident that the total number of atoms,  $\sim nR^3$  is conserved during the expansion as must be the case.

We thus find that

$$T_m(z) = T_{m,0}(1 + z)^2 \quad \text{for } z \leq 150 - 200 \quad (120)$$

with

$$T_m(150 \text{ to } 200) \simeq T_r(150 \text{ to } 200) \quad (121)$$

The adiabatic expansion concept may be used to link the derivations of equations (113) and (119) for the temperature-redshift relations. In an adiabatic expansion, it is well known that

$$TV^{(\gamma-1)} = \text{const.} \quad (122)$$

where the quantity,  $\gamma$ , here is the ratio of specific heat at constant pressure to that at constant temperature and  $V$  is the volume of the gas (in this case the volume of the universe) which from (98) is given by

$$V(z) = V_0(1 + z)^{-3} \quad (123)$$

For photons and monatomic gases at relativistic temperatures ( $pc \simeq E$ ),  $\gamma = 4/3$ , whereas for nonrelativistic gases  $\gamma = 5/3$ . Thus, from (123) and (122) one can immediately obtain both equation (113) for photons and relativistic gases and (119) for nonrelativistic gases.

We can use these equations to take into account the cosmological effects in computing the extragalactic gamma-ray spectrum from Compton interactions between cosmic-ray electrons and photons of the universal blackbody radiation field in intergalactic space. The local ( $z = 0$ ) spectrum is given from equation (11) as

$$I_{e,0}(E_\gamma) = \frac{2}{3} \sigma_T c H_0^{-1} f(\Gamma) (mc^2)^{(1-\Gamma)} (3.6k)^{\left(\frac{\Gamma-3}{2}\right)} k_{e,0} \rho_{r,0} \times T_{r,0}^{\left(\frac{\Gamma-3}{2}\right)} E_\gamma^{-\left(\frac{\Gamma+1}{2}\right)} \quad (124)$$

for Compton gamma-rays produced by cosmic-ray electrons having a power law energy spectrum of the form

$$I(E_e) = K_{e,0} E_e^{-\Gamma} \quad (125)$$

Under the conditions where (125) is valid over all redshifts from 0 to  $z$  and where electron energy losses other than those from the universal expansion are neglected, the transformation from  $K_{e,0}$  to  $K_e(z)$  is given by

$$\begin{aligned}
K_e(z) &= K_{e,0} (1+z)^3 (1+z)^{\Gamma-1} \\
&= K_{e,0} (1+z)^{\Gamma+2}
\end{aligned}
\tag{126}$$

where the first factor of  $(1+z)^3$  represents the density effect and the factor of  $(1+z)^{\Gamma-1}$  represents the transformation of the power-law energy spectrum from a burst of relativistic cosmic-ray electrons occurring at  $z_{\max} \geq z$ .

Using equations (114) and (115), as well as (126) and substituting them into the general formula (105), we find

$$I_c(E_\gamma) = I_{c,0}(E_\gamma) \int_0^{z_{\max}} dz \frac{(1+z)^\Gamma}{\sqrt{1+\Omega z}}
\tag{127}$$

so that under these conditions, the power-law form for the Compton  $\gamma$ -ray spectrum is maintained but the cosmological flux is enhanced by a factor given by the integral over  $z$  in equal (124).

However, Brecher and Morrison (1967) showed that the true situation is not as simple as that given by equation (127) under the conditions when the high energy end of the electron spectrum is steepened owing to energy losses from the Compton interactions themselves. Since the blackbody radiation density is proportional to  $(1+z)^4$ , electrons lose energy primarily from Compton interactions with the energy loss rate being given by

$$\left(\frac{d\gamma}{dt}\right)_c = -\frac{4}{3} \frac{\sigma_T c \rho_r}{m_e c^2} \gamma^2 = \frac{(1+z)^4}{\tau_0} \gamma^2
\tag{128}$$

with

$$\tau_0 \equiv \frac{3m_e c^2}{4\sigma_T c \rho_{r,0}} = 7.7 \times 10^{19} \text{ s} \quad (129)$$

The energy loss from the universal expansion is given by

$$\left(\frac{d\gamma}{dz}\right)_{\text{exp}} = \frac{\gamma}{1+z} \quad (130)$$

From (130) and (106), we obtain

$$\left(\frac{d\gamma}{dz}\right)_c = \left(\frac{d\gamma}{dt}\right)_c \left(\frac{dt}{dz}\right) = \frac{(1+z)^2 \gamma^2}{H_0 \tau_0 \sqrt{1+\Omega z}} \quad (131)$$

The two energy loss rate terms are equal at the critical energy,  $E_c = \gamma_c m_e c^2$ ,

where

$$\gamma_c = \frac{H_0 \tau_0 \sqrt{1+\Omega z}}{(1+z)^3} \simeq \frac{256 (1+\Omega z)^{1/2}}{(1+z)^3} \quad (132)$$

or

$$E_c \simeq 130 \frac{\sqrt{1+\Omega z}}{(1+z)^3} \text{ MeV} \quad (133)$$

For  $E < E_c$ , the electron spectrum maintains its power-law form since these electrons lose their energy through the universal expansion and equation (126) is therefore valid. However, for  $E > E_c$ , the equilibrium electron flux is given by the solution of a rate balance equation under the conditions when Compton losses dominate. Under these conditions,

$$\frac{\partial}{\partial \gamma} \left[ K_e \gamma^{-\Gamma'} \frac{(1+z)^4 \gamma^2}{\tau_0} \right] = k_q \gamma^{-\Gamma} \quad (134)$$

(Brecher and Morrison, 1967), where  $k_q \gamma^{-\Gamma}$  is the original (injection) electron spectrum and  $\Gamma'$  is the exponent of the resulting equilibrium electron spectrum.

It follows from equation (134) that

$$\Gamma' = \Gamma + 1 \quad (135)$$

and

$$K_e = \frac{k_q \tau_0}{\Gamma (1+z)^4} \quad (136)$$

so that the equilibrium electron spectrum is depleted by a factor proportional to  $(1+z)^4$  by Compton interactions with the universal radiation field and, in addition, the exponent of the electron spectrum is steepened by one power of  $E_e$ .

This steepening in the electron spectrum corresponds to a change of 1/2 in the exponent of the Compton gamma-ray spectrum at an energy

$$E_{\gamma,c} = \left\langle \frac{4}{3} \epsilon_0 \right\rangle \gamma_c^2 = 33 \left[ \frac{1 + \Omega z}{(1+z)^5} \right] \text{ eV} \quad (137)$$

Thus, the Compton gamma-rays are expected to be produced by the steepened electron spectrum at all gamma-ray energies. From (136), Brecher and Morrison conclude that unless there is a large evolutionary factor in the electron production spectrum, i.e.,  $k_q \sim (1+z)^m$ , where  $m \gtrsim 4$ , there will be no significant enhancement of Compton gamma-rays at large redshifts over those produced at the present epoch.

The local gamma-ray spectrum from relativistic bremsstrahlung interactions is given by (36) as

$$I_{b,0}(E_\gamma) = 3.4 \times 10^{-26} n_0 c H_0^{-1} \frac{I_e(> E_\gamma)}{E_\gamma} \quad (138)$$

Making use of equations (105) and (126), we obtain for the cosmological bremsstrahlung production spectrum

$$\begin{aligned} I_b(E_{\gamma 0}, Z_{\max}) &= \frac{3.4 \times 10^{-26} n_0 c H_0^{-1} K_{e,0}}{\Gamma - 1} \\ &\times \int_0^{z_{\max}} dz \frac{(1+z)^3 (1+z)^{\Gamma+2} [(1+z) E_{\gamma 0}]^{-\Gamma}}{(1+z)^4 \sqrt{1+\Omega z}} \\ &= \frac{3.4 \times 10^{-3} \Omega}{\Gamma - 1} K_{e,0} E_{\gamma 0}^{-\Gamma} \int_0^{z_{\max}} dz \frac{(1+z)}{\sqrt{1+\Omega z}} \\ &= \frac{6.8 \times 10^{-3}}{\Gamma - 1} K_{e,0} E_{\gamma 0}^{-\Gamma} \left[ \left(1 + \frac{z}{3} - \frac{2}{3\Omega}\right) \sqrt{1+\Omega z} - \left(1 - \frac{2}{3\Omega}\right) \right] \end{aligned} \quad (139)$$

In particular, for the Einstein-de Sitter universe where  $\Omega = 1$ ,

$$I_b(E_{\gamma 0}, z_{\max}) = \frac{2}{3} I_{b,0}(E_{\gamma 0}) [(1 + z_{\max})^{3/2} - 1] \quad (140)$$

and for the low density model where  $\Omega z \ll 1$ ,

$$I_b(E_{\gamma 0}, z_{\max}) = \frac{1}{2} I_{b,0}(E_{\gamma 0}) [(1 + z_{\max})^2 - 1] \quad (141)$$

Where electron steepening by Compton interactions with the 2.7K radiation is important, the situation is more complicated and a more detailed treatment of this problem has been given by Stecker and Morgan (1972).

## 6. Gamma-Ray Absorption Processes at High Redshifts

In Section 4, we discussed in detail the processes which result in the absorption of cosmic gamma-rays. In that section, we pointed out that there are three main absorption processes of importance under the conditions in interstellar and intergalactic space: 1) pair-production interactions of cosmic gamma-rays with the universal blackbody radiation field, 2) Compton interactions of cosmic gamma-rays with electrons the interstellar or intergalactic gas, and 3) pair-production interactions of cosmic gamma-rays with atoms of the interstellar or intergalactic gas. In this section, we will show how the effectiveness of these absorption processes is enhanced at high redshifts due to increased photon and matter densities at these redshifts when the universe was in a more compact state. We will also derive the energy-dependence of these absorption processes, taking cosmological factors into account.

We begin our discussion by considering the absorption of cosmic gamma-rays by pair-production interactions with photons of the universal blackbody radiation field, viz., reaction (53) whose absorption coefficients are given by equations (61)-(63).

For cosmological applications, we must take into account the redshift dependences of  $T$  and  $E_\gamma$  in an expanding universe,

$$T = T_0(1 + z)$$

and

(142)

$$E_\gamma = E_{\gamma 0}(1 + z)$$

where the subscript zero refers to presently observed ( $z = 0$ ) quantities, so that

$$T_0 = 2.7 \text{ K.}$$

Taking the  $z$ -dependence into account, we then find that the condition  $\nu \gg 1$  in equation (63) is applicable in the energy range

$$E_\gamma \ll \frac{1.12 \times 10^6 \text{ GeV}}{(1 + z)^2} \quad (143)$$

The optical depth of the universe to gamma-rays is then given by

$$\begin{aligned} \tau(E_\gamma, z_{\max}) &= \int_0^{\ell_{\max}(z_{\max})} d\ell \kappa_{\gamma\gamma}(E_\gamma, z) \\ &= \int_0^{z_{\max}} dz \kappa_{\gamma\gamma}(E_\gamma, z) \left( \frac{d\ell}{dz} \right) \end{aligned} \quad (144)$$

where, from equation (106)

$$\frac{d\ell}{dz} \simeq \frac{10^{28} \text{ cm}}{(1 + z)^2 (1 + 10^5 n_0 z)} \quad (145)$$

$n_0$  being the present mean atomic density of all the matter in the universe. We will consider here two types of model universes: 1) a "flat" or Einstein-de Sitter model with  $n_0 \sim 10^{-5} \text{ cm}^3$  and 2) an "open" model with  $n_0 \ll 10^{-5} z$ .

For the flat model, equation (144) reduces to

$$\tau(E_{\gamma 0}, z_{\max}) = 3.9 \times 10^8 E_{\gamma 0}^{-1/2} \int_0^{z_{\max}} dz \frac{\exp - [1.12 \times 10^6 / (1+z)^2 E_{\gamma 0}]}{(1+z)^{1/2}} \quad (146)$$

with  $E_{\gamma 0}$  in GeV.

For  $z_{\max} \gg 1$ , equation (146) can be further simplified to yield

$$\tau(E_{\gamma 0}, z_{\max}) \simeq 1.7 \times 10^2 E_{\gamma 0}^{1/2} (1+z_{\max})^{1/2} \exp - \left( \frac{1.12 \times 10^6}{(1+z_{\max})^2 E_{\gamma 0}} \right) \quad (147)$$

A numerical solution found by setting equation (144) for  $(E_{\gamma 0}, z_{\text{crit}}) = 1$ , which defines the critical redshift where the universe becomes opaque to gamma-rays of energy  $E_{\gamma 0}$  can be well approximated by the expression

$$1 + z_{\text{crit}} \simeq 2.60 \times 10^2 E_{\gamma 0}^{-0.484} \quad (148)$$

For the open model, we find

$$\tau(E_{\gamma 0}, z_{\max}) = 3.9 \times 10^8 E_{\gamma 0}^{-1/2} \int_0^{z_{\max}} dz \exp - \left( \frac{1.12 \times 10^6}{(1+z)^2 E_{\gamma 0}} \right) \quad (149)$$

For  $z_{\max} \gg 1$ , equation (149) may be approximated by

$$\tau(E_{\gamma 0}, z_{\max}) \simeq 1.7 \times 10^2 E_{\gamma 0}^{1/2} (1+z_{\max}) \exp - \left( \frac{1.12 \times 10^6}{(1+z)^2 E_{\gamma 0}} \right) \quad (150)$$

Thus, there is no significant difference between the opacities of the open and flat model universes. This being the case, we may invert equation (148) to obtain an expression for the predicted cut-off energy,  $E_c$ , above which gamma-rays originating at a redshift,  $z_{\max}$ , cannot reach us. This relation is then given by

$$E_c \simeq \left( \frac{2.60 \times 10^2}{1 + z_{\max}} \right)^{2.60} \quad (151)$$

and is graphed in Figure 26.

In the other extreme,  $\nu \ll 1$ , we find that as we consider higher and higher energies, the universe will not become transparent to gamma-rays again until we reach an energy  $E_{tr}$ , where the optical depth,  $\tau(E_{tr}, z_{\max})$ , again falls to unity. The expression for the optical depth when  $\nu \ll 1$  in equation (63) is given for a flat universe by

$$\tau(E_{\gamma 0}, z_{\max}) \simeq 4.4 \times 10^{13} E_{\gamma 0}^{-1} \int_0^{z_{\max}} dz (1+z)^{-3/2} \quad (152)$$

$$\simeq 8.8 \times 10^{13} E_{\gamma 0}^{-1} (1 + z_{\max})^{-1/2} \text{ for } z_{\max} \gg 1$$

and for an open universe by

$$\tau(E_{\gamma 0}, z_{\max}) \simeq 4.4 \times 10^{13} E_{\gamma 0}^{-1} \int_0^{z_{\max}} dz (1+z)^{-1} \simeq 4.4 \times 10^{13} E_{\gamma 0}^{-1} \ln(1 + z_{\max}) \quad (153)$$

In both cases we find that  $E_{tr} > 10^{13}$  GeV so that we may safely assume that the universe, due to the blackbody radiation field, is essentially opaque to gamma-rays of all energies greater than  $E_c$ .

Gamma-ray absorption by pair production and Compton interactions with intergalactic gas at high redshifts has been examined by Rees (1969) and by Arons and McCray (1969). Our discussion here essentially follows theirs. The absorption cross section for Compton interactions is given in equations (66) and (67);

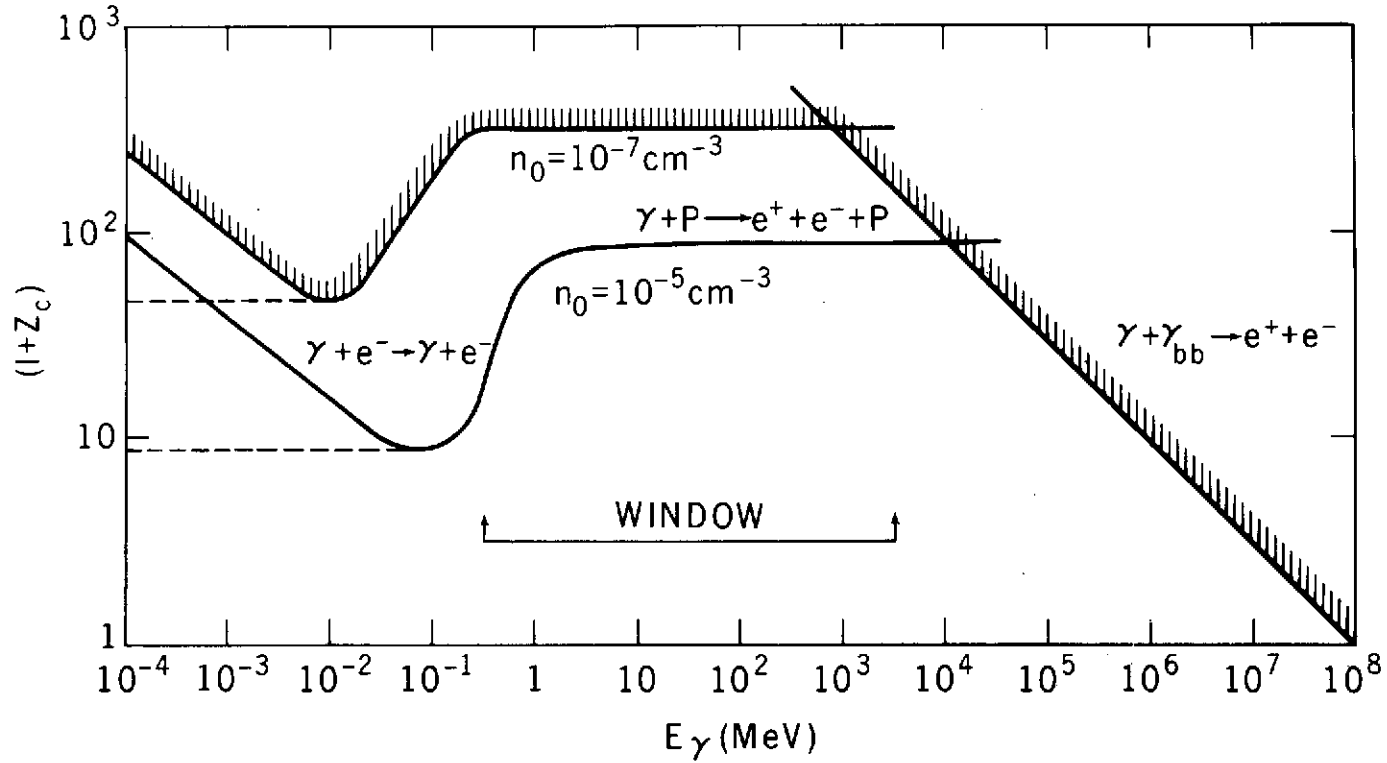


Figure 26. The redshift at which the universe becomes opaque to photons given as a function of observed gamma-ray energy. Gamma-rays originating at all redshifts below the curve can reach us unattenuated with the energy indicated. The two curves on the left side of the figure are for attenuation by Compton scattering with intergalactic electrons having the densities indicated and for pair production and are based on the calculations of Arons and McCray (1969). The right-hand curve results from attenuation of gamma-rays by interactions with the microwave blackbody radiation and is based on the discussion of Fazio and Stecker (1970).

that for pair production in equation (69). The cross sections for these processes are graphed in Figure 8. The total absorption cross section above 100 MeV energy is roughly constant equals  $1.8 \times 10^{-26}$  cm<sup>2</sup>. For the case of a constant absorption cross section, the optical depth as a function of redshifts,  $z_{\max}$ , is given by equations (144) and (145) as

$$\begin{aligned}
 \tau(z_{\max}) &= \int_0^{z_{\max}} dz n(z) \sigma \left( \frac{d\ell}{dz} \right) \\
 &= \frac{n_c \sigma c \Omega}{H_0} \int_0^{z_{\max}} dz \frac{(1+z)}{\sqrt{1+\Omega z}} \\
 &= \frac{2}{3} \tau_c \cdot \left[ \left( 3 + z - \frac{2}{\Omega} \right) \sqrt{1 + \Omega z} - \left( 3 - \frac{2}{\Omega} \right) \right]
 \end{aligned} \tag{154}$$

where

$$\tau_c \equiv n_c \sigma c H_0^{-1} = 1.8 \times 10^{-3} \tag{155}$$

a result which was first obtained by Gunn and Peterson (1965).

For an Einstein-de Sitter universe ( $\Omega = 1$ ),

$$\tau(z_{\max}) = \frac{2}{3} \tau_c [(1 + z_{\max})^{3/2} - 1] \tag{156}$$

and for a low density universe ( $\Omega z \ll 1$ )

$$\tau(z_{\max}) = \frac{\Omega}{2} \tau_c [(1 + z_{\max})^2 - 1] \tag{157}$$

At lower energies, when the cross section is not constant, the calculation is more complex.

Figure 26 shows the critical redshift for absorption of  $\gamma$ -radiation plotted as a function of observed energy. At lower energies absorption is due to Compton interactions with intergalactic matter, in the intermediate range absorption is due to pair-production interactions with intergalactic matter (Arons and McCray 1969 Rees 1969). At the higher energies absorption is due to pair production interactions with blackbody photons (Fazio and Stecker 1970). As one can see from the figure, there is a natural "window" between  $\sim 1$  MeV and  $\sim 10$  GeV which defines the optimal energy range for studying cosmological  $\gamma$ -rays.

In the case of pair production interactions, i.e., those which are important for  $E_\gamma \gtrsim 1$  MeV as shown in Figure 26, the photon completely disappears and the effect is a true absorption effect. In those cases, particularly above 10 GeV,  $z_c$  can be used as an upper limit on the integral given by equation (105) for evaluating the background energy spectrum. This immediately implies a steepening of the background spectrum above 10 GeV. However, in the case of Compton scattering, important for  $E_\gamma \lesssim 1$  MeV, we do not have a pure absorption process but rather a process in which a photon of some initial energy  $E'$  is replaced by one at some lower energy  $E$ . Thus, in order to calculate the theoretical background spectrum properly one must solve an integrodifferential scattering equation (Arons 1971 a, b). We will refer to this equation as the cosmological photon transport (CPT) equation. We can write this equation in the form

$$\frac{\partial \mathcal{I}}{\partial t} + \frac{\partial}{\partial E} [-EH(z) \mathcal{I}] = \mathcal{Q}(E, z) - \kappa_{AB}(E, z) \mathcal{I} + \int_E^{\mathcal{E}(E)} dE' \kappa_{SC}(E, z) \mathcal{I}(E|E') dE' \quad (158)$$

where  $E$  is the photon energy  $\kappa_{AB}$  and  $\kappa_{SC}$  are the photon absorption and scattering rates (which are a function of  $z$  because the intergalactic gas density is assumed to scale as  $(1+z)^3$  because of the expansion of the universe. The script quantities for the  $\gamma$ -ray intensity and production rate

$$\mathcal{I}(E, z) \equiv (1+z)^{-3} I(E, z) \quad (159)$$

and

$$\mathcal{Q}(E, z) \equiv (1+z)^{-3} Q(E, z)$$

are quantities co-moving with the expansion, defined so that their redshift-density dependence cancels out  $\mathcal{E}(E)$  is an upper limit on the scattering integral defined by the Compton process and  $H(z)$  is the Hubble parameter which, in terms of the Hubble  $H_0$ , is given by the relation

$$H(z) = H_0 (1+z) \sqrt{1 + \Omega z} \quad (160)$$

where  $\Omega$  is the ratio of the mean gas density in the universe to the density needed to close the universe gravitationally. The term

$$\frac{\partial \mathcal{I}}{\partial t} = - (1+z) H(z) \frac{\partial \mathcal{I}}{\partial z} \quad (161)$$

and the second term in equation (158) expresses the energy loss of the  $\gamma$ -rays because of the expansion redshift.

The third term in equation (158) is the source function or production function of  $\gamma$ -radiation produced with energy  $E$  at redshift  $z$ . The fourth term represents

the true absorption due to pair-production processes as well as the total scattering cross section for Compton scattering as a function of redshift and energy. Because all of the scattered photons "disappear" at energy  $E'$  but reappear at some lower energy  $E$ , the integral term in the right-hand side of the equation has to be included. This term is equivalent to a source term of photons at lower energies. The upper limit on the integral is determined by the kinematics of Compton scattering and is given by

$$\mathcal{E}(E) = \begin{cases} E/[m_e c^2 (1 - 2E/m_e c^2)], & E < \frac{1}{2} m_e c^2 \\ \infty, & E \geq \frac{1}{2} m_e c^2 \end{cases} \quad (162)$$

The CPT equation was solved numerically by Stecker, Morgan and Bredekamp (1971) in their study of the spectrum of background-radiation to be expected from cosmological matter-antimatter annihilation. Part of their results are shown in Figure 25. The curve labeled "no absorption" shows the result with the terms involving  $\kappa_{AB}$  and  $\kappa_{SC}$  set equal to zero. The curve labeled "absorption without transport" shows the result when the integral term involving  $\kappa_{SC}$  is set equal to zero. This is equivalent to removing all of the scattered photons and not replacing them at lower energies. The solid line shows the full solution.

Figure 26 shows the effect of increasing the mean gas density in the intergalactic medium and therefore the mean density of Compton scattering electrons. It clearly demonstrates the increase in the absorption due to Compton scattering at low energies as the mean density increases.

*J*

## 7. Interpretation of the Diffuse $\gamma$ -Ray Background Observations

It must have been evident very early, in an implicit way that the only source of matter large enough to give a significant background of isotropic radiation of a truly astronomical nature is the universe itself. Therefore, the connection with cosmology has been clearly the prime motivation for interest in an isotropic background radiation since Morrison's 1958 paper.

Theoretical discussions of various types may be found in the literature long before the first solid observational evidence of the existence of a gamma-ray background.

The mechanisms listed by Morrison (1958) to be of possible significance in producing continuum radiation were synchrotron radiation, cosmic-ray electron bremsstrahlung,  $\pi^0$ -meson decay (from cosmic ray-nucleon interactions) and antimatter annihilation. To these four, one more mechanism, viz., Compton interactions between cosmic-ray electrons and starlight (Felten and Morrison, 1963) was added. It later became apparent when the 3K blackbody radiation was discovered that these photons would be orders of magnitude more numerous than starlight photons in intergalactic space as targets for cosmic-ray electrons and should thus be the prime Compton radiation generators of cosmological interest. That the significance of this was readily grasped is obvious from the plethora of independent suggestions made immediately after the discovery of the microwave background radiation (Felten 1965, Gould 1965, Hoyle 1965, Fazio, Stecker and Wright 1966, Felten and Morrison 1966). The relative weakness of intergalactic

magnetic fields, evidenced by data on the non-thermal radio background, eliminated synchrotron radiation as a prime contender in generating the diffuse gamma-ray background so that four mechanisms were left

- (a) electron bremsstrahlung
- (b) electron-photon interactions (Compton effect)
- (c) cosmic-ray produced  $\pi^0$ -decay
- (d) decay of  $\pi^0$ -mesons from matter-antimatter annihilations

Evidence for a diffuse background above 50 MeV was reported by Kraushaar and Clark (1962) from measurements on Explorer 11. The interpretation of Felten and Morrison (1963) that both the Ranger 3 and Explorer 11 results could be fitted reasonably well by a single power law of the type expected from Compton interactions seemed logical despite a possible flattening above 1 MeV reported by Arnold, et al. (1962) and it was expected that data in the two energy decades between 1 and 100 MeV would exhibit nothing more exciting than a smooth power law spectrum as extrapolated from the sub-MeV ("X-ray") energies.

In the late 60's the author, after having made detailed thesis calculations of gamma-ray spectra from cosmic-ray produced secondary particles and from proton-antiproton annihilation (Stecker 1967), became interested in the effects cosmology might have on such spectra and on the implications of these effects for cosmology itself. Cosmic-ray  $\pi^0$ -decay was suspected to play a major role in generating galactic gamma-rays (Pollack and Fazio 1963) and it remained a viable possibility the extragalactic background flux above 100 MeV. But if such

interactions are occurring in intergalactic space now, why not in the distant past when gas and cosmic-ray densities were higher (in an expanding universe)? If so, large fluxes of extragalactic cosmic-rays (comparable to galactic fluxes) need not exist now to explain the 100 MeV background (Stecker 1968, 1969a). Also, the spectrum would be redshifted and would be softer than the galactic spectrum (Stecker 1969b). Similar ideas were being independently worked on by Ginzburg (1968) in the context of the Lamaitre cosmological model and by Rozental and Shukalov (1969) for the standard expanding universe model. In these models, various cosmological effects come into play to distort the spectrum from  $\pi^0$  decay and redshift its characteristic peak from an energy of  $m_\pi c^2/2 \simeq 70$  MeV to lower energies (see extensive discussions in the monographs by Stecker (1971a) and Ozernoi, Prilutsky and Rozental (1973)). The result was the prediction of a possible enhancement in the gamma-ray background spectrum between 1 and 100 MeV deviating from the simple power law extrapolation of the X-ray background.

Figure 29 shows a two component model normalized for a best-fit to the observations involving the production of intergalactic gamma-rays from cosmic-ray interactions with intergalactic gas producing  $\pi^0$ -mesons out to a maximum redshift of 100 (Stecker 1969b, c, 1971b). Three problems arise with this explanation: 1) even with a relatively steep assumed cosmic-ray spectrum ( $\sim E^{-2.7}$ ) the bulge in the theoretical spectrum may be too large to fit the observations, although this discrepancy may not be too serious considering

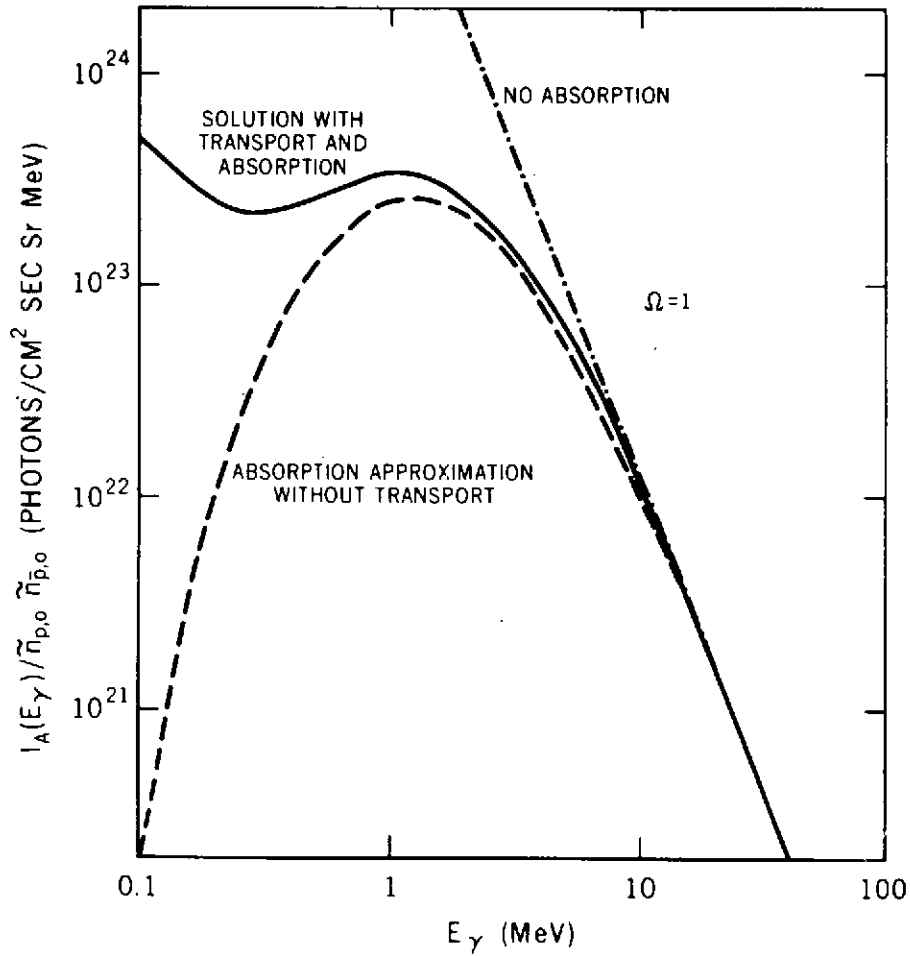


Figure 27. The cosmological  $\gamma$ -ray spectrum from matter-antimatter annihilation calculated by solving the CPT equation numerically for  $\Omega = 1$ . The solid line represents the complete solution. The other curves represent the effect of neglecting the absorption and scattering (transport) terms in equation (158).

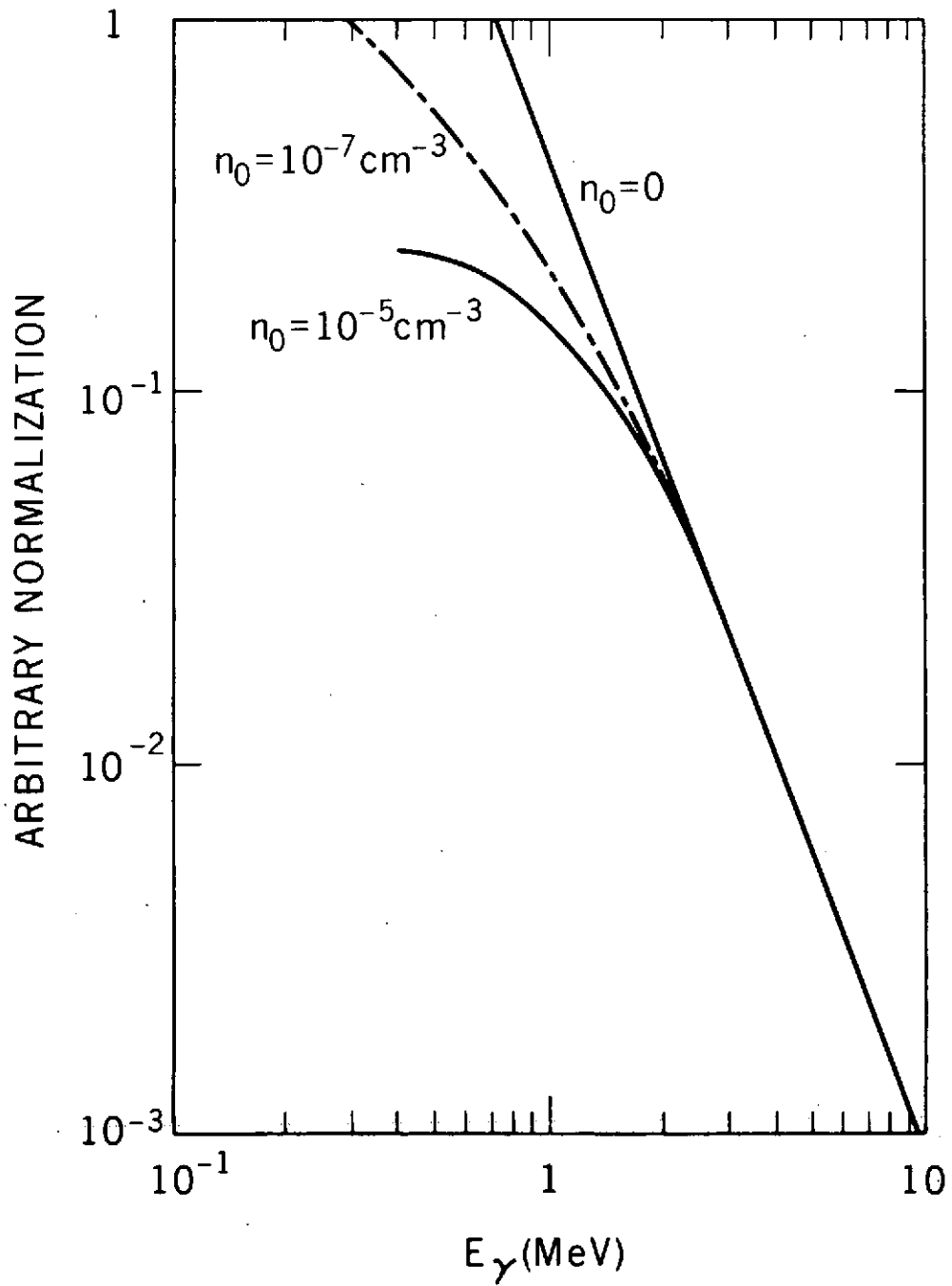


Figure 28. The effect of absorption of  $\gamma$ -rays at high redshifts by the protogalactic gas.

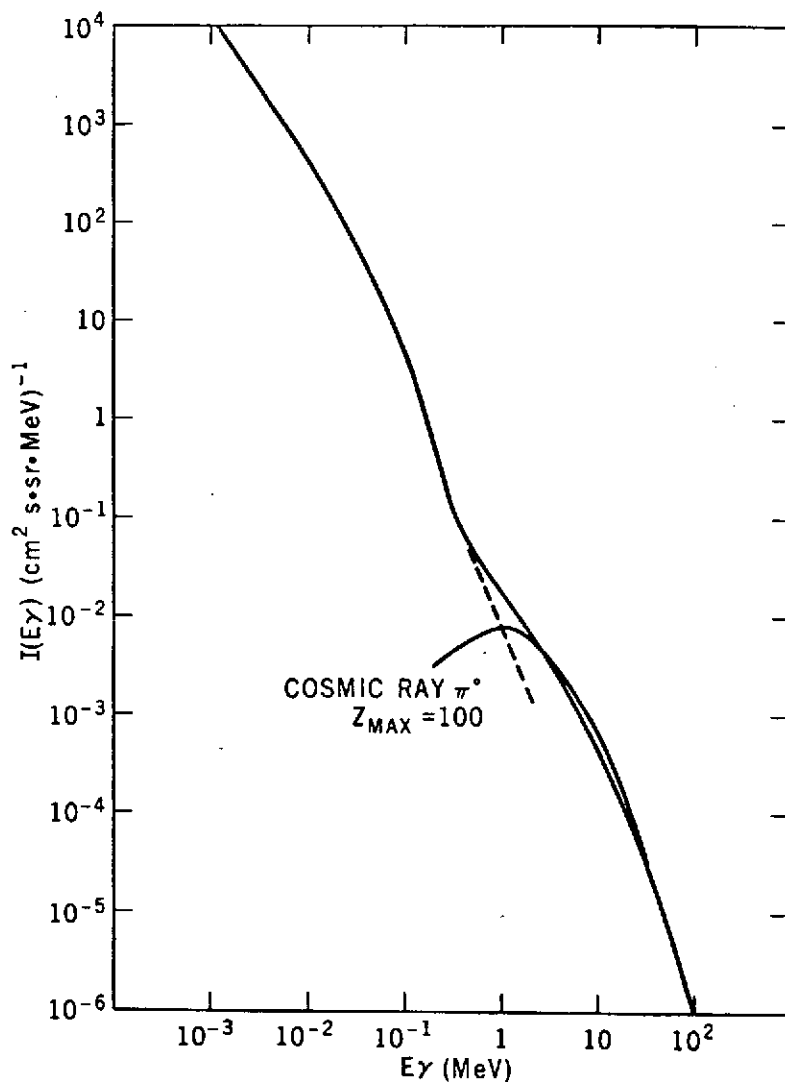


Figure 29. Comparison of the observed background with a two-component model involving the production and decay of neutral pions produced in intergalactic cosmic-ray interactions at red-shifts up to 100.

observational uncertainties, 2) large amounts of energy are needed in cosmic-rays at high-red-shifts, requiring the existence of strong primordial cosmic-ray sources (protars) which are either pregalactic or protogalactic. Such objects may have been the "spinars" suggested by Morrison (1969) if spinars existed at such redshifts of about 70-100 (Stecker 1971b). If it is considered that each spinar produces approximately  $10^{62}$  ergs over a time scale of  $10^7$ - $10^8$  years (Morrison 1969), a time comparable to the Hubble time at these redshifts, then at most 20 percent of the presently observed galaxies are needed to have arisen from this early spinar state in order to provide the cosmic-ray energy needed to account for the diffuse  $\gamma$ -radiation above 1 MeV. At a redshift of about 70, the free-fall time for forming spinars from gas clouds is comparable to the Hubble time. This may provide a natural upper limit to the redshift,  $z_{\text{MAX}}$ , for primordial cosmic-ray production in the spinar model. (It should, however, be noted that such spinars may arise in other ways (see Stecker 1971b) and that they may now be a class of moribund objects unrelated to galaxies as we see them now). 3) The third problem with this hypothesis is that the maximum redshift for cosmic ray production  $z_{\text{max}}$  is a free parameter chosen to fit the observations.

A related hypothesis examined by Stecker et al. (1971) and Stecker and Puget (1972) is that the  $\gamma$ -ray background is from redshifted  $\pi^0$ -decay  $\gamma$ -rays but that  $\pi^0$ -mesons are the result of nucleon-antinucleon annihilation at an early epoch in the history of the universe. The annihilation hypothesis does not suffer from

the above mentioned problems of the cosmic-ray protar hypothesis. The parameter  $z_{\max}$  does not enter into the theory; annihilations occur at all redshifts and the 1 MeV-flattening is an absorption effect as discussed earlier. The transport equation (158) was solved to determine the exact form of the spectrum. Energy considerations do not present a problem. Another advantage of the theory is that it arises as a natural effect in a cosmology such as that suggested by Omnès (1972 and references therein) Figure 30 shows a detailed comparison of the annihilation hypothesis spectrum with present observations. The dashed line shows the effect of adding in an additional component which is a power-law extrapolation of the x-ray background. The two component model shown provides an excellent fit to the observational data.

Early observations of gamma-radiation by Kraushaar and Clark (1962) had clearly indicated that if antimatter exists in the universe in large amounts, it must clearly be separated from matter so that the average annihilation rate is quite small. In 1969, Omnès suggested a baryon symmetric (equal amounts of matter and antimatter) cosmology based on a possible phase transition effect which could separate matter from antimatter at an early stage in the big-bang corresponding to nuclear density for the cosmic plasma. The phase transition effect was also studied by Aldrovandi and Caser (1972) and Cisneros (1973). Further work by Omnès (1972 and references therein) showed that the separate domains of matter and antimatter could grow to contain masses of the size of galaxies by the recombination epoch. This result has recently been refined by

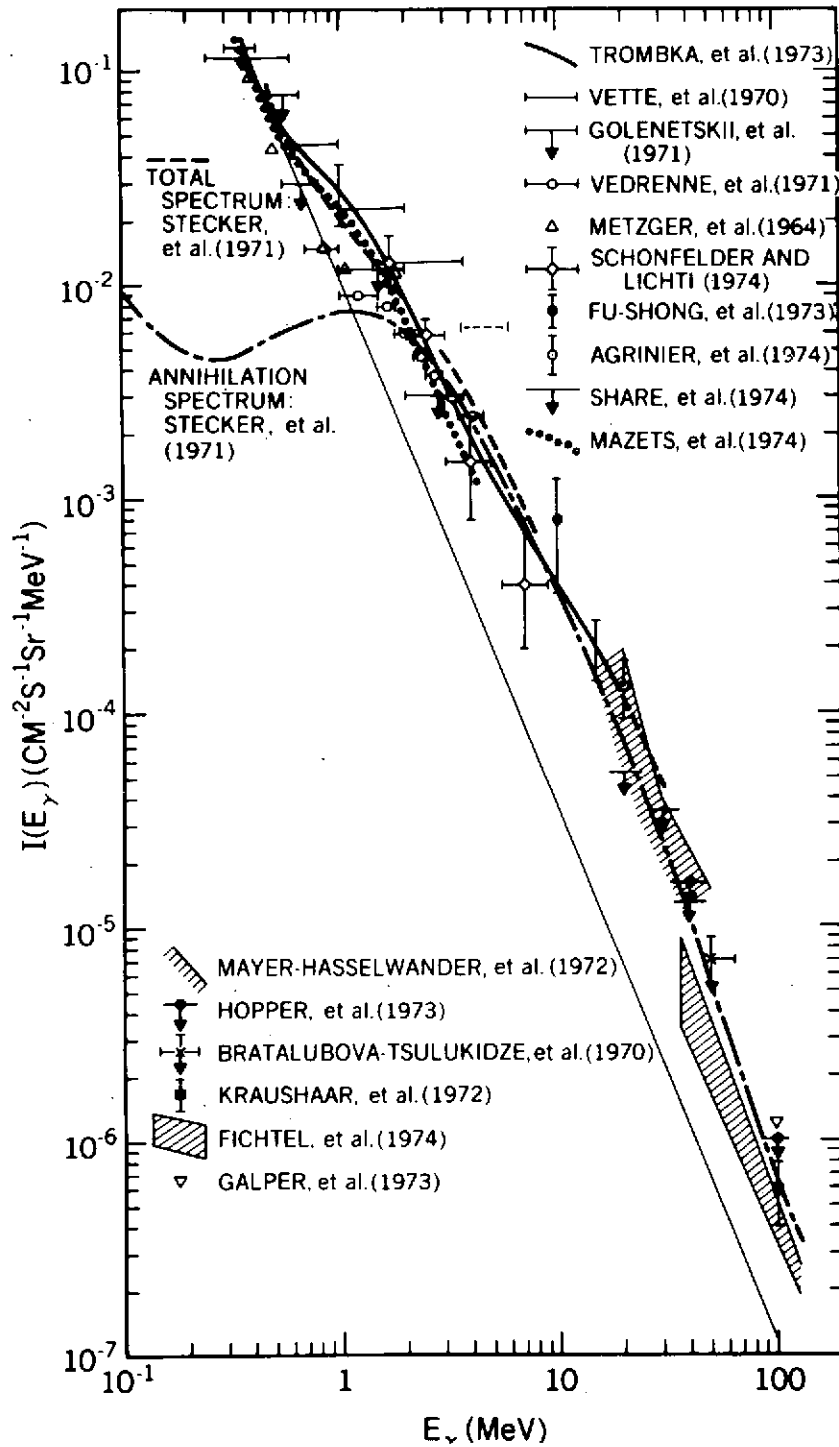


Figure 30. A comparison of the data given in Figure 25 with the annihilation model discussed by Stecker, Morgan and Bredekamp (1971) and Stecker and Puget (1972).

Aldrovandi et al. (1973). It was to be expected that boundary-region annihilations in this picture would also produce redshifted  $\pi^0$ -decay radiation and absorption effects would cut off the resultant flux below 1 MeV. Therefore, Stecker, Morgan and Bredekamp (1971) were motivated to make a detailed calculation of the resultant diffuse background spectrum to be expected, and the results agreed fairly well with the observations then available. The encouraging enhancement in the 1 to 100 MeV range is partially due to the existence of a "gamma-ray window" in this energy range as shown in Figure 26. The results were encouraging enough to examine further the evolution of the Omnès cosmology for redshifts less than  $10^3$  (Stecker and Puget 1972). This study had several exciting implications

- (a) separate regions containing masses the size of galaxy clusters could be obtained.
- (b) turbulence produced by annihilation pressure could provide enough energy to trigger galaxy formation.
- (c) estimates obtained placed the galaxy formation stage at redshifts of the order of 60.
- (d) mean densities and angular momenta of galaxies could be estimated in this picture consistent with observation and related to the annihilation rates calculated by the model and implied by the observations.

The general scheme of the galaxy formation model is shown in Figure 31.

The observational implications of the model are outlined in Figure 32.

## GENERAL SCHEME OF MODEL

- MATTER AND ANTIMATTER EXIST IN EQUAL AMOUNTS IN SEPARATE REGIONS.
- MIXING OCCURS ALONG BOUNDARY REGIONS OF THICKNESS  $\sim \lambda_A$ .
- RESULTING RAPID HEATING OF PLASMA WITHIN A DISTANCE  $\sim \lambda_X$  OF BOUNDARY BY ANNIHILATION PRODUCTS PRODUCES EXPANSION AWAY FROM BOUNDARY.
- RESULTING EXPANSION OF PLASMA INDUCES HIGH-VELOCITY GAS MOTIONS.
- DURING THE NEUTRALIZATION ERA (POSSIBLY EVEN SOMEWHAT BEFORE) GAS MOTIONS BECOME TURBULENT ( $\sim 500 \leq Z \leq \sim 3000$ ).
- WHEN GAS GOES FROM PLASMA TO ATOMIC STATE ( $\sim 400 \leq Z_N \leq \sim 600$ ):
  - A) DUE TO DECOUPLING OF MATTER FROM RADIATION FIELD, VISCOSITY DROPS BY ALMOST 8 ORDERS OF MAGNITUDE AND SOUND VELOCITY DROPS BY FOUR ORDERS OF MAGNITUDE.
  - B) THIS CAUSES TURBULENCE TO BECOME SUPERSONIC AND TO EXTEND THE EDDY SPECTRUM DOWN TO A SCALE OF THE ORDER OF  $10^{-3}$  pc.
  - C) THE SUPERSONIC TURBULENCE INDUCES DENSITY FLUCTUATIONS  $\Delta\rho/\rho \sim 1$  OVER THE WHOLE RANGE OF EDDY SCALES.
- AT A REDSHIFT OF  $\frac{2}{15}Z_N$  OR ABOUT 60, VIRIAL THEOREM BECOMES SATISFIED FOR BINDING OF GAS CLOUDS INTO PROTOGALAXIES DUE TO DENSITY FLUCTUATIONS INDUCED BY SUPERSONIC TURBULENCE.

Figure 31. Outline of the galaxy formation theory of Stecker and Puget (1972).

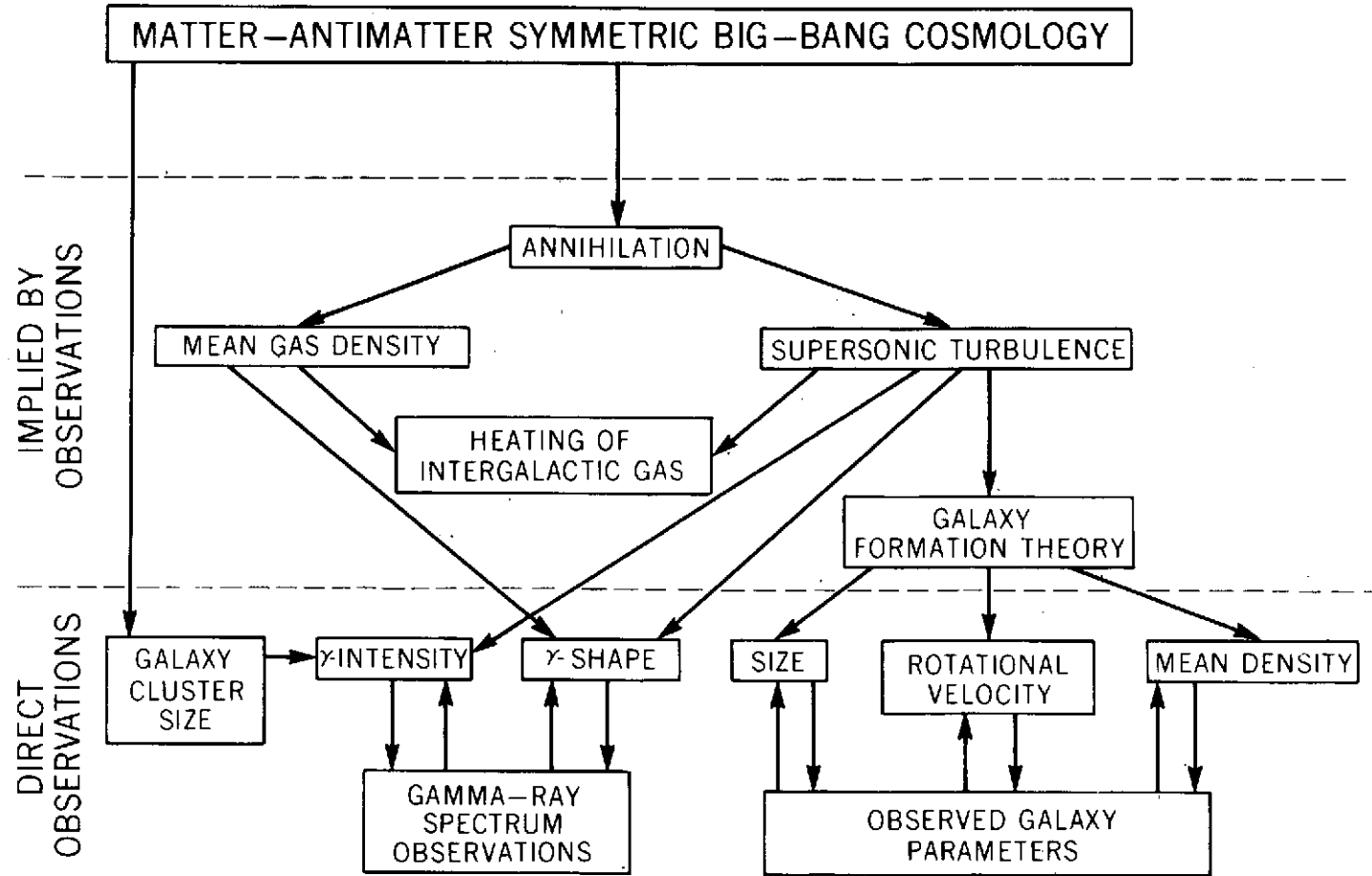


Figure 32. Observational implications of baryon symmetric cosmology.

Several other models of isotropic  $\gamma$ -ray production have been put forward. One suggestion is that the whole spectrum in the  $10^{-3}$ - $10^2$  MeV range is due to Compton interactions of intergalactic electrons with the universal blackbody radiation (Felton 1965, Gould 1965, Hoyle 1965, Fazio, Stecker and Wright 1966, Felten and Morrison 1966). In its most recent version Brecher and Morrison (1969) have attempted to explain the observed spectral features using the Compton hypothesis, however, Cowsik and Kobetich have done a more detailed calculation indicating that the Compton mechanism generates a smooth featureless power-law spectrum.

Figure 32 shows the energy spectrum  $J(E_\gamma) \equiv E_\gamma I(E_\gamma)$  of the background radiation between  $10^{-3}$  and 200 MeV as based on the review paper of Schwartz and Gursky (1973) and the data shown in Figure 23. An extrapolation of the data between 30 keV and 1 MeV is shown by the dashed line. A strong deviation from a power-law spectrum is indicated.

A critical test between the cosmic ray proton and annihilation hypotheses lies in a study of the energy spectrum. Figure 33 shows the present range of the data, indicated by the shaded region, along with the extrapolated power-law spectrum (X) the annihilation spectrum (A) and the high energy form of the spectrum predicted for redshifted cosmic-ray  $\pi^0$ -decay gamma-rays (CR). The annihilation spectrum should exhibit a sharp cutoff slightly below 1 GeV because the energy of the gamma-rays is limited by the rest-energy available to them from baryon-antibaryon annihilations. A detailed discussion of this

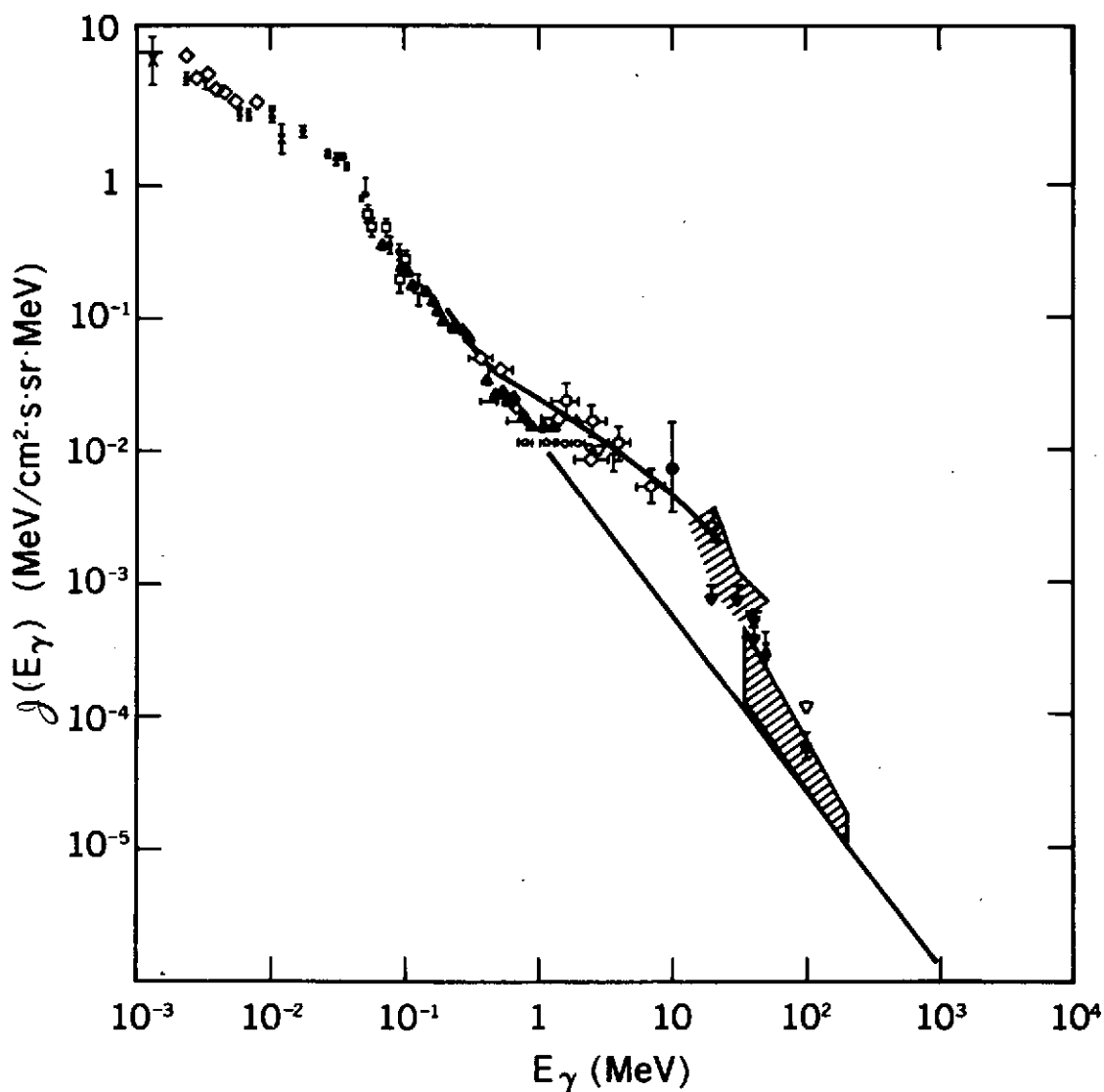


Figure 33. Energy flux spectrum of the x-ray and gamma-ray background based on Schwartz and Gursky (1973) and the data given in Figure 25. The straight diagonal line indicates an extrapolation of the 30 keV to 1 MeV spectrum.

may be found in Stecker (1971a). The cosmic-ray produced spectrum, on the contrary, can continue up to higher energies with a steepening induced around 10 GeV by pair-production losses through interactions with the microwave background (Fazio and Stecker 1970). This steepening should amount to an increase of 0.5 in the spectral index for a closed Einstein-de Sitter universe and an increase of 0.75 in the spectral index for a low-density open universe (Stecker 1971a). It should be kept in mind that the cutoff in the annihilation spectrum may be somewhat obscured by the presence of other background radiations having relatively lower intensities below 200 GeV.

Various other mechanisms which have been discussed in connection with the interpretation of the origin of the  $\gamma$ -ray background may be found in a review last year by the author (Stecker 1973c).

Another recent hypothesis for the origin of the background radiation which also involves primordial cosmic rays is that of Strong, et al. (1973). This hypothesis is based on the model of Hillas (1967) that the observed cosmic rays, at least those above  $\sim 10^6$  GeV, are universal and primordial. Hillas showed that if the observed cosmic rays originated at a redshift  $z_{\text{max}} \simeq 15$ , energy losses that these cosmic rays would undergo in pair-production interactions with the black-body photons of the type



would steepen the spectrum at the presently observed energy of  $\sim 3 \times 10^6$  GeV.

At a redshift of  $\sim 15$ , when these interactions took place, the blackbody photons had an energy of  $\sim 10^{-2}$  eV and the cosmic rays had an energy of  $\sim 5 \times 10^7$  GeV. The electron-positron pairs produced would then produce a shower of lower energy  $\gamma$ -rays through a repeated two-stage interaction process with the blackbody radiation field involving Compton scattering followed by pair production, i.e.,

$$e^{\pm} + \gamma_{\text{blackbody}} \rightarrow e^{\pm} + \gamma_{\text{high energy}}$$

followed by

(164)

$$\gamma_{\text{blackbody}} + \gamma_{\text{High energy}} \rightarrow e^+ + e^-$$

The resultant spectrum based on a complex model is shown in Figure 35. Both the Hillas model and the hypothesis of Strong, et al. require an exceedingly low intergalactic gas density,  $n_0 \lesssim 10^{-9} \text{ cm}^{-3}$ , in order that the  $\gamma$ -rays produced by the cosmic ray model of Stecker (1969b) do not exceed the observed background level.

If the intergalactic gas density should turn out to be of the order of  $10^{-9} \text{ cm}^{-3}$  which is only about 1% of the mean matter density in galaxies, we would have to radically alter our ideas about galaxy formation in order to account for 99% of the mass in the universe to be bound into galaxies.

Present observations give a background flux of  $\gamma$  radiation above 100 MeV of about

$$J = \frac{qL}{4\pi} = 3 \times 10^{-5} \text{ cm}^{-2} \text{ s}^{-1} \text{ Sr}^{-1} \quad (165)$$

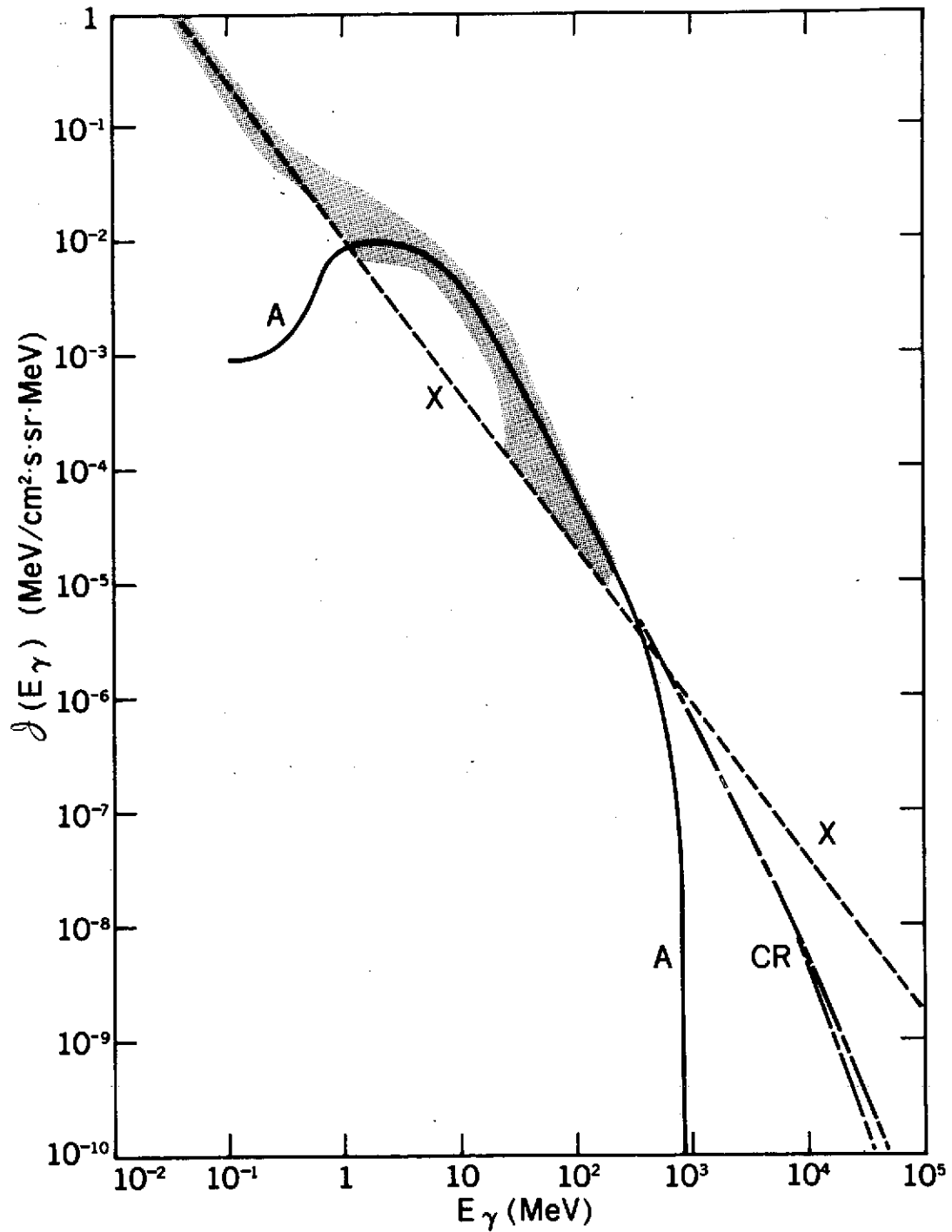


Figure 34. Predicted energy flux spectra from the annihilation model (A) and cosmic ray (protar) model (CR) as discussed in the text. Also shown is the scatter area covered by the observational data (shaded) and the extrapolated x-ray background spectrum (X). The two curves shown for the CR spectrum above 7 GeV are for closed (Einstein-de Sitter) and open universes as discussed in the text (Stecker 1971a).

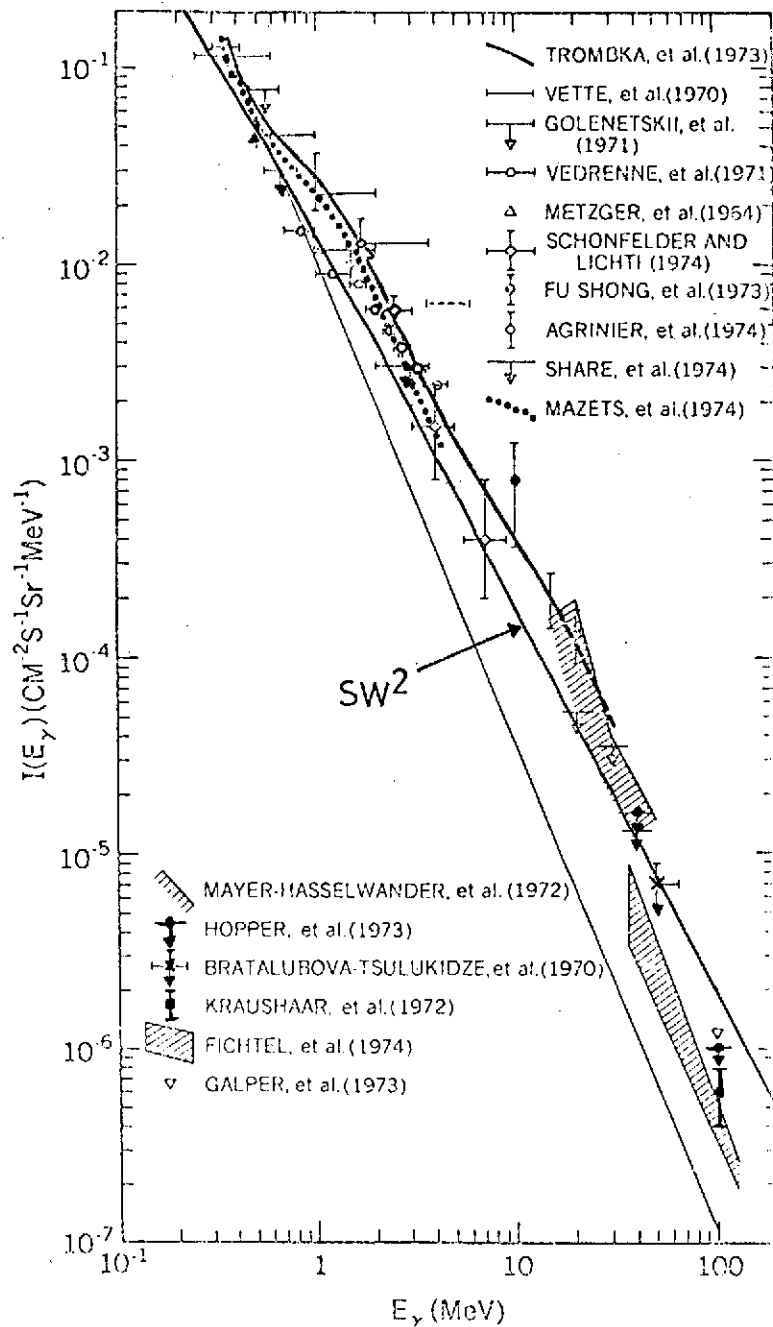


Figure 35. The  $\gamma$ -ray background calculated from the Hillas model by Strong, et al. (1973) ( $SW^2$ ). Also shown are the data from Figure 25 for comparison.

where the path length

$$L \simeq \frac{c}{H_0} \simeq 10^{28} \text{ cm} \quad (166)$$

and the production rate

$$\begin{aligned} q &\simeq 1.3 \times 10^{-25} n_H \zeta \\ &\simeq 10^{-30} \Omega \xi \end{aligned} \quad (167)$$

where  $\xi$  is the ratio of intergalactic to galactic cosmic ray intensity if part of the background is produced by noncosmological (contemporary  $z = 0$ ) cosmic rays. If we call the fraction of the background produced by contemporary cosmic rays  $f$ , then from equations (165) to (167)

$$3 \times 10^{-5} f \simeq 10^{-3} \Omega \xi \quad (168)$$

because the background spectrum is observed to be quite steep, conservatively  $f \lesssim 1/3$  so that the limit on the product of intergalactic gas density and cosmic ray intensity becomes

$$\Omega \xi \lesssim 10^{-2} \quad (169)$$

This excludes the possibility of both universal cosmic rays ( $\xi = 1$ ) and a closed universe ( $\Omega = 1$ ).

More stringent upper limits can be placed on primordial cosmic rays (Stecker 1971b) and the antimatter annihilation rate (Stecker, et al. 1971), Stecker and Puget 1972). Thus it would seem that  $\gamma$ -ray astronomy at present can with

certainty only put limits on our speculations about the origin of cosmic rays. But on the other hand we can say that speculations about the origin of cosmic  $\gamma$ -rays have broadened our conceptions about high-energy astrophysics and cosmology.

#### REFERENCES

1. Agrinier, B., Forichon, M., Laray, J. P., Parlier, B., Montmerle, T., Boella, G., Maraschi, L., Sacco, B., Scarsi, L., Da Costa, J. M., and Palmeria, R. 1973, Proc. 13th Int. Conf. on Cosmic Rays, Denver, 1, 8.
2. Aldrovandi, R., and Caser, S. 1972. *Nuc. Phys.* B38, 593.
3. Aldrovandi, R., Caser, S., Omnes, R. and Puget, J. L. 1973. *Astron. and Astrophys.* 28, 253.
4. Allen, C. W. 1973. Astrophysical Quantities, Athbone Press, London.
5. Arnold, J. R., Metzger, A. E., Anderson, E. C. and Van Dilla, M. A. 1962. *J. Geophys. Res.* 67, 4878.
6. Arons, J. and McCray, R. 1969. *Astrophys. J.* 158, L91.
7. Arons, J. 1971a. *Astrophys. J.* 164, 437.
8. Arons, J. 1971b. *Astrophys. J.* 164, 457.
9. Bignami, G. F. and Fichtel, C. E. 1974. *Astrophys. J.* 189, L65.
10. Boldt, E. and Serlemitsos, P. 1969. *Astrophys. J.* 157, 557.
11. Bratalubova-Tsulukidze, L. I., Grigorov, N. L., Kalinkin, L. F., Melioransky, A. S., Pryakhin, E. A., Savenko, I. A., and Yufarkin, V. Ya. 1970. *Acta Phys.* 29, Suppl. 1.

12. Brecher, K. and Morrison, P. 1967. *Astrophys. J.* 150, L61.
13. Brecher, K. and Morrison, P. 1969. *Phys. Rev. Lett.* 23, 802.
14. Brown, J. W., Stone, E. C. and Vogt, R. E. 1973. Proc. 13th. Int. Conf. on Cosmic Rays, Denver, 484.
15. Cavallo, G. and Gould, R. J. 1971. *Nuovo Cimento* B2, 77.
16. Cisneros, A. 1973. *Phys. Rev.* D7, 362
17. Clark, D. H., Caswell, J. L. and Green, A. J. 1973. *Nature* 246, 28.
18. Comstock, G. M., Hsieh, K. C., and Simpson, J. A. 1972. *Astrophys. J.* 173, 691.
19. Cowsik, R. and Kobetisch, E. J. 1972. *Astrophys. J.* 177, 585.
20. Dovzhenko, O. I., and Pomanskii, A. A. 1964. *Sov. Phys. JETP* 18, 187.
21. Fazio, G. G., Stecker, F. W. and Wright, J. P. 1966. *Astrophys. J.* 144, 611.
22. Fazio, G. G. and Stecker, F. W. 1970. *Nature* 226, 135.
23. Feenberg, E. and Primakoff, H. 1947. *Phys. Rev.* 73, 449.
24. Felten, J. E. and Morrison, P. 1963. *Phys. Rev. Lett.* 10, 453.
25. Felten, J. E. 1964. *Phys. Rev. Lett.* 15, 1003.
26. Felten, J. E. and Morrison, P. 144, 241.
27. Fermi, E. 1954, *Astrophys. J.* 119, 1.
28. Fichtel, C. E., Hartman, R. C., Kniffen, D. A. and Sommer, M. 1972. *Astrophys. J.* 171, 31.
29. Fichtel, Kniffen, D. A. and Hartman, R. C. 1973. *Astrophys. J.* 186, L99.

30. Frye, G. M. and Smith, L. H. 1966. *Phys. Rev. Lett.* 17, 733.
31. Frye, G. M., Albats, P. A., Zych, A. D., Starb, J. A. Hopper, V. D.,  
Rawlinson, W. R., and Thomas, J. A. 1974. *Proc. ESLAB Symposium on  
the Context and Status of  $\gamma$ -Ray Astronomy, Frascati, Reidel, in press.*
32. Fu-Shong, K., Frye, G. M., and Zych, A. D., 1973. *Astrophys. J. Lett.*  
186, L51.
33. Golenetskii, S. V., Mazets, E. P., Il'insky, V. N., Aptekhar, R. L., Bredov,  
M. M., Gur'yan, Yu. A. and Panov, V. N. 1971, *Astrophys. Lett.* 9, 69.
34. Garmire, G. and Kraushaar, W. L. 1965. *Space Sci. Rev.* 4, 123.
35. Ginzburg, V. L. and Syrovatsky, S. I. 1964. *The Origin of Cosmic Rays*,  
MacMillan, New York.
36. Ginzburg, V. L. 1968. *Astrophys. and Space Sci.* 1, 1.
37. Gould, R. J. 1965. *Phys. Rev. Lett.* 12, 511.
38. Gould, R. J. and Schréder, G. P. 1966 *Phys. Rev. Lett.* 16, 252.
39. Gould, R. J. and Schréder, G. P. 1967a. *Phys. Rev.* 155, 1404.
40. Gould, R. J. and Schréder, G. P. 1967b. *Phys. Rev.* 155, 1408.
42. Greisen, K. 1966. *Phys. Rev. Lett.* 16, 748.
43. Gunn, J. E. and Peterson, B. A. 1965. *Astrophys. J.* 142, 1633.
44. Hayakawa, S. 1952. *Prog. Theor. Phys.* 8, 571.
45. Heitler, W. 1960. *The Quantum Theory of Radiation*, Oxford Press,  
London.
46. Helmkin, H. and Hoffman, J. 1973. *Nature Phys. Sci.* 243, 6.

47. Hillas, A. M. 1968. *Can. J. Phys.* 46, S623.
48. Hoffman, W. F. and Frederick, C. L. 1969. *Astrophys. J. Lett.* 155, L12.
49. Hollenback, D. J. and Salpeter, E. E. 1971. *Astrophys. J.* 163, 155.
50. Hollenback, D. J., Werner, M. W. and Salpeter, E. D. 1971. *Astrophys. J.* 163, 165.
51. Hoyle, F. 1965. *Phys. Rev. Lett.* 15, 131.
52. Hopper, V. D., Mace, O. B., Thomas, J. A., Albats, P., Frye, G. B., Thomson, G. B. and Staib, J. A. 1973. *Astrophys. J.* 186, L55.
53. Hutchinson, G. W. 1952. *Phil. Mag.* 43, 847.
54. Ilovaisky, S. A. and Lequeux, J. 1972. *Astron. and Astrophys* 20, 347.
55. Jauch, J. M. and Rohrlich, F. 1955. *The Theory of Photons and Electrons*, Addison-Wesley, Cambridge, Mass..
56. Jelly, J. V. 1966 *Phys. Rev. Lett.* 16, 479.
57. Jones, F. C. 1965. *Phys. Rev.* 137B, 1306.
58. Jones, F. C. 1967. *Can. J. Phys.* 46, S1003.
59. Kniffen, D. A. Hartman, R. C. Thompson, D. J. and Fichtel, C. E. 1973. *Astrophys. J.* 186, L105.
60. Kraushaar, W. L. and Clark, G. W. 1962. *Phys. Rev. Lett.* 8, 106.
61. Kraushaar, W. L., Clark, G. W., Garmire, G. P., Borken R., Higbie, P., Leong, C. and Thorsos, T. 1972. *Astrophys. J.* 177, 341.
62. Mayer-Hasselwander, H. A., Pfefferman, E., Pinkau, K., Rothermel, H., and Sommer, M. 1972. *Astrophys. J. Lett.* 175, L23.

63. Mazetz, E. P., Golenetskii, S. V., Il'inskii, V. N., Gur'yan, Yu. A., and Kharitonova, T. V. 1974. A. F. Joffe Physico-Technical Institute Preprint No. 468.
64. Metzger, A. E., Anderson, E. C., Van Dilla, M. A. and Arnold, J. R. 1964, Nature, 204, 766.
65. Morrison, P. 1958. Il Nuovo Cimento 1, 858.
66. Morrison, P. 1969. Astrophys. J. 157, L75.
67. Nikishov, A. I., 1962. Sov. Phys. JETP 14, 393.
68. O'Dell, F. W., Shapiro, M. M., Silberberg, R., and Tsao, C. H. 1973. Proc. 13th. Intl. Conf. on Cosmic Rays, Denver, 490.
69. Omnès, R. 1972, Physics Reports 3C, 1.
70. Oort, J. H. 1970. Galactic Astronomy, (ed. H. Y. Chiu and A. Muriel) Gordon and Breach, New York, 129.
71. Ozernoi, L. M., Prilutsky, O. F. and Rozental, I. L. 1973. Astrofizika Visokikh Energy Atomizdat, Moscow, USSR.
72. Pollack, J. B. and Fazio, G. G. 1963. Phys. Rev. 131, 2684.
73. Puget, J. L. and Stecker, F. W. 1974. Astrophys. J. 191, 323.
74. Rees, M. J. 1969. Astrophys. Lett. 4, 113.
75. Rozental, I. L. and Shukalov, I. 1969. Astron. Zh. 46, 779 (Trans. 1970 Sov. Astron. A. J. 13, 612).
76. Samimi, J. Share, G. H. and Kinzer, R. L. 1974. Proc. ESLAB Symposium on the Context and Status of  $\gamma$ -Ray Astronomy, Frascati, Reidel, in press.

77. Sanders, R. H. and Wrixon, G. T. 1972. *Astronomy and Astrophysics* 18, 92.
78. Sanders, R. H. and Wrixon, G. T. 1973, *Astron. and Astrophys.* 26, 365.
79. Schmidt, M. 1965. Galactic Structure (ed. A. Blaauw and M. Schmidt)  
U. of Chicago, Press, Chicago, Ill., 513.
80. Schwinger, J. 1949. *Phys. Rev.* 75, 1912.
81. Schönfelder, V., and Lichti, G. 1974. *Astrophys. J.* 191, L1.
82. Schwartz, D. and Gursky, H. 1973. Gamma Ray Astrophysics, (F. W. Stecker  
and J. I. Trombka, ed.) NASA SP-339 U.S. Gov't. Printing Office, Washington,  
D. C., 15.
83. Shane, W. W. 1972. *Astron and Astrophys.* 16, 118.
84. Share, G. H., Kinzer, R. L. and Seeman, N. 1974. *Astrophys. J.* 187, 45.
85. Share, G. H., Kinzer, R. L., and Seeman, N. 1974. *Astrophys. J.*, 187, 511.
86. Solomon, P. M., and Wickramasinghe, N. C. 1969. *Astrophys. J.*, 158, 449.
87. Solomon, P. M. and Stecker, F. W. 1974. *Proc. ESLAB Symposium on the  
Context and Status of  $\gamma$ -Ray Astronomy, Frascati, Reidel, in press.*
88. Sood, R. K., Bennett, K. Clayton, P. G. and Rochester, G. K. 1974. *Proc.  
ESLAB Symposium on the context and Status of  $\gamma$ -Ray Astronomy Frascati,  
Reidel, in press.*
89. Spitzer, L., Drake, J., Jenkins, E. B., Morton, D. C., Rogerson, J. B. and  
York, D. G. 1973. *Astrophys. J.* 181, L116.
90. Stecher, T. P., and Stecker, F. W. 1970. *Nature* 226, 1234.
91. Stecker, F. W. 1967. *Smithsonian Astrophys. Obs. Spec. Rpt. No.* 261.

92. Stecker, F. W. 1968a. Phys. Rev. Lett. 21, 1016.
93. Stecker, F. W. 1968b. Nature, 220, 675.
94. Stecker, F. W. 1969a. Nature, 222, 1157.
95. Stecker, F. W. 1969b. Astrophys. J. 157, 507.
96. Stecker, F. W. 1969c. Nature, 224, 870.
97. Stecker, F. W. 1970. Astrophys. & Space Sci. 6, 377.
98. Stecker, F. W. 1971a. Cosmic Gamma Rays, Mono Book Corp.,  
Baltimore, Md.
99. Stecker, F. W. 1971b. Nature, 229, 105.
100. Stecker, F. W. 1973a. Astrophys. J. 185, 499.
101. Stecker, F. W. 1973b. Astrophys. and Space Sci. 20, 47.
102. Stecker, F. W. 1973c. Gamma Ray Astrophysics, (F. W. Stecker and  
J. I. Trombka, ed.) NASA SP-339, U. S. Gov't Printing Office, Washington,  
D. C., 211.
103. Stecker, F. W. and Morgan, D. L. 1972. Astrophys. J. 171, 201.
104. Stecker, F. W. Morgan, D. L. and Bredekamp. J. 1971, Phys. Rev. Lett.  
27, 1469.
105. Stecker, F. W., Puget, J. L., Strong, A. W. and Bredekamp, J. H., 1974.  
Astrophys. J. 188, L59.
106. Stecker, F. W. and Trombka, J. I. 1973. Gamma Ray Astrophysics, NASA  
SP-339, U. S. Gov't Printing Off. Washington, D. C.

107. Strong, A. W., Wdowczyk, J. and Wolfendale, A. W., 1973. *Nature*, 241, 109.
108. Strong, A. W. 1974. *J. Phys. A*.
109. Tanaka, Y. 1974. Proc. ESLAB Symposium on the Context and Status of  $\gamma$ -Ray Astronomy, Frascati, Reidel, in press.
110. Thompson, D., Fichtel, C. E. Hartman, R. C., Kniffen, D. A. and Bignami, G. F. 1974. Proc. ESLAB Conf. on the Context and Status of  $\gamma$ -Ray Astronomy, Frascati, Reidel, in press.
111. Thompson, D. J. Fichtel, C. E., Kniffen, D. A. and Hartman, R. C. 1974a. Proc. ESLAB Conf. on the Context and Status of  $\gamma$ -Ray Astronomy, Frascati, Reidel, in press.
112. Trombka, J. I., Metzger, A. E., Arnold, J. R., Matteson, J. L., Reedy, R. C. and Peterson, L. E., 1973. *Astrophys. J.*, 181, 737.
113. Trower, W. P. 1966, Univ. of Cal., Lawrence Rad. Lab. Rpt. UCRL-2426, Vol. 2.
114. Van der Kruit, P. C. 1971. *Astron. and Astrophys.* 13, 405.
115. Vedrenne, G. E. Albernhe, F. Martin, I. and Talon, R. 1971, *Astron. and Astrophys.* 15, 50.
116. Vette, J. I., Gruber, D., Matteson, J. L. and Peterson, L. E. 1969 Proc. IAU Symp. no. 37, Rome, (L. Gratton, Ed.), 335, Reidel Pub. Co., Dordrecht, Holland.

117. Vette, J. I., Gruber, D., Matteson, J. L. and Peterson, L. E. 1970.  
Astrophys. J. Lett., 160, L161.
118. Wdowczyk, J. Tkaczyk, W. and Wolfendale, A. W. 1972, J. Phys. A5, 1419.
119. Zatsepin, G. and Kuz'min, V. 1966. Zh. E. T. F. Pis'ma 4, 114 (Translation:  
JETP Lett. 19, 1199 (1967)).
120. Zel'dovich, Y. B., Kurt, V. G., and Syunyaev, R. A., 1969. Sov. Phys.  
JETP 28, 146.